

Design, Synthesis and studies directed towards the photophysical properties of the polycyclic aromatic hydrocarbons

Rekha Sharma
Marquette University

Recommended Citation

Sharma, Rekha, "Design, Synthesis and studies directed towards the photophysical properties of the polycyclic aromatic hydrocarbons" (2011). *Master's Theses (2009 -)*. Paper 109.
http://epublications.marquette.edu/theses_open/109

DESIGN, SYNTHESIS AND STUDIES DIRECTED TOWARDS THE
PHOTOPHYSICAL PROPERTIES OF THE POLYCYCLIC
AROMATIC HYDROCARBONS

by
Rekha Sharma

A Thesis Submitted to the Faculty of the Graduate School,
Marquette University,
In Partial Fulfillment of the Requirements for
the Degree of Master of Science

Milwaukee, Wisconsin

August 2011

ABSTRACT
DESIGN, SYNTHESIS AND STUDIES DIRECTED TOWARDS THE
PHOTOPHYSICAL PROPERTIES OF THE POLYCYCLIC
AROMATIC HYDROCARBONS

Rekha Sharma

Marquette University, 2011

The cross conjugated molecules are also known as cruciforms, which effectively allow the HOMO-LUMO separation. The term Cruciform is used for diaxial chromophores in which the properties of the two axes can be manipulated upon suitable substitution with auxochromic substituents. Originally designed for molecular electronic applications, the discovery that these cruciforms possess a platform where Frontier Molecular Orbitals can be tuned, led to their investigative research as sensory fluorophores. In the majority of organic chromophores, the HOMO and the LUMO are congruent. Thus, upon binding to an analyte both HOMO and LUMO are almost equally affected and hence large shifts in emission are not observed. However, with spatially separated donor and acceptor units the independently addressable FMOs can be used to modulate photophysical properties. Accordingly synthesis of a cross conjugated molecule having electron donor substituent on one branch and electron acceptor substituent on the other branch was undertaken and photophysical properties was studied.

Synthesis of novel fluorene-containing ligands and their complexes with ruthenium and rhenium metal was also developed and the role of fluorene rings on Ruthenium bipyridine and Rhenium complexes were investigated.

ACKNOWLEDGEMENTS

Rekha Sharma

I am thankful to Professor ***Rajendra Rathore*** for the opportunity to work in his laboratory. I wish to express my thanks to the committee members, Professor ***Mark G. Steinmetz*** and Professor ***James R. Gardinier***. Finally I wish to thank those who made it possible for the completion of this thesis in its final form.

TABLE OF CONTENTS

ACKNOWLEDGEMENTS.....	i
LIST OF TABLES.....	iv
LIST OF FIGURES.....	v
LIST OF SCHEMES.....	vii
 CHAPTER 1. Cross Conjugated Polycyclic Aromatic Hydrocarbons: Synthesis and Photophysical properties.	
INTRODUCTION.....	2
RESULTS AND DISCUSSION.....	6
Synthesis of (9, 9-Dihexyl-6, 7-dimethoxy-9H-fluorene Boronic Ester)..	6
Synthesis of Fluorene Derivative 15	9
Synthesis of Cross Conjugated Compound 18.....	12
Electrochemistry, Cation radical Spectra.....	15
Absorption/Emission spectroscopy.....	17
Summary and Conclusions.....	22
EXPERIMENTAL SECTION.....	23
 CHAPTER 2. Synthesis and Photophysical Properties of Ruthenium and Rhenium Complexes of Fluorene Based Bipyridine Ligands.	
INTRODUCTION.....	55
RESULTS AND DISCUSSION.....	60
Synthesis of Fluorene Based Bipyridine Ligands.....	60
Synthesis and Characterization of Ruthenium Metal Complexes of Methyl Bipyridine and Fluorene Based Bipyridine Ligands.....	63

Synthesis and Characterization of Rhenium Metal Complexes of Fluorene Based Bipyridine Ligands.....	66
Electrochemistry, Absorption/Emission Spectroscopy of Ru Complexes	68
Absorption and Emission Spectra of Rhenium metal complexes.....	70
Summary and Conclusions.....	71
EXPERIMENTAL SECTION.....	71

REFERENCES AND FOOTNOTES

CHAPTER 1.....	105
CHAPTER 2.....	107

LIST OF TABLES**CHAPTER 1**

TABLE 1	Absorption/Emission data of cross conjugated molecule 18.....	31
TABLE 2	Crystal data and structure refinement for compound 17.....	48

CHAPTER 2

TABLE 1	Crystal data and structure refinement for ligand (6).....	94
TABLE 2	Crystal data and structure refinement for 5, 5'-Bis-[9-(9-hexyl-9H-fluoren-9-ylmethyl)-9H-fluoren-9-ylmethyl]-[2, 2'] bipyridinyl ligand (4).....	95
TABLE 3	Crystal data and structure refinement for Ruthenium metal complex of methyl bipyridine (9).....	97
TABLE 4	Crystal data and structure refinement for Rhenium metal complex of fluorene based ligand (12).....	99
TABLE 5	Crystal data and structure refinement for Rhenium metal complex of fluorene based ligand (13).....	100

LIST OF FIGURES

CHAPTER 1

FIGURE 1	The structures of recently reported cross conjugated molecules.....	13
FIGURE 2	Showing the HOMO-LUMO of compound 18, obtained by density functional theory calculations at the B3LYP/6-31G* level.....	15
FIGURE 3	¹ H NMR spectra of 9, 9-Dihexyl-6, 7-dimethoxy-9H-fluorene boronic ester (8) in CDCl ₃ at 22 °C.....	18
FIGURE 4	¹ H NMR spectra of fluorene derivative (15) in CDCl ₃ at 22°C	21
FIGURE 5	¹ H NMR spectra of compound 17, 18 in CDCl ₃ at 22°C.....	23
FIGURE 6	Cyclic Voltammogram of compound (18) in CH ₂ Cl ₂ containing 0.2 M <i>n</i> -Bu ₄ NPF ₆ at various scan rates at 22 °C.....	25
FIGURE 7	Square wave (blue trace) in CH ₂ Cl ₂ containing 0.2 M <i>n</i> -Bu ₄ NPF ₆ at a scan rate of 200 mV/s at 22 °C.....	26
FIGURE 8A	Spectral changes observed upon the reduction of MB^{+•} SbCl ₆ ⁻ by an incremental addition of 18 to its radical cation in CH ₂ Cl ₂ at 22 °C.....	27
FIGURE 8 B	Plot of depletion of absorbance of MB^{+•} SbCl ₆ ⁻ (blue circles) and an increase of the absorbance of 18 ^{+•} (pink circles,) against the equivalent of added neutral 18	27

FIGURE 9	(A) Normalised absorption and emission spectra in CH ₂ Cl ₂ solution at 22 °C. (B) Emission spectra of compound 18 in concentration range of 1.0*10 ⁻⁷ M to 7.9*10 ⁻⁶ , in CH ₂ Cl ₂ solution at 22 °C.....	28
FIGURE 10	Emission spectra of compound 18 in concentration range of 2.99*10 ⁻⁷ M to 5.96*10 ⁻⁶ M, in Toluene at 22 °C.....	18
FIGURE 11	Emission spectra of compound 18 in concentration range of 2.99*10 ⁻⁷ M to 5.96*10 ⁻⁶ M, in Hexane at 22 °C.....	29
FIGURE 12	Emission spectra of compound 18 in concentration range of 2.99*10 ⁻⁷ M to 5.96*10 ⁻⁶ M, in Acetonitrile solvent at 22 °C.....	30
FIGURE 13	Emission spectra of compound 18 in Methanol, at 22 °C.....	30
FIGURE 14	Comparison of the emission spectra in different solutions at 22 °C.....	31.

CHAPTER 2

FIGURE 1	Representative examples of reported Ru (II) –complexes.....	66
FIGURE 2	Representative examples of electro-active materials obtained using fluorene framework.....	67
FIGURE 3	The proposed structure of Ru (II) –complexes based on polyfluorene substituted bipyridine ligands.....	68
FIGURE 4	¹ H NMR spectra of ligand 4, 6 in CDCl ₃ at 22 °C.	72

- FIGURE 5** ^1H NMR spectra of Ru complexes 9-11 in CD_3CN at $22\text{ }^\circ\text{C}$ 75
- FIGURE 6** ^1H NMR spectra of Re complexes 12-13 in CDCl_3 at $22\text{ }^\circ\text{C}$ 77
- FIGURE 7** Cyclic voltammograms of 9, 10, and 11 in CH_3CN measured at a scan rate of $\nu = 100\text{ mV s}^{-1}$ at $22\text{ }^\circ\text{C}$78
- FIGURE 8** Comparison of the normalized absorption and emission spectra of Ru $(\text{Bp})_2\text{.BpyMe}$, $\text{Ru}(\text{Bpy})_2(\text{F1Bpy})$ and $\text{Ru}(\text{Bpy})_2(\text{F2BPy})_2$. All spectra were recorded at a concentration of 2×10^{-3} in CH_3CN 79
- FIGURE 9** Comparison of the normalized absorption (A) and emission spectra (B) of $\text{Re}(\text{CO})_3\text{Br}(\text{MeBpy})$, $\text{Re}(\text{CO})_5(\text{F1Bpy})$ and $\text{Re}(\text{CO})_5(\text{F2BPy})$. All spectra were recorded at a concentration of 2×10^{-3} in CH_3CN 80

LIST OF SCHEMES**CHAPTER 1**

SCHEME 1 Synthesis of (9, 9-Dihexyl-6,7-dimethoxy-9H-fluorene boronic ester)...17

SCHEME 2 Schematic representation of Synthesis of fluorene derivative 15..... 20

SCHEME 3 Assembly of Cross- conjugated molecule 18 using 15 and 8..... 22

CHAPTER 2

SCHEME 1 Schematic representation of the synthesis of Ruthenium metal complexes of fluorene based bipyridine ligands..... 69

SCHEME 2 Schematic representation of the synthesis of 5, 5'-Bis-[9-(9-hexyl-9H-fluorene-9-ylmethyl)-9H-fluorene-9-ylmethyl]-[2, 2'] bipyridinyl ligand...71

SCHEME 3 Schematic representation of the synthesis of Ruthenium metal complexes of methyl bipyridine and fluorene based bipyridine ligands..... 74

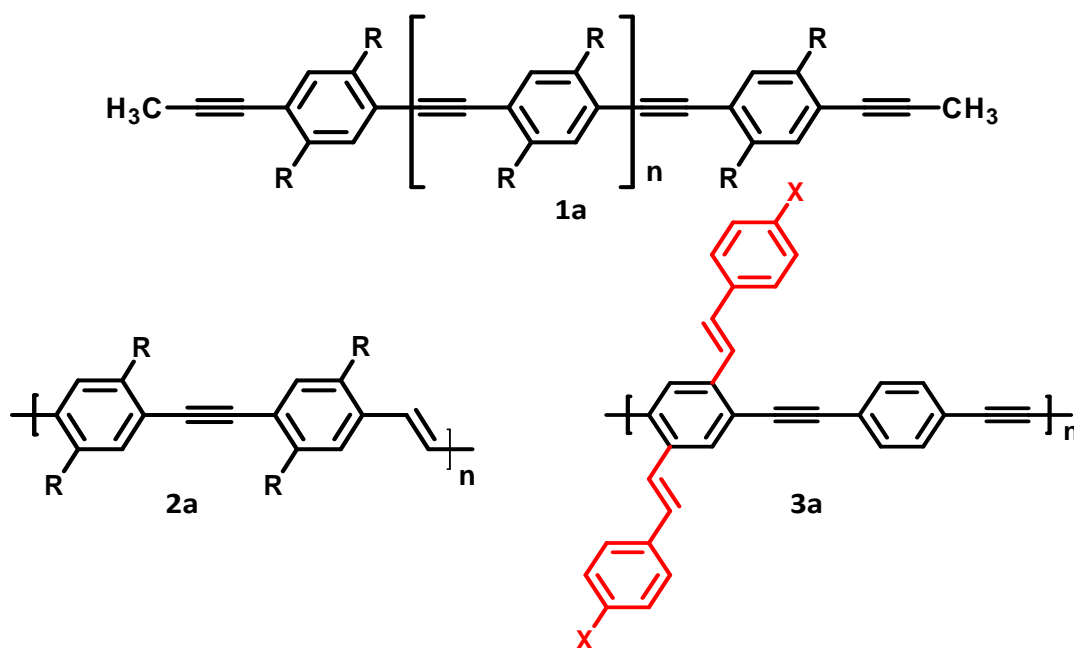
SCHEME 4 Schematic representation of the synthesis of Rhenium Metal Complexes of fluorene based bipyridine ligands.....76

Chapter-1

Cross Conjugated Polycyclic Aromatic Hydrocarbons: Synthesis and Photophysical Properties

Introduction

Polycyclic aromatic hydrocarbons are very important because of their application in the field of molecular electronics and photovoltaic devices such as light-emitting diodes, field-effect transistors; liquid crystal displays and solar cells.¹ For molecular electronic applications, PPEs (para-phenylene ethynynes) were known long back². But compared to the PPVs (poly phenylene vinylenes), the PPEs are at a disadvantage for applications in OLEDs. In these polymers hole injection was a problem due to the electron withdrawing nature of the alkyne group (structure 1a). So to remove this problem first vinyl group was introduced into the main chain but it did not improve the performance (structure 2a). In a second attempt styryl groups in the side chain was introduced which significantly improved the performance (structure 3a), these materials were more electron rich and the solution and solid state band gap reduced and hole injection considerably facilitated.² (structure 3a).



To understand the properties of these polymers better Bunz and coworkers³ introduced this new class of cross-conjugated (4a-9a) “X-shaped” molecules also known as cruciforms in which HOMO and LUMO were spatially separated. Term cruciform was first used by Collin Nuckolls⁴ for a class of molecules with two perpendicular disposed π -systems connected through a central aromatic core.

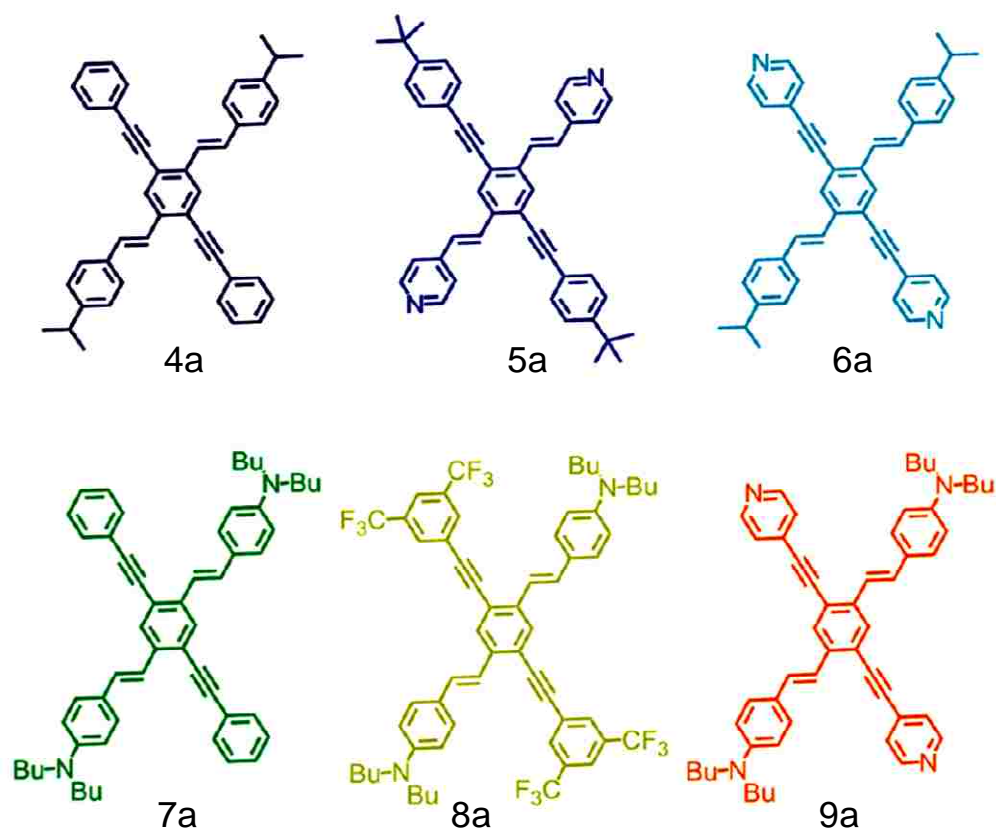
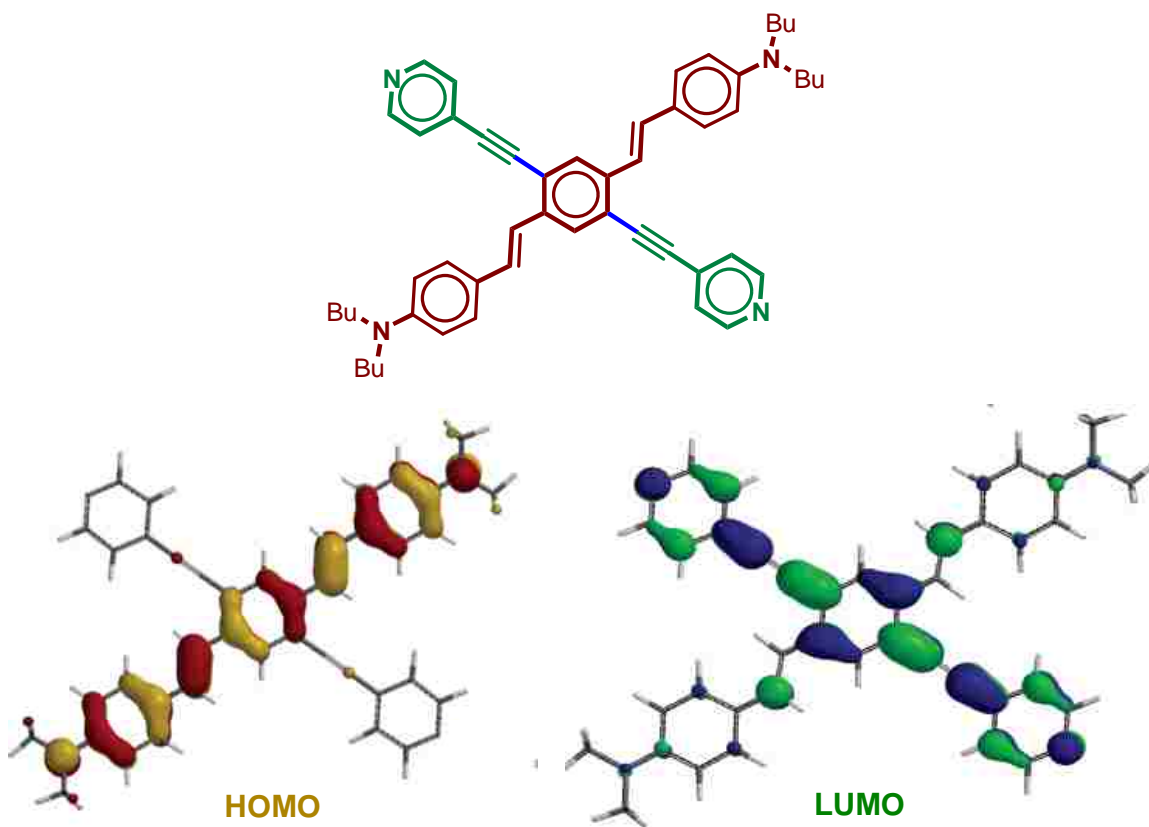


Figure 1. The structures of recently reported cross conjugated molecules.

The term ‘cruciform’ is used for diaxial chromophores in which properties of the two axes can be manipulated upon suitable substitution with auxochromic substituents.² These cruciforms possess the structure where Frontier Molecular Orbitals (FMOs) can be adjusted.

In most of the organic chromophores, the HOMO and LUMO are spatially superimposable upon each other. Thus upon binding to an analyte both HOMO and LUMO are almost equally affected. Hence large shifts in emission bands are not observed.² However with spatially separated donor and acceptor units (i.e. one axis is donor substituted and other axis is acceptor substituted) FMOs can be separated.



In these cross conjugated molecules, the HOMO lies on the distyryl branch of the molecule while LUMO is situated on the ethynyl branch of the molecule.² As a consequence, the intramolecular charge transfer emissions and absorptions of these cruciforms are dependent on solvent polarity and exhibits dramatic spectral shifts which makes them functional scaffolds for metal sensor arrays.

Accordingly, we have undertaken the synthesis of a cross conjugated molecule having electron donor substituents on one branch and electron acceptor substituents on the other branch (see Figure 2). It is envisioned that such an arrangement of donor/acceptor groups in molecule 18 will allow the effective separation of HOMO and LUMO. Herein, we will describe the preparation, absorption and emission spectroscopic studies, and electrochemical properties as follows.

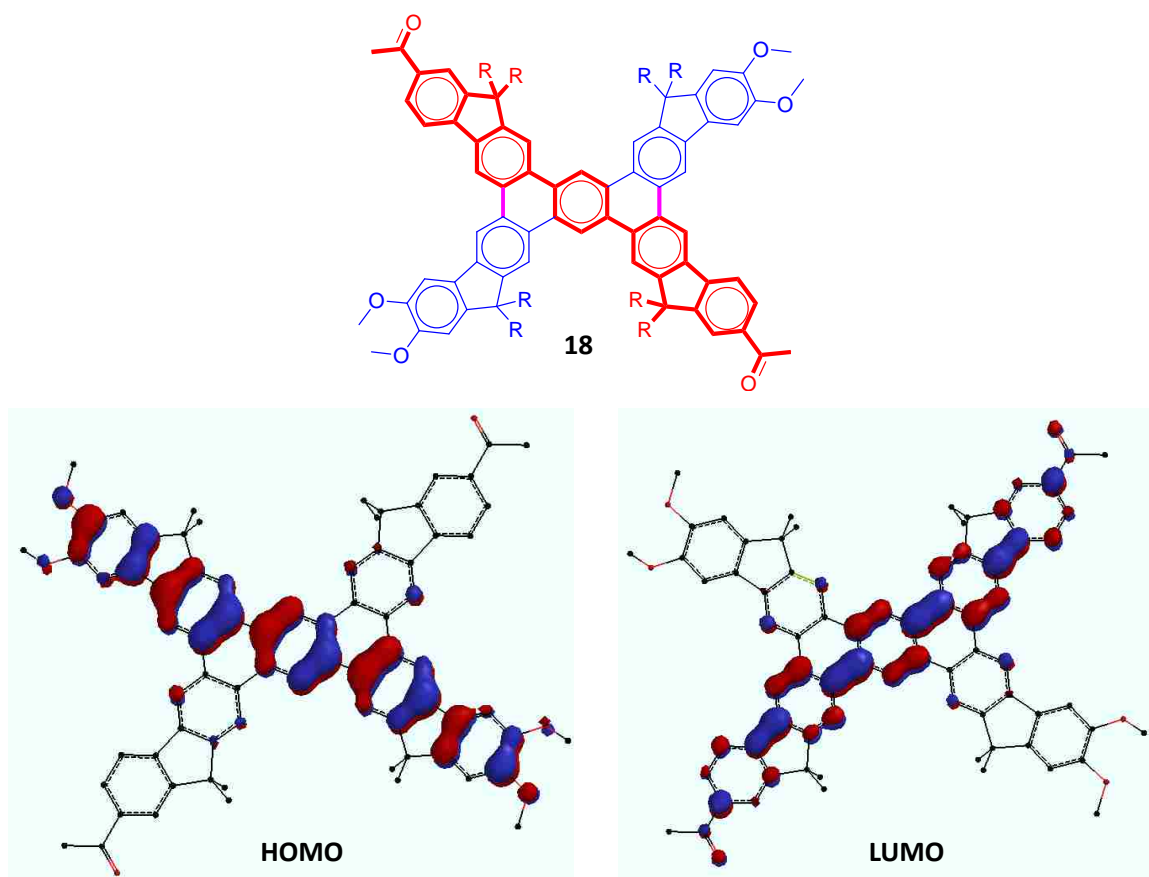
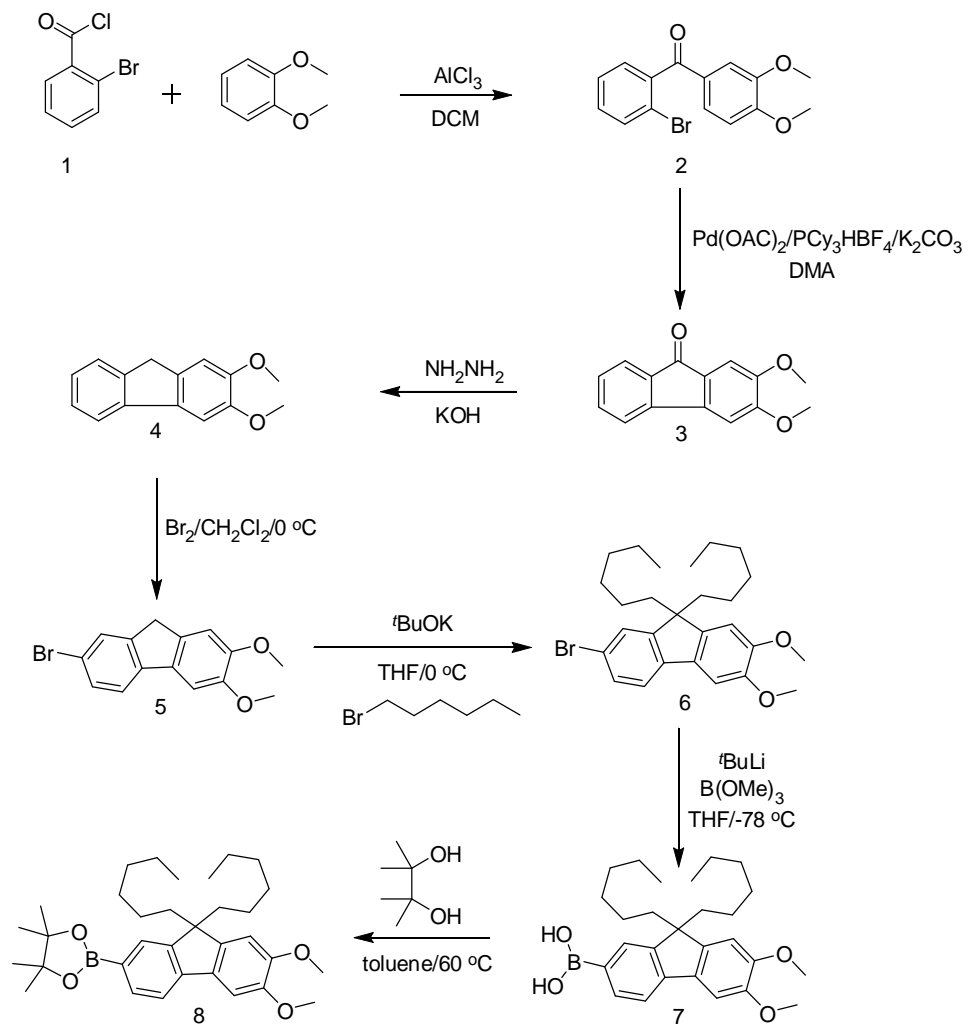


Figure 2. Showing the HOMO-LUMO of compound 18, obtained by density functional theory calculations at the B3LYP/6-31G* level.

Results and discussions

Synthesis of (9, 9-Dihexyl-6, 7-dimethoxy-9H-fluorene boronic ester) (8). General synthetic strategy (see Scheme 1) for the compound 18 begins with commercially available 2-bromobenzoyl chloride and veratrol. Thus, a standard Friedel-Craft reaction between 1 and veratrol yields the ketone 2 in 84% yield after a simple recrystallization. Bromo- ketone 2 was then subjected to a palladium-catalyzed intramolecular Heck coupling to furnish the fluorenone 3 in excellent yield. The fluorenone 3 was easily reduced to corresponding fluorene 5 in excellent yield using standard Wolf-Kishner reduction. A selective bromination of 5 afforded 7-bromo-2,3-dimethoxy-9,9-dihexylfluorene (6), which was subjected to an alkylation reaction using potassium-*tert*-butoxide (2.1 equivalents) and 1-bromohexane in THF at room temperature to afford 7-bromo-9,9-dihexyl-2,3-dimethoxyfluorene (6). The bromofluorene derivative 6 was converted to corresponding boronic acid by a reaction with butyllithium and trimethyl borate in THF at -78 °C. The resulting boronic acid was treated with excess pinacol in toluene at 60°C to yield corresponding pure boronic ester after column chromatography in 50% yield. The boronic ester was characterized by ¹H NMR and ¹³C NMR spectroscopy (see Figure 3).

Scheme 1: Synthesis of 9,9-Dihexyl-6,7-dimethoxy-9H-fluorene boronic ester (8)



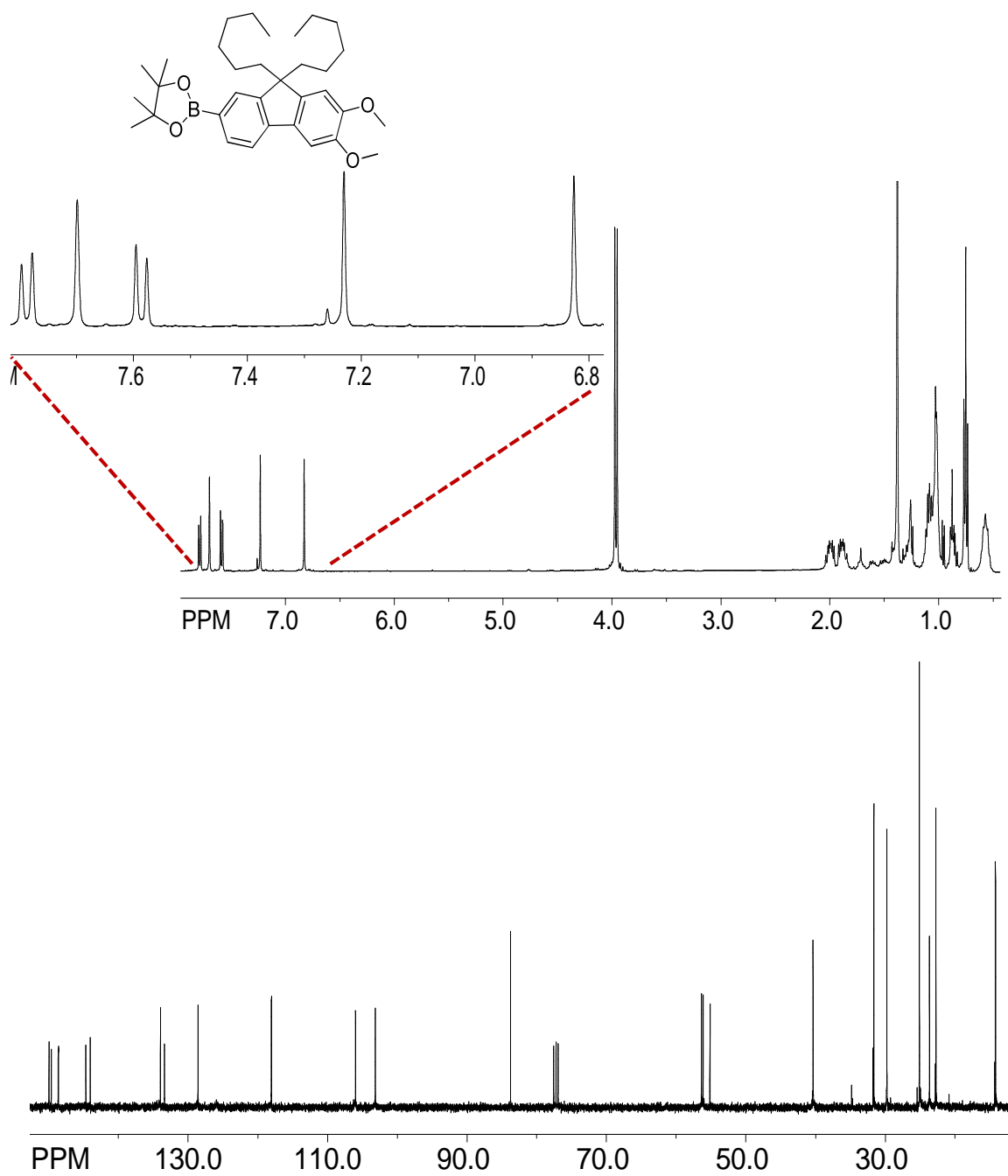
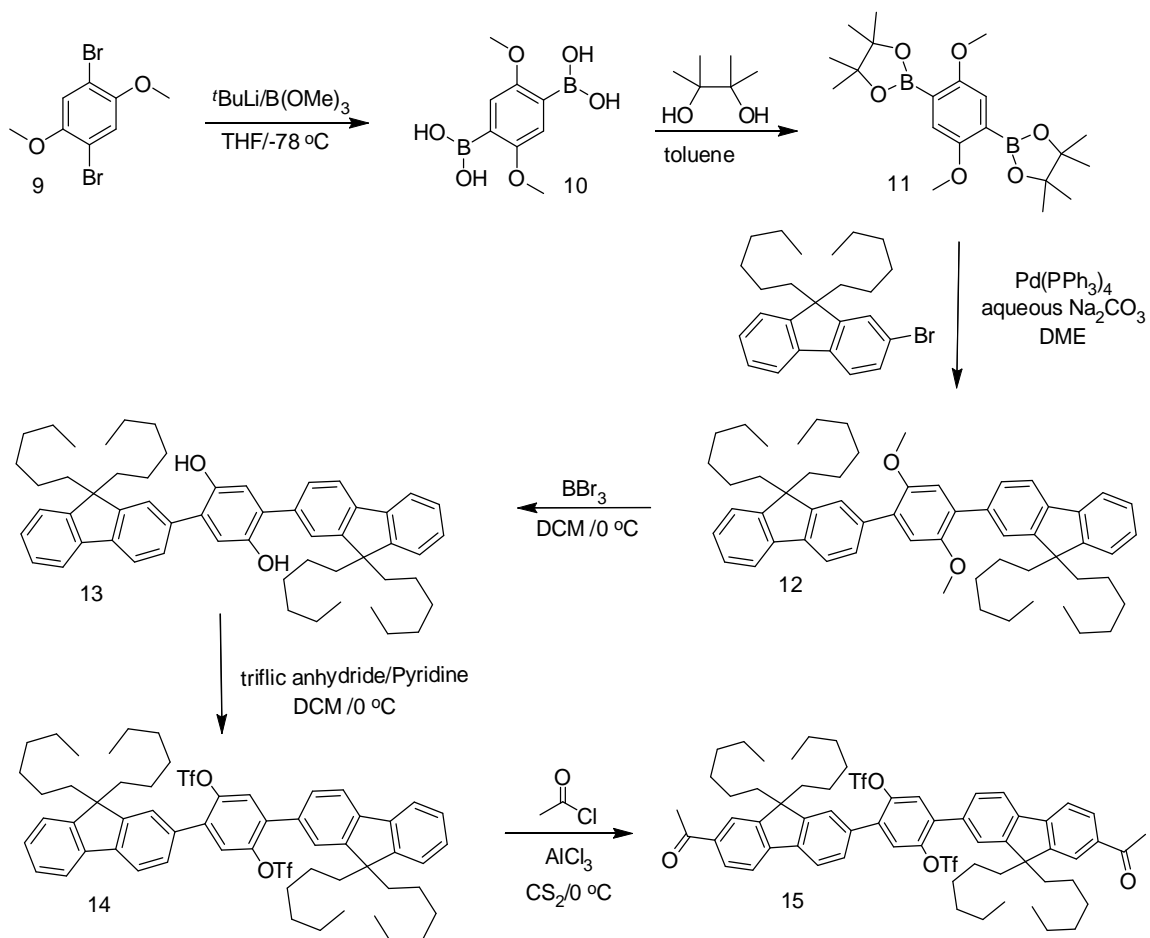


Figure 3. ^1H and ^{13}C NMR spectra of 9,9-Dihexyl-6,7-dimethoxy-9H-fluorene boronic ester (8) in CDCl_3 at 22 $^\circ\text{C}$.

Synthesis of fluorene derivative 15. Diboronic ester of 1,4-dimethoxy-2,5-dibromobenzene (obtained using standard procedures, see Experimental section) was subjected to Suzuki coupling with 2 equivalent of 9,9-dihexyl-2-bromofluorene in refluxing 1,2-dimethoxyethane (DME) in the presence of a catalytic amounts of *tetrakis*-triphenylphosphinepalladium [Pd(PPh₃)₄, 0.1 mol%] to afford the intermediate 12 in 58% yield after column chromatography purification. A demethylation of the methoxy groups of 12 using BBr₃ in dichloromethane at 0 °C produced the corresponding dihydroxy intermediate 13 in good yield. The hydroxyl functional groups of 13 were transformed into triflate functional groups in 90% yield using triflic anhydride and pyridine in dichloromethane . The resultant ditriflet 14 was subjected to Friedal-Craft acylation using acetyl chloride and AlCl₃ in dichloromethane to afford compound 15. The compound 15 was characterized by ¹H NMR and ¹³C NMR spectroscopy (see Scheme 2 and Figure 4).

Scheme 2: Synthesis of *bis*-fluorene derivative 15.

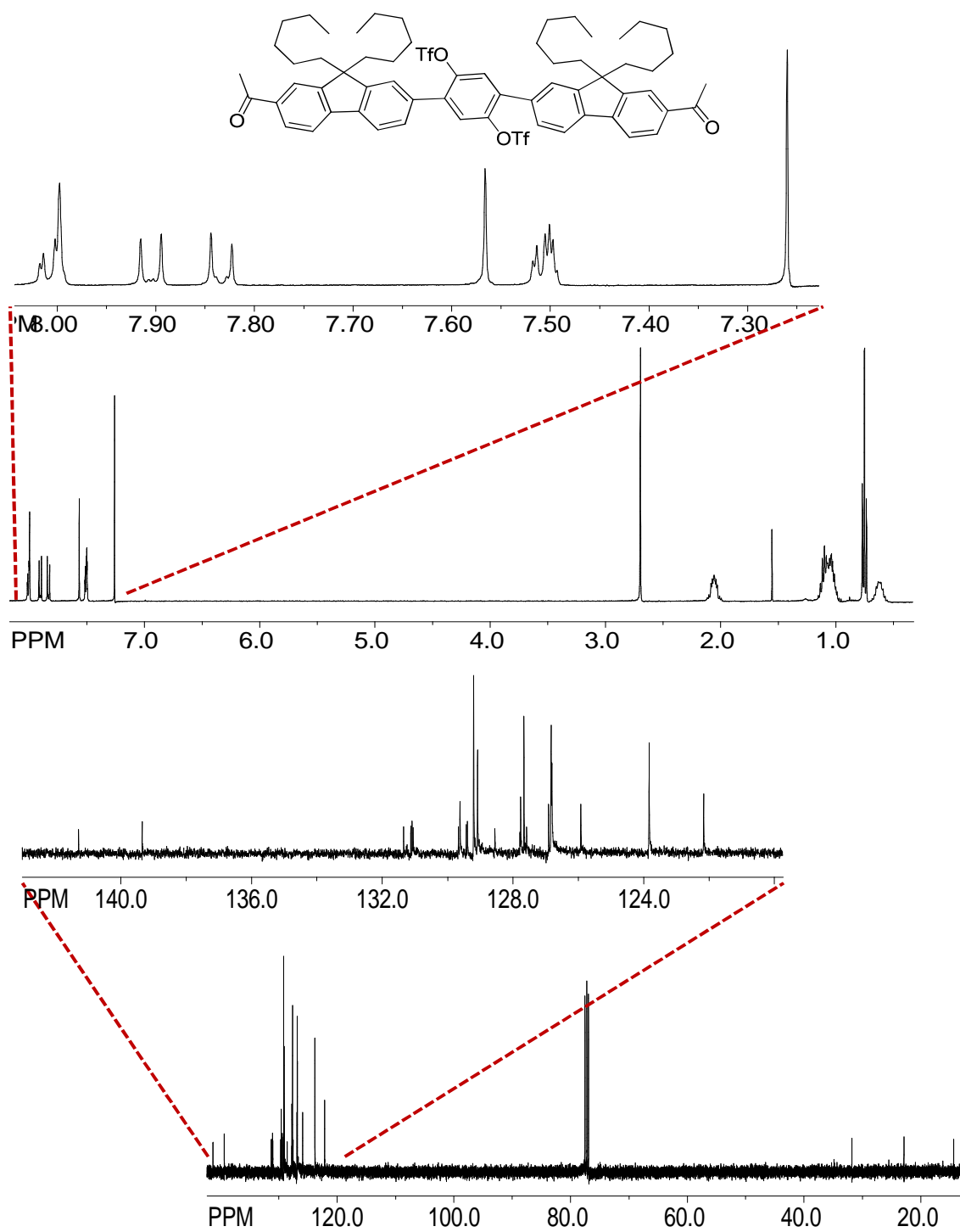
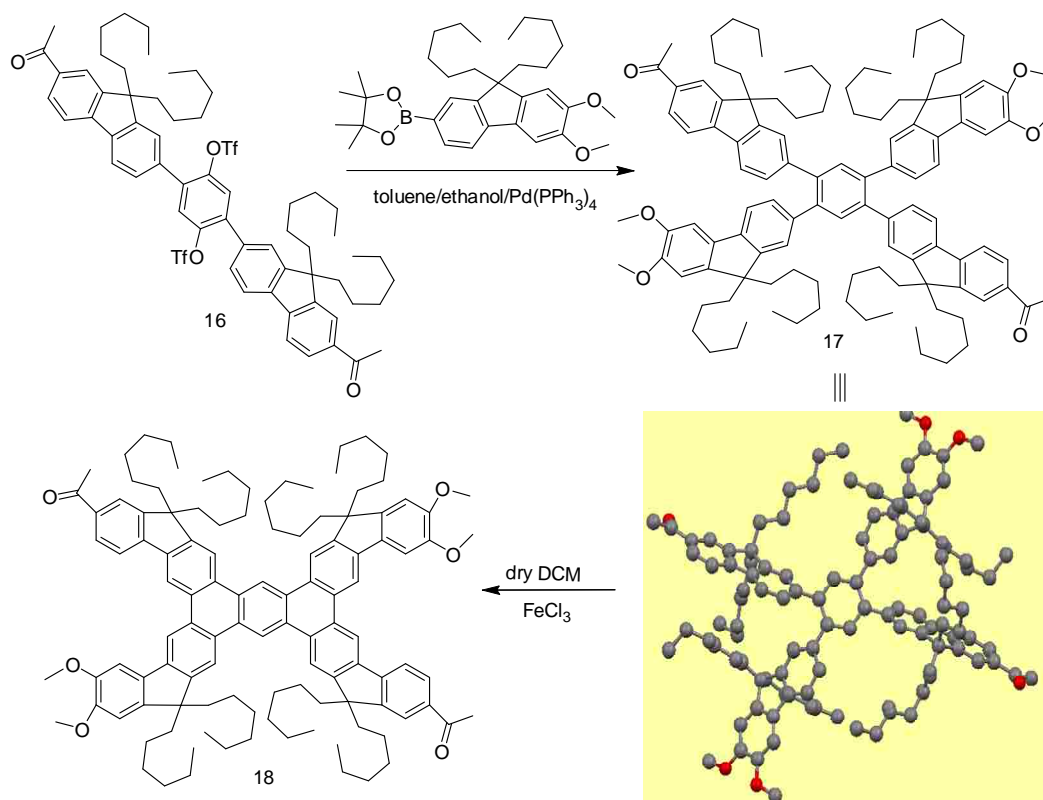


Figure 4. ^1H and ^{13}C NMR spectra of 15 in CDCl_3 at 22°C .

Assembly of cross-conjugated molecule 18 using 15 and 8. The preparation of cross-conjugated molecule 18 was completed in two steps using 15 and 8. Thus a standard Suzuki coupling reaction of 15 (Scheme 2) with boronic ester 9 (Scheme 1) in refluxing toluene in the presence of a catalytic amounts of $\text{Pd}(\text{PPh}_3)_4$ (0.1 mol) and aqueous sodium carbonate afforded the precursor 17 in 50% yield after column chromatography. The molecular structure of 17 was confirmed by X-ray crystallography (Scheme 3). An oxidative cyclization of 17 using 10 equivalent of FeCl_3 in dichloromethane finally furnished the cyclized cross conjugated compound 18, which was carefully characterized by ^1H NMR and ^{13}C NMR spectroscopy (Figure 5).

Scheme 3: Assembly of cross-conjugated molecule 18 using 15 and 8.



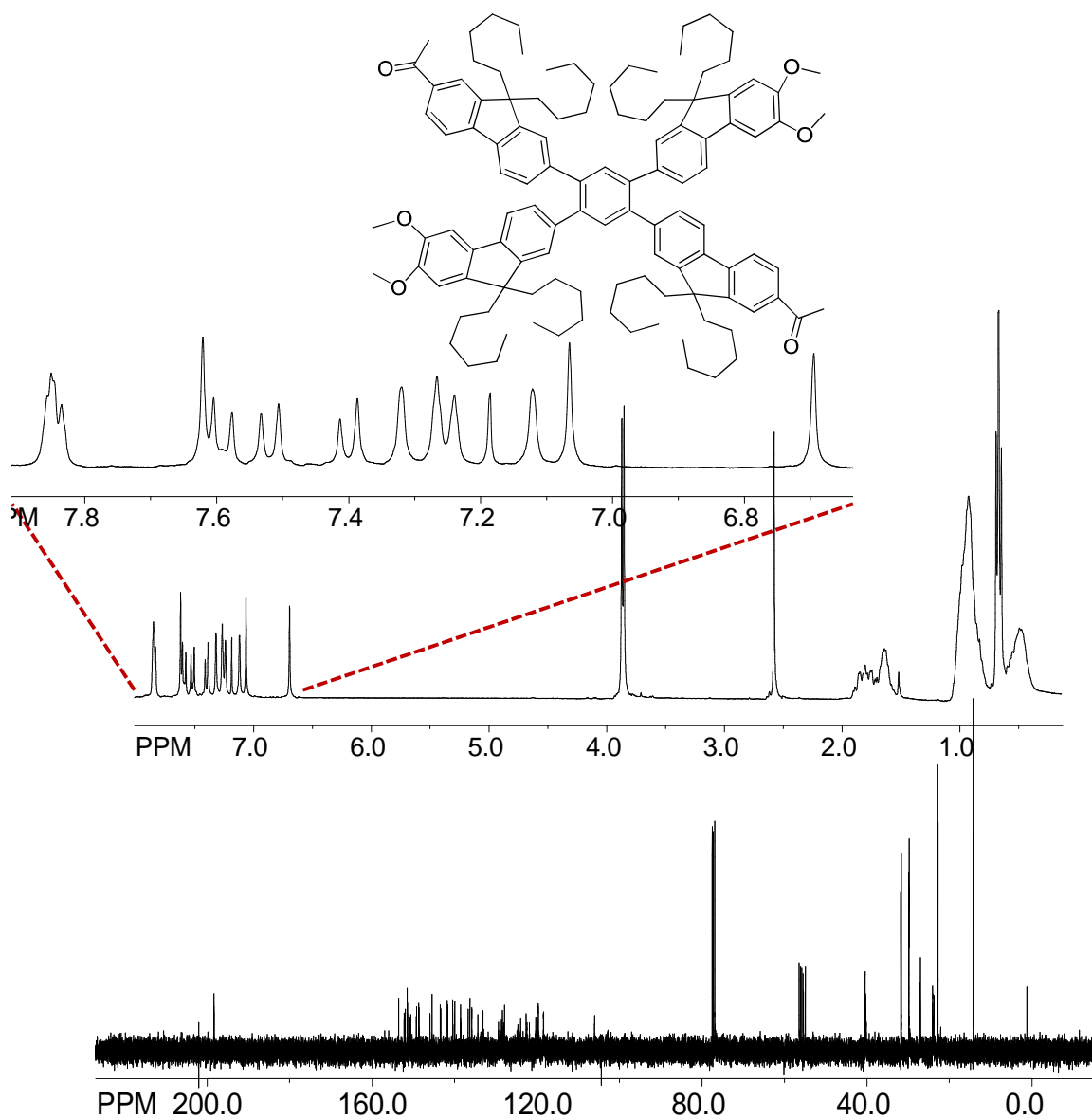


Figure 5a. $^1\text{H}/^{13}\text{C}$ NMR spectra of compound 17 in CDCl_3 at 22°C .

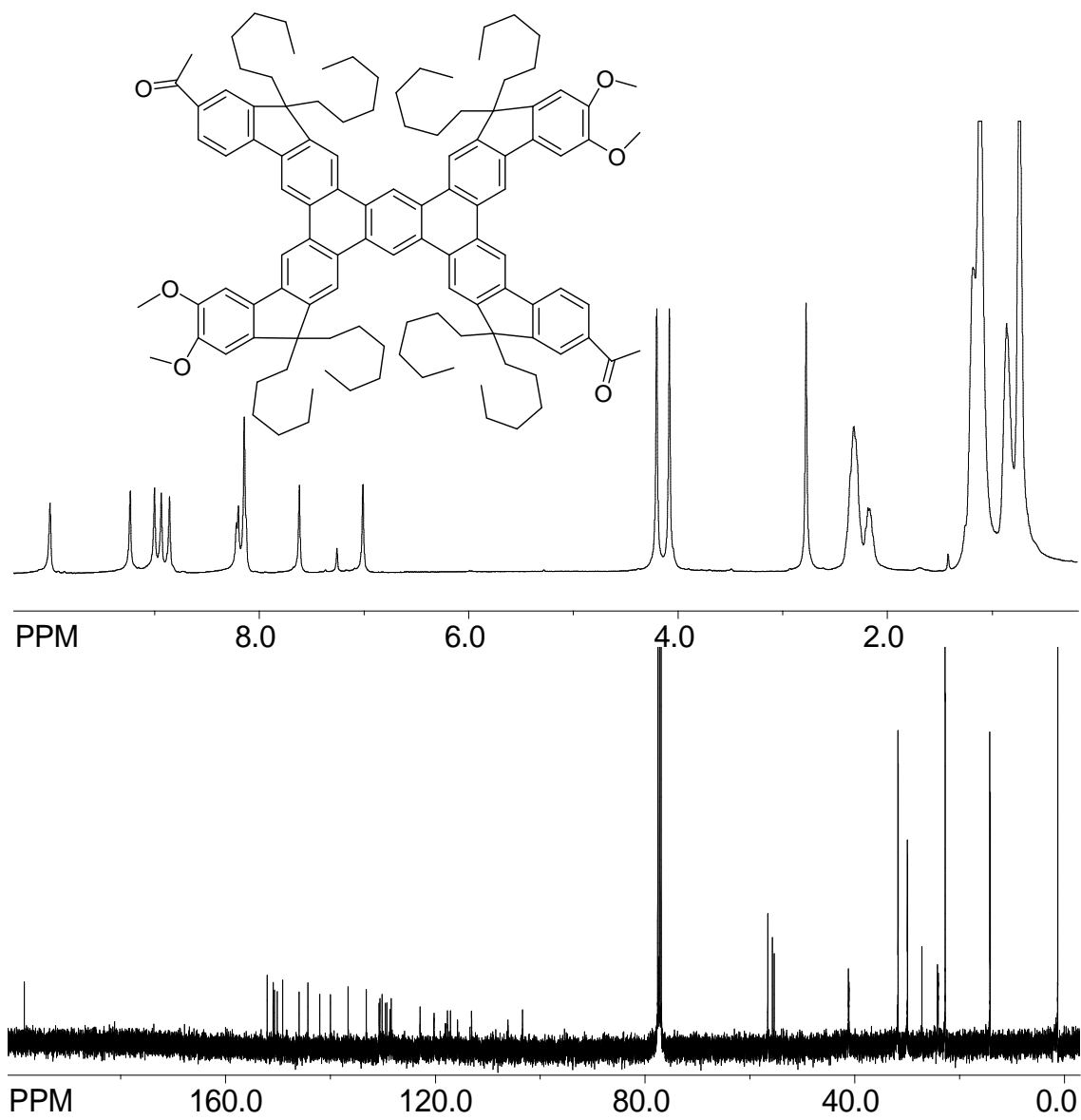


Figure 5b. $^1\text{H}/^{13}\text{C}$ NMR spectra of compound 18 in CDCl_3 at 22°C .

Electrochemistry

The redox properties of compound 18 was determined by electrochemical oxidation at a platinum electrode as 2×10^{-3} M solution in anhydrous dichloromethane containing 0.2 M tetra-*n*-butyl ammonium hexafluorophosphate as the supporting electrolyte. The cyclic voltammograms exhibit one reversible oxidation at 1.04V, for the removal of the first electron at varying scan rates of 50–500 mV s^{-1} , and the second oxidation wave at 1.13 V for the removal of second electron. The third and fourth oxidation waves at 1.60V and 1.82V, respectively, were quasireversible (Figures 6 and 7).

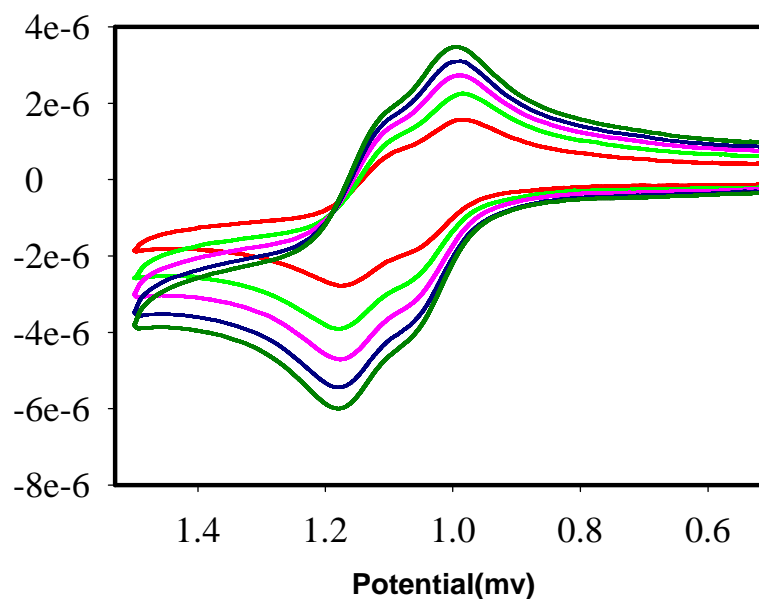


Figure 6. Cyclic voltammogram of compound 18 in CH_2Cl_2 containing 0.2 M *n*- Bu_4NPF_4 at different scan rates (50–500 mV s^{-1}) at 22 °C.

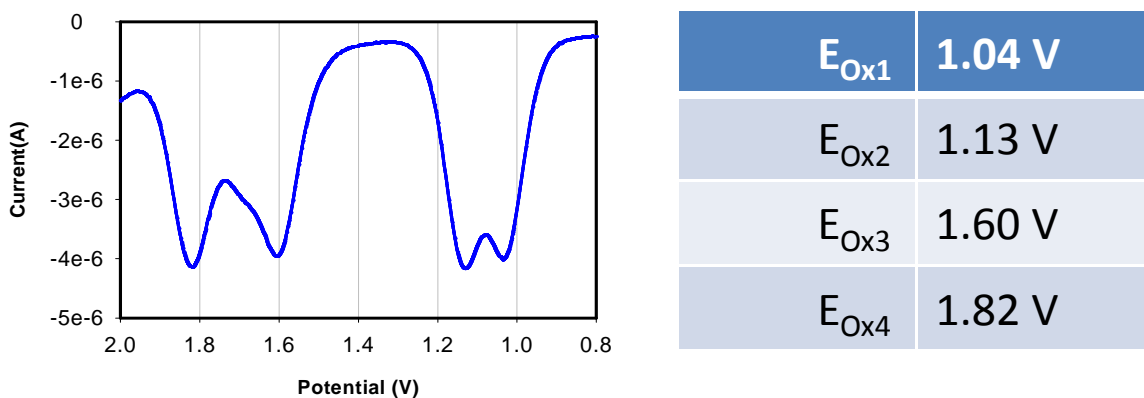


Figure 7. Square wave (left) in CH_2Cl_2 containing 0.2 M $n\text{-Bu}_4\text{N PF}_6$ at a scan rate of 200 mV/s at 22 °C. (Right): Tabulation of the oxidation potentials of 18.

Generation of the cation radical of 18 and its electronic spectra: The cation radical of compound 18 was generated using an aromatic cation-radical salts ($\text{MB}^{+\bullet} \text{SbCl}_6^-$), derived from triarylamine.

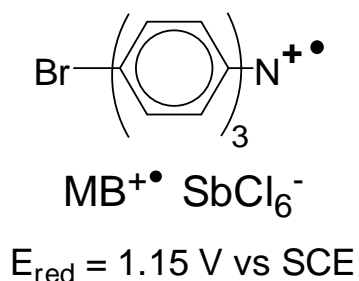


Figure 3 shows the spectral changes observed upon an incremental addition of sub-stoichiometric amounts of 18 to a solution of $\text{MB}^{+\bullet} \text{SbCl}_6^-$ in dichloromethane at 22 °C. Moreover, a plot of formation of $18^{+\bullet}$ (i.e. an increase of absorbance at 2000 nm) and a consumption of $\text{MB}^{+\bullet} \text{SbCl}_6^-$ (i.e. a decrease of absorbance at 728 nm) against the increments of added neutral 18 established that $\text{MB}^{+\bullet} \text{SbCl}_6^-$ was completely consumed

after addition of 1 equiv. of **18**; and the resulting absorption spectrum remained unchanged upon further addition of neutral **18**, i.e. Eq 1.

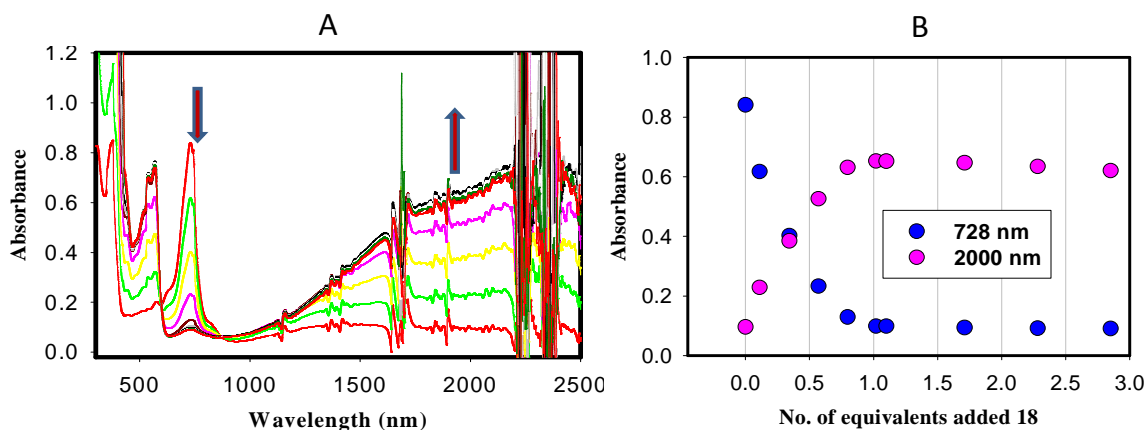
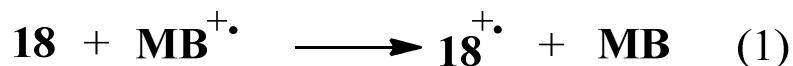


Figure 8. (A) Spectral changes observed upon the reduction of $\mathbf{MB}^{+\bullet} \text{SbCl}_6^-$ by an incremental addition of **18** in CH_2Cl_2 at 22°C . (B) Plot of depletion of absorbance of $\mathbf{MB}^{+\bullet} \text{SbCl}_6^-$ (blue circles) and an increase of the absorbance of $\mathbf{18}^{+\bullet}$ (pink circles,) against the equivalent of added neutral **18**.

Absorption/emission spectroscopy of **18**.

The electronic absorption and emission spectra of **18** were recorded in dichloromethane, THF, toluene, hexane, acetonitrile and methanol under the identical conditions and temperature (22°C). The absorption and emission spectra in DCM are shown in figure 5. The absorption spectra possess transition around 350 and 399nm. The emission spectra of compound **18** have emission maxima at 470nm, in the concentration range of 10^{-7} to 10^{-6} as shown in figure 5B. Red shift was observed in emission maxima in solvents from

hexane to acetonitrile (Table 1) in the concentration range of 10^{-7} - 10^{-6} (Figure 10). However there was no trend observed in quantum yields. The fluorescence quantum yields were determined using quinine sulphate ($\Phi = 0.54$) as a standard and compound showed fluorescence quantum yields 0.16 in DCM, 0.17 in hexane, 0.24 in THF, 0.28 in Toluene and 0.05 in Acetonitrile.

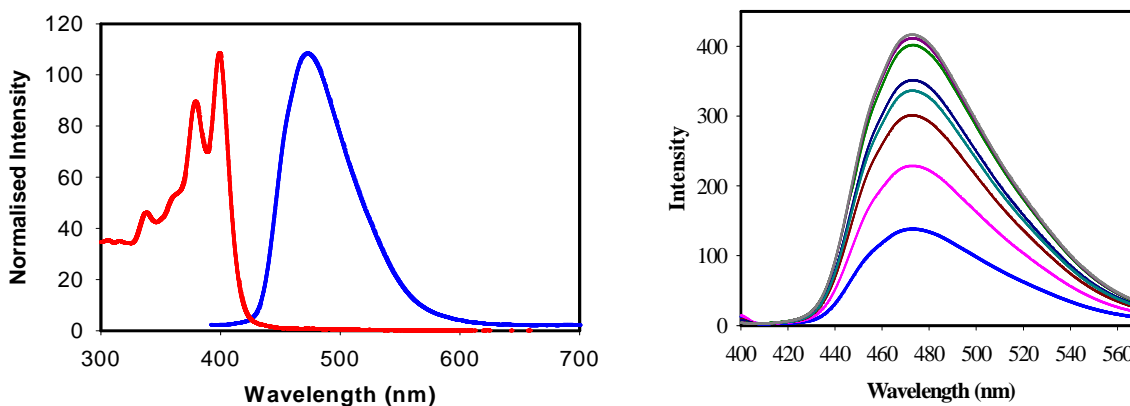


Figure 9. (Left) Normalised absorption and emission spectra of 18 in CH_2Cl_2 at 22 °C. (B) Emission spectra of compound 18 in concentration range of 1.0×10^{-7} to 7.9×10^{-6} in dichloromethane at 22 °C. Emission maximum at $\lambda_{\text{max}} = 470$ nm.

The emission spectra in toluene and hexane showed well defined vibrational structure (Figures 10 and 11), with the position of emission maxima shifting towards blue. In toluene, the emission band was centered at 446 nm while in hexane the band was centered at 436 nm (Figures 10 and 11).

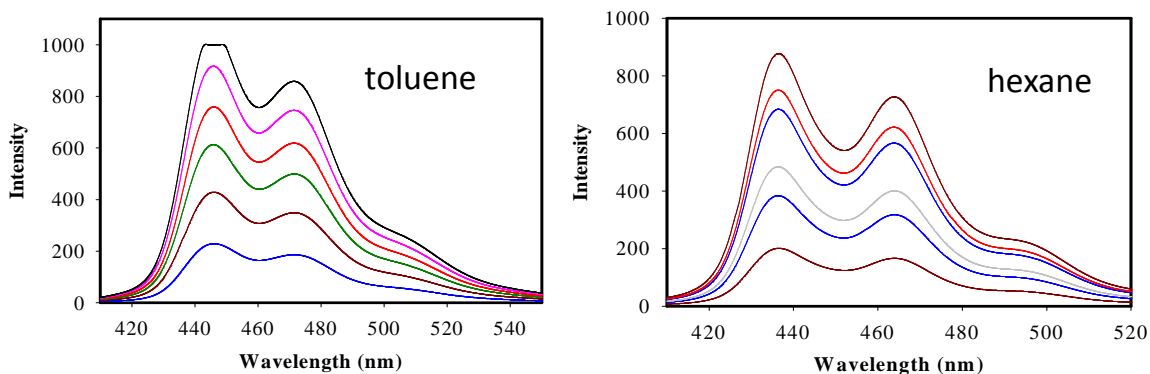


Figure 10/11. (Left) Emission spectra of compound 18 in concentration range of 2.99×10^{-7} to 5.96×10^{-6} M, $\lambda_{\text{max}} = 446$ nm, in toluene at 22 °C. (Right) Emission spectra of compound 18 in concentration range of 2.99×10^{-7} to 5.96×10^{-6} M, $\lambda_{\text{max}} = 436$ nm, in hexane at 22 °C.

In acetonitrile, the emission band for 18 was observed at 480 nm and was unchanged in the concentration range of 10^{-7} to 10^{-6} M as shown in Figure 12. In methanol compound was not soluble so emission study based on concentration could not be done, however it showed emission maxima at 480 nm (Figure 13).

The emission spectra for 18 are compared in Figure 14 and the values of both absorption and emission bands as well as the quantum yield for emission from 18 in different solvents are compiled in Table 1. The Table 1 and Figure 14 clearly suggest that the emission band shows a bathochromic shift with the increasing polarity of the solvent.

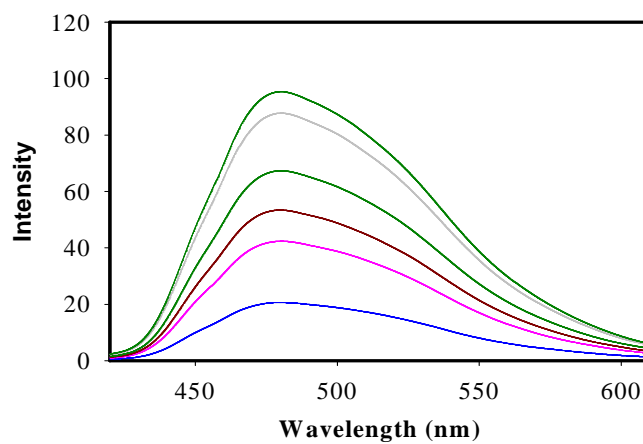


Figure 12. Emission spectra of 18 in acetonitrile in the concentration range of 2.99×10^{-7} to 5.96×10^{-6} M, $\lambda_{\text{max}} = 480$ nm, at 22 °C.

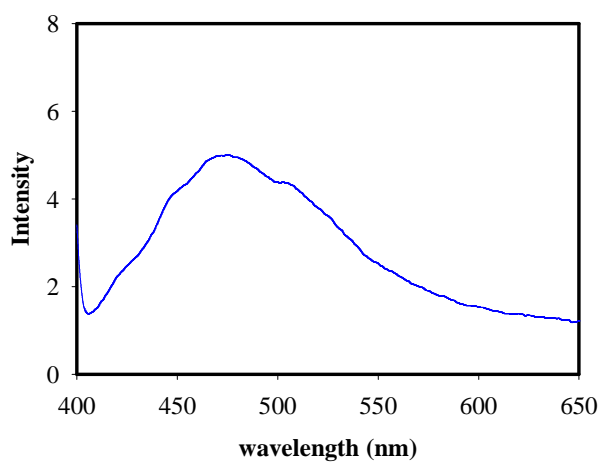


Figure 13. Emission spectra of compound 18 in methanol, $\lambda_{\text{max}} = 480$ nm, at 22 °C.

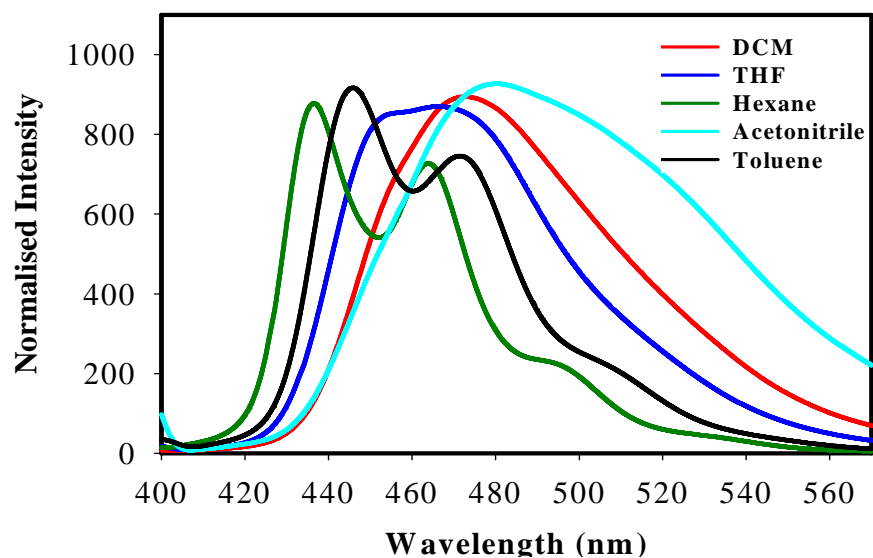


Figure 14. Comparison of the emission spectra in different solvents.

Table 1. Absorption/Emission data of compound **18**.

	Hexane	Toluene	THF	DCM	ACN
Emission $\lambda_{\text{Max}}(\text{nm})$	436	446	460	470	480
Quantum Yield	0.17	0.28	0.24	0.16	0.05
Absorption $\lambda_{\text{Max}}(\text{nm})$	395	400	398	399	376

Summary and Conclusions

We have successfully synthesized and characterized the structure of a cross conjugated molecule (i.e. compound 18) which contains electron donor substituents on one branch and the electron acceptor substituents on the other branch. The successful synthesis of 18 demonstrated that a spatial separation of HOMO and LUMO can be achieved in a planarized polycyclic aromatic hydrocarbon. The cross conjugated molecule 18 also showed that the position of emission maximum shifts red with the increasing solvent polarity.

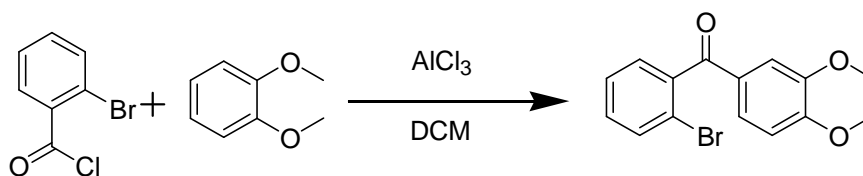
Experimental Section

General Experimental Methods and Materials. All reactions were performed under argon atmosphere using conventional vacuum-line techniques unless otherwise noted. All commercial reagents were used without further purification unless otherwise noted. Anhydrous tetrahydrofuran (THF) was prepared by refluxing the commercial tetrahydrofuran (Aldrich) over lithium tetrahydroaluminate under an argon atmosphere for 24 hours followed by distillation. It was stored under an argon atmosphere in a Schlenk flask equipped with a Teflon valve fitted with Viton O-rings. Dichloromethane (Aldrich) was repeatedly stirred with fresh aliquots of conc. Sulfuric acid (~10% by volume) until the acid layer remained colorless. After separation it was washed successively with water, aqueous sodium bicarbonate, water, and saturated aqueous sodium chloride and dried over anhydrous calcium chloride. The dichloromethane was distilled twice from P₂O₅ under an argon atmosphere and stored in a Schlenk flask equipped with a Teflon valve fitted with Viton O-rings. The hexanes and toluene were distilled from P₂O₅ under an argon atmosphere and then refluxed over calcium hydride (~12 hrs). After distillation from CaH₂, the solvents were stored in Schlenk flasks under argon atmosphere.

Cyclic Voltammetry (CV). The CV cell was of an air-tight design with high vacuum Teflon valves and Viton O-ring seals to allow an inert atmosphere to be maintained without contamination by grease. The working electrode consisted of an adjustable platinum disk embedded in a glass seal to allow periodic polishing (with a fine emery cloth) without changing the surface area (~1 mm²) significantly. The reference SCE

electrode (saturated calomel electrode) and its salt bridge were separated from the catholyte by a sintered glass frit. The counter electrode consisted of platinum gauze that was separated from the working electrode by ~3 mm. The CV measurements were carried out in a solution of 0.1 to 0.2 M supporting electrolyte (tetra-*n*-butylammonium hexafluorophosphate, TBAH) and the substrate in dry dichloromethane under an argon atmosphere. All the cyclic voltammograms were recorded at a sweep rate of 200 mV sec⁻¹, unless otherwise specified and were IR compensated. The oxidation potentials ($E_{1/2}$) were referenced to SCE, which was calibrated with added (equimolar) ferrocene ($E_{1/2} = 0.450$ V vs. SCE). The $E_{1/2}$ values were calculated by taking the average of anodic and cathodic peak potentials in reversible cyclic voltammograms or directly from square-wave voltammograms in irreversible cyclic voltammograms.

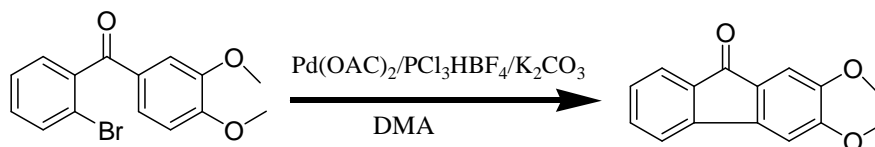
Synthesis of (2-Bromo-phenyl)-(3,4-dimethoxy-phenyl)methanone (2).



To a stirred solution of (6.0 gm, 27.33 mmol) bromobenzoyl chloride in (100 ml) dichloro methane at 0°C, (5.46 gm, 40.99 mmol) AlCl₃ was added portion wise, after 15 minutes (3.48 ml, 27.33 mmol) Veratrol was added with the help of dropping funnel. Reaction was stirred for 24hr.

After completion, reaction mixture was cooled with dry ice under argon atmosphere, acidified with 25 ml dil HCl followed by extraction with DCM. Organic layer was dried over MgSO₄. Filtrate was concentrated to yield the product. Product was purified by Recrystallization with DCM and Hexane. Yield: 7.47 gm, 84%; mp 139-141 °C; ¹H NMR δ (CDCl₃): 3.94 (s, 6H), 6.85 (d, 1H, *J* = 8.39), 7.21 (dd, 1H, *J* = 8.17), 7.30-7.45 (m, 3H), 7.58-7.67 (m, 2H). ¹³C NMR δ (CDCl₃): 56.38, 110.10, 111.06, 119.68, 126.71, 127.29, 128.94, 129.39, 131.04, 133.27, 141.16, 149.50, 154.20, 194.77.

Synthesis of 2, 3-Dimethoxy-fluoren-9-one (3).

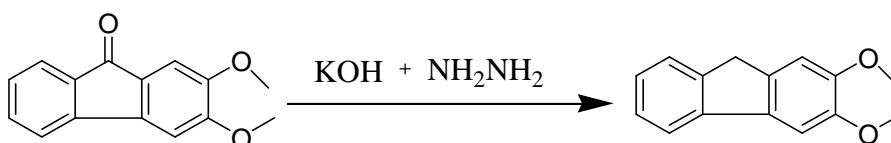


To a stirred solution of compound 2 (10.0 gm, 31.09 mmol) in 150 ml DMA, Pd(OAc)₂, (69 mg, 0.31 mmol), PCy₃HBF₄ (0.228 gm, 0.62 mmol) was added. Mixture was degassed and refilled with argon. Then potassium carbonate was added. Reaction mixture was heated in a oil bath maintained ~130°C. Reaction mixture was refluxed for 24 hr.

After completion, reaction mixture was cooled to room temperature. Dilute HCl was added followed by extraction with DCM to yield product. Yield: 7.12 gm, 95%; mp 134-136 °C; ¹H NMR δ (CDCl₃): 3.92 (s, 3H), 4.01 (s, 3H), 7.00 (s, 1H), 7.16-7.23 (m, 2H), 7.33-7.24 (m, 2H), 7.55 (dt, 1H, *J* = 7.32). ¹³C NMR δ (CDCl₃): 56.53, 103.54,

107.22, 119.26, 123.86, 126.97, 128.32, 134.36, 134.88, 139.63, 144.08, 149.85, 154.70, 193.31.

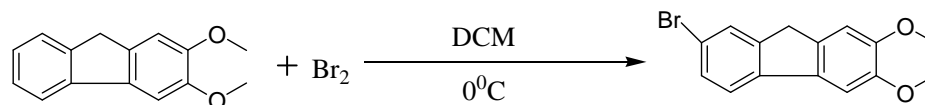
Synthesis of 2,3-Dimethoxy-9H-fluorene (4).



To a stirred solution of compound 3 (5.8 g, 24.09 mmol) in 100 mL diethylene glycol, KOH was added under argon followed by hydrazine hydrate. Reaction mixture was refluxed on heating metal at 180-190°C. Reaction was stirred for 24 hours.

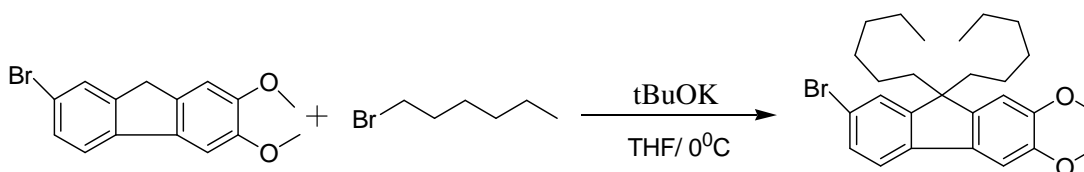
After completion, reaction mixture was added in cold water and HCl. It was extracted with DCM. The organic layer was dried over magnesium sulfate and concentrated in vacuum to afford the product which was further purified by silica column chromatography using 10 % ethyl acetate in hexanes mixture to afford the product. Yield: 2.88 gm, 51% ; mp 128-130 °C; ^1H NMR δ (CDCl_3): 3.79 (s, 2H), 3.92 (s, 3H), 3.96 (s, 3H), 7.07 (s, 1H), 7.17-7.24 (m, 2H), 7.32 (t, 1H, $J = 15.43$), 7.47 (d, 1H, $J = 7.45$), 7.64 (d, 1H, $J = 7.98$). ^{13}C NMR δ (CDCl_3): 37.03, 56.38, 56.41, 103.18, 108.46, 119.02, 123.82, 125.02, 125.70, 126.92, 134.47, 135.96, 142.33, 143.59, 148.96.

Synthesis of 7-Bromo-2, 3-dimethoxy-9H-fluorene (5).



To a stirred solution of compound 4 (2.8 g, 12.34 mmol) in 100 mL DCM under argon at 0 °C bromine (1.97 g, 12.34 mmol) was added with the aid of a dropping funnel. Reaction was stirred for 2 hr. After completion, reaction was quenched with DCM. Organic layer was washed with sodium bisulphite and dried over MgSO₄ and concentrated in vacuum to yield the product, which was purified by recrystallization from DCM and hexane. Yield: 3.3 g, 87%; mp 98-100 °C. ¹H NMR δ (CDCl₃): 3.75 (s, 2H), 3.93 (s, 3H), 3.96 (s, 3H), 7.04 (s, 1H), 7.20 (s, 1H), 7.43-7.50 (m, 2H), 7.58-7.61 (m, 1H). ¹³C NMR δ (CDCl₃): 36.74, 56.28, 56.30, 103.01, 108.21, 119.24, 120.12, 128.10, 129.86, 133.33, 135.60, 141.24, 145.47, 148.99, 149.25.

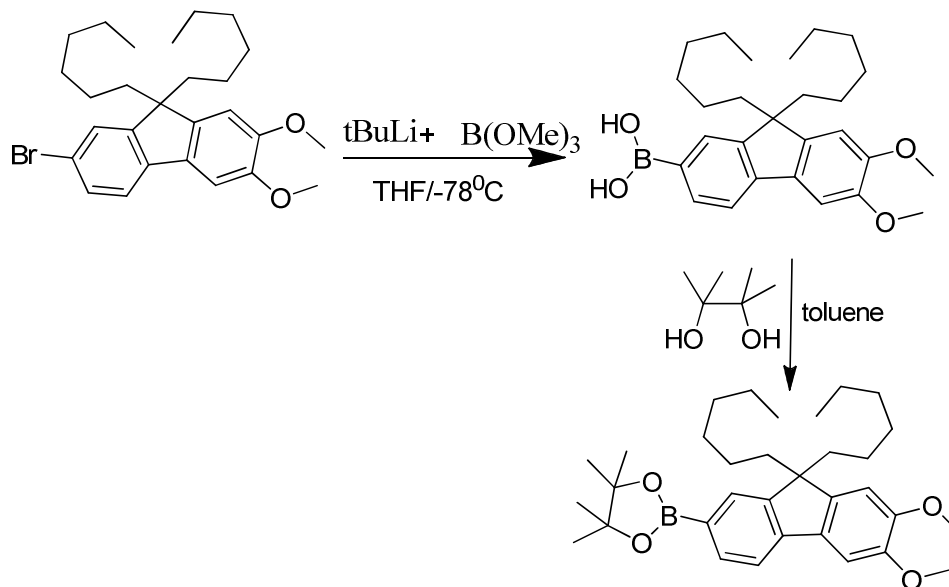
Synthesis of 7-Bromo-9, 9-dihexyl-2,3-dimethoxy-9H-fluorene (6).



To a stirred solution of compound 5 (3.3 g, 10.79 mmol) in 35 mL dry THF at 0°C potassium *tert*-butoxide (2.54 g, 22.65 mmol) was added, After 15 minutes (3.18 mL, 22.65 mmol) bromohexane was added with the aid of a dropping funnel. The resulting mixture was stirred for 2 hrs.

Reaction was quenched with water followed by extraction with DCM to afford the product. Yield: 3.78 g, 73%; mp 58-60 °C; ^1H NMR δ (CDCl_3): 0.48-0.64 (m, 4H), 0.77 (t, 6H, $J = 14.0$), 0.96-1.16 (m, 12H), 1.79-1.94 (m, 4H), 3.94 (s, 3H), 3.97 (s, 3H), 6.79 (s, 1H), 7.15 (s, 1H), 7.38-7.43 (m, 3H). ^{13}C NMR (CDCl_3) δ : 14.22, 22.77, 29.81, 35.67, 40.47, 55.46, 56.26, 56.46, 102.95, 106.00, 119.84, 120.09, 126.02, 129.95, 132.58, 140.68, 143.04, 148.85, 149.65, 153.15.

Synthesis of (9,9-Dihexyl-6,7-dimethoxy-9H-fluorene boronic ester) (8).

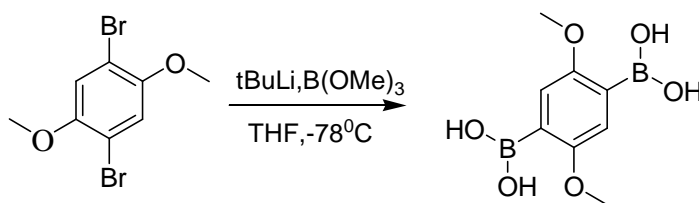


To a stirred solution of compound 6 (1.0 g, 2.11 mmol) in 15 mL dry THF under argon at -78°C (1 mL, 2.32 mmol) butyllithium was added dropwise followed by (0.387 mL, 3.48 mmol) trimethylborate. Reaction was stirred for 24 hrs. After completion, reaction mixture was poured in beaker containing 200 g ice and 7 mL H_2SO_4 . This reaction

mixture was stirred for 1 hour and then extracted with ether to yield the boronic acid which was used in next step without further without purification.

Thus, boronic acid (2.56 g, 5.84 mmol) was dissolved in 70 mL toluene. Pinacol (0.69 g, 5.84 mmol) was added and the resultant mixture refluxed for 2 h in a flask equipped with a Dean-Stark trap and condenser. After completion, reaction mixture was cooled to room temperature and solvent was removed in vacuo to yield the product, which was purified by column chromatography using 2% ethyl acetate in hexanes. Yield: 1.5 g, 50%; mp 65-67 °C. ^1H NMR δ (CDCl_3): 0.47-0.66 (m, 4H), 0.75 (t, 6H, $J = 14.79$), 0.97-1.15 (m, 12H), 1.81-2.07 (m, 4H), 3.95 (s, 3H), 3.97 (s, 3H) 6.82 (s, 1H), 7.23 (s, 1H), 7.58 (d, 1H, $J = 7.67$), 7.69 (s, 1H), 7.78 (d, 1H, $J = 7.67$). ^{13}C NMR (CDCl_3) δ : 14.17, 22.71, 23.65, 25.08, 29.77, 31.62, 40.36, 55.13, 56.11, 56.35, 83.76, 103.13, 105.97, 118.05, 128.58, 133.40, 133.96, 144.05, 144.69, 148.62, 149.63, 149.94.

Synthesis of boronic acid of dibromo dimethoxy Benzene (10).

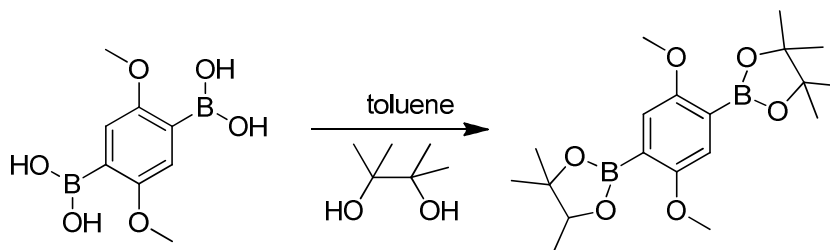


In a oven dried Schlenk flask, a solution of dibromodimethoxybenzene (4.7 g, 15.8 mmol) in anhydrous THF (100 mL) was cooled to -78°C (dry ice-acetone bath) under argon atmosphere and *n*-butyllithium (2.5 M in hexane, 18.96 ml, 47.4 mmol) was added

dropwise. After the addition of butyllithium, the temperature was slowly raised to $-10\text{ }^{\circ}\text{C}$. After 2hr, reaction mixture was cooled again to $-78\text{ }^{\circ}\text{C}$ and (7.70 mL, 69.36 mmol) trimethyl borate was added dropwise, and let the temperature slowly rise to room temperature. Reaction mixture was stirred for additional 12 h at room temperature.

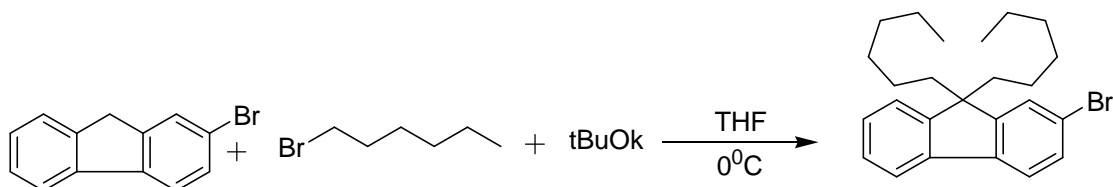
After completion, reaction mixture was quenched with 10% HCl and it was stirred for 40 minutes then extracted with ether; and combined organic layers were dried over MgSO_4 and concentrated in vacuo to afford the product, which was purified by recrystallization with DCM and hexane. Yield: 1.4 g, 40%; mp $>460\text{ }^{\circ}\text{C}$. $^1\text{H NMR } \delta$ (DMSO): 3.77 (s, 6H), 7.15 (s, 2H), 7.81 (s, 4H).

Synthesis of boronic ester of dibromo dimethoxy Benzene (11).



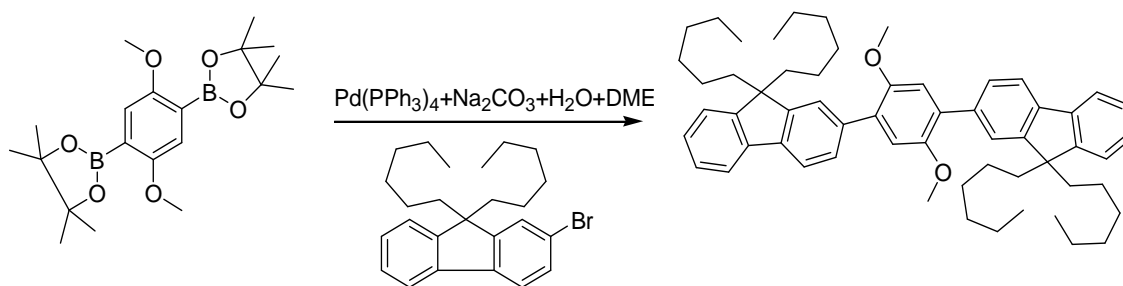
Boronic acid (1.07 gm, 4.75 mmol) was dissolved in 60 mL toluene and (1.12 g, 9.5 mmol) pinacol was added. The resulting mixture was refluxed for 2 h in a flask equipped with Dean-Stark trap. After completion, reaction mixture was cooled and solvent was removed by evaporation to yield the product. Yield: 1.76 g, 95%; $^1\text{H NMR } \delta$ (CDCl_3): 1.35 (s, 24H), 3.81 (s, 3H), 7.14 (s, 1H). $^{13}\text{C NMR } \delta$ (CDCl_3): 25.02, 57.17, 83.78, 119.04, 158.28.

Synthesis of 2-Bromo-9,9-dihexyl-9H-fluorene.



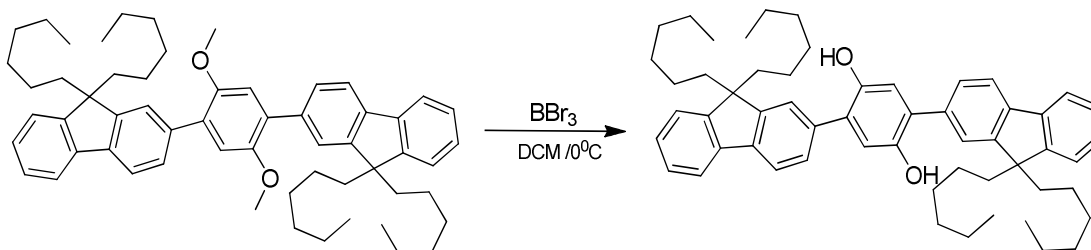
Bromofluorene (10.0 g, 40.79 mmol) was dissolved in 100 mL THF at 0 °C and then potassium t-butoxide (9.15 g, 81.58 mmol) was added. After 5 min, bromohexane (11.45 mL, 81.58 mmol) was added with dropping funnel. Reaction mixture was stirred for 2 hr. After completion, reaction was quenched with water and extracted with DCM. Combined organic layers were dried over MgSO_4 and concentrated in vacuo to afford the product. Yield: 14.86 g, 88%; ^1H NMR δ (CDCl_3): 0.43-0.58 (m, 4H), 0.66 (t, 6H, $J = 13.6$), 0.87-1.08 (m, 12H), 1.77-1.91(m, 4H), 7.21 (d, 3H, $J = 3.13$), 7.30-7.41(m, 2H), 7.44 (d,1H, $J = 8.0$), 7.53-7.59(m, 1H). ^{13}C NMR δ (CDCl_3): 14.22, 22.79, 23.86, 29.85, 31.67, 40.51, 55.56, 119.94, 121.22, 123.05, 126.31, 127.11, 127.66, 130.66, 140.22, 140.32, 150.49, 153.15,

Synthesis of compound 12.



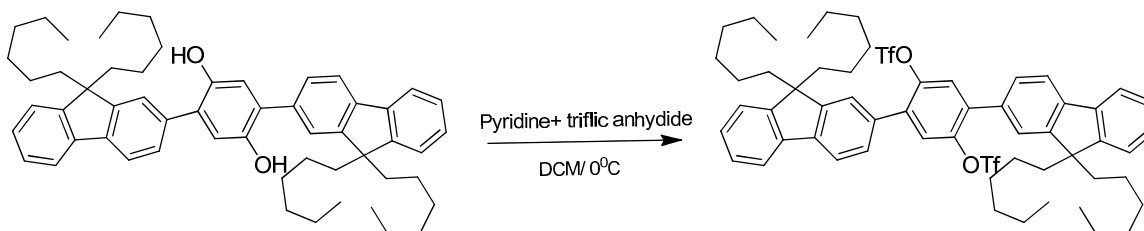
A solution of sodium carbonate (23 g) in water (70 mL) was prepared in a Schlenk flask and degassed (3x) and kept under argon atmosphere. In a separate Schlenk flask, bromohexylfluorene (6.35 g, 15.38 mmol), dimethoxybenzene bis-boronic ester (3.0 g, 7.69 mmol), and DME (70 mL) were added under an argon atmosphere and the Schlenk flask was degassed (5x). Under an argon flow, a catalytic amount of Pd(PPh₃)₄ (100 mg) was added and the flask was covered by aluminum foil and degassed (3x). Into this mixture, the aqueous sodium carbonate solution was transferred and the reaction was degassed again (3x). The resulting mixture was heated to reflux for ~24 hours, after completion reaction mixture was cooled under argon atmosphere, extracted with water and dichloromethane. The organic layer was then dried over magnesium sulfate and concentrated in vacuum to afford crude solid which was further purified by silica column chromatography using 1% ethyl acetate: hexane mixtures to afford the product. Yield: 3.62 g, 58%; mp 103-105 °C. ¹H NMR δ (CDCl₃): 0.53-0.83 (m, 10H), 0.88-1.13 (m, 12H), 1.78-2.04 (m, 4H), 3.70 (s, 3H), 7.0 (s, 1H), 7.14-7.29 (m, 3H), 7.46 (d, 1H, *J* = 7.84), 7.54 (s, 1H), 7.63 (dd, 2H, *J* = 15.13). ¹³C NMR (CDCl₃): 22.80, 24.08, 29.98, 31.73, 40.52, 55.19, 56.92, 115.65, 119.51, 119.90, 123.03, 124.61, 126.94, 127.13, 128.08, 131.29, 137.07, 140.29, 141.05, 150.52, 151.22, 151.36.

Synthesis of compound 13.



To a stirred solution of compound 12 (2.6 g, 3.23mmol) in 70 mL dry DCM at 0 °C, BBr₃ solution in DCM was added with the aid of a dropping funnel over the period of 45 min. and the resulting reaction mixture was stirred for 2 hr. After completion, reaction was quenched with methanol at 0 °C and extracted with water and DCM. Organic layer was dried over MgSO₄ and concentrated in vacuo to yield the product. Yield; 2.28 g, 91%; ¹H NMR δ(CDCl₃): 0.64-0.86 (m, 10H), 1.01-1.23 (m, 12H), 1.96-2.12 (m, 4H), 5.15 (s, 1H), 7.07 (s, 1H), 7.33-7.46 (m, 3H), 7.51-7.59 (m, 2H), 7.74-7.81 (m, 1H), 7.83-7.89 (m, 1H). ¹³C NMR (CDCl₃): 14.19, 22.77, 24.07, 29.89, 31.68, 40.52, 55.45, 117.27, 120.10, 120.61, 123.15, 123.73, 127.10, 127.50, 127.62, 129.15, 135.33, 140.56, 141.26, 146.54, 151.11, 152.28.

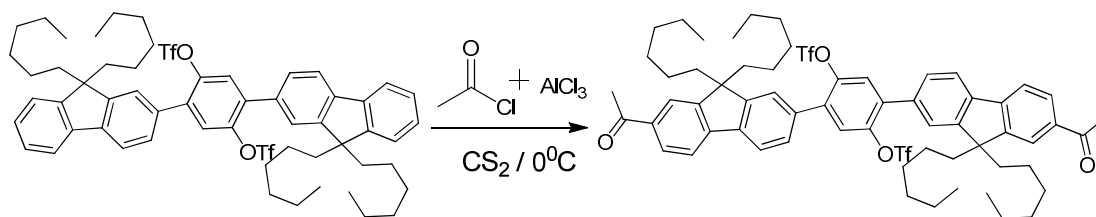
Synthesis of compound 14.



In a schlenk flask, under an argon atmosphere, compound 13 (2.28 g, 2.94 mmol) and pyridine (1.42 mL, 17.60 mmol) were dissolved in dry DCM (50 mL). The solution was cooled at $-10\text{ }^{\circ}\text{C}$ with ice acetone bath. In a dropping funnel, a solution of triflic anhydride (1.32 mL, 8.23 mmol) in DCM (10 mL) was taken and was added to the above cooled solution over 10 min under an argon atmosphere. The reaction mixture was stirred for 6 hr at $0\text{ }^{\circ}\text{C}$.

After completion, reaction mixture was concentrated in vacuum. Residual brown oil is diluted with ethyl acetate washed with 5% HCl and then saturated sodium bicarbonate and sodium chloride. Then dried over MgSO_4 and concentrated in vacuo to yield the product. Yield: 2.99 g, 90%; mp $68\text{-}70\text{ }^{\circ}\text{C}$ ^1H NMR $\delta(\text{CDCl}_3)$: 0.60-0.74 (m, 3H), 0.78 (t, 6H, $J = 13.59$), 1.0-1.20 (m, 13H), 2.04 (t, 4H, $J = 16.38$), 7.35-7.43 (m, 3H), 7.46-7.52 (m, 2H), 7.59 (s, 1H), 7.78 (d, 1H, $J = 6.27$), 7.85 (d, 1H, $J = 7.67$). ^{13}C NMR $\delta(\text{CDCl}_3)$: 14.15, 22.74, 23.92, 29.87, 31.69, 4.60, 55.60, 116.98, 120.17, 120.28, 120.40, 123.17, 123.95, 125.64, 127.13, 127.99, 128.31, 132.49, 136.87, 140.28, 142.48, 145.83, 151.37, 151.69.

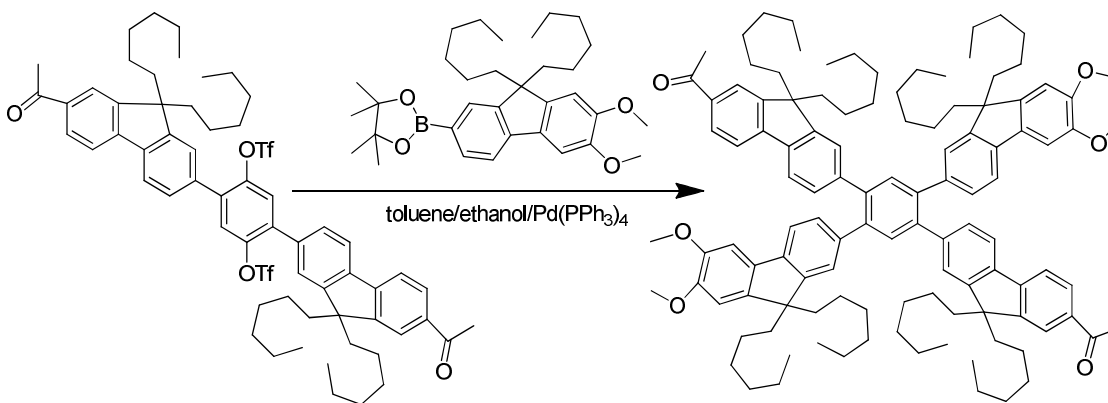
Synthesis of compound 15.



To a stirred solution of acetyl chloride (0.52 mL, 8.85 mmol) in 100 mL CS₂, AlCl₃ was added at 0 °C. After 15 min, compound 14 dissolved in CS₂ was added by dropping funnel over a period of 30 min. Then reaction mixture was refluxed on heating mantle for 36 hr.

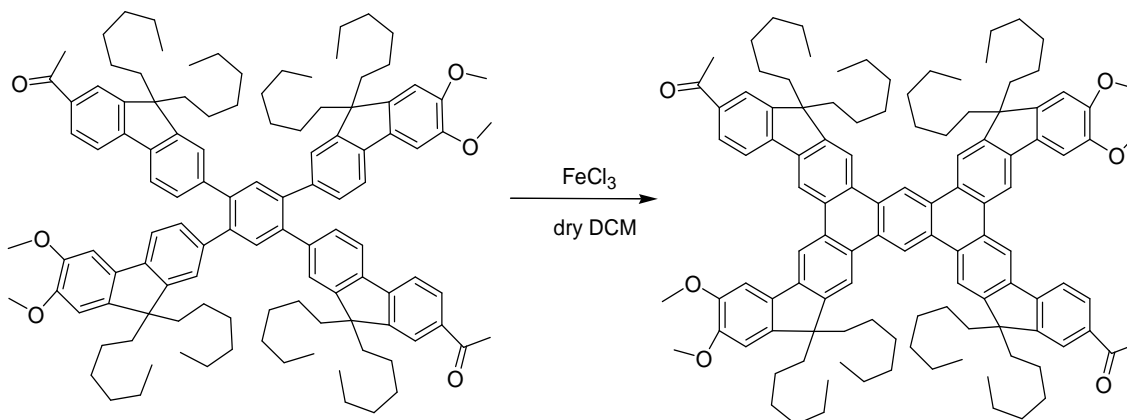
After completion, reaction mixture was cooled to 0 °C then quenched with 50 mL 1:1 HCl-water mixture, and extracted with DCM. Organic layer was washed with brine, and dried over MgSO₄, and concentrated in vacuo to yield the product. Yield: 1.28 g, 50%; mp 127-129 °C. ¹H NMR δ (CDCl₃): 0.54-0.689 (m, 4H), 0.75 (t, 6H, *J* = 14.30), 0.95-1.16 (m, 12H), 1.98-2.13 (m, 4H), 2.69 (s, 3H), 7.48-7.52 (m, 2H), 7.56 (s, 1H), 7.83 (d, 1H), 7.90 (d, 1H), 7.98-8.0 (m, 2H). ¹³C NMR (CDCl₃): 14.35, 22.87, 31.80, 122.15, 123.82, 125.91, 126.79, 126.81, 126.89, 127.56, 127.65, 127.75, 127.77, 128.54, 129.07, 129.18, 129.38, 129.41, 129.60, 129.66, 131.04, 131.07, 131.11, 131.33, 139.33, 141.28.

Synthesis of compound 17.



9, 9-Dihexyl-6, 7-dimethoxy-9H-fluorene boronic ester (0.71 g, 1.37 mmol) and acylated compound 16 (0.70 g, 0.623 mmol) were mixed in 30 mL toluene and ethanol under an argon atmosphere, followed by successive addition of a catalytic amount of Pd(PPh₃)₄ (100mg) and aqueous sodium carbonate solution (5 g in 20 mL water). The resulting mixture was degassed and refilled with argon and refluxed for 72 h. After completion, the reaction contents were cooled under an argon atmosphere, extracted with water and dichloromethane. The organic layer was then dried over magnesium sulfate and concentrated in vacuo to afford crude solid which was purified by silica column chromatography using 5 % ethyl acetate: hexane mixtures to afford 500 mg of the desired product as a white solid. Yield: 500 mg, 50%; mp 165-167 °C; ¹H NMR δ (CDCl₃): 0.36-0.61(m, 10H), 0.61-0.72 (t, 11H, *J* = 14.0), 0.76-1.09 (m, 23H), 1.47-1.94 (m, 8H), 2.57(s, 3H), 3.86 (d, 6H, *J* = 5.5), 6.69 (s, 1H), 7.06 (s, 1H), 7.12(s, 1H), 7.24 (s, 1H), 7.26 (s, 1H), 7.31(s, 1H), 7.40 (d, 1H, *J* = 8.28), 7.52 (d, 1H, *J* = 8.28), 7.56-7.65 (m, 2H), 7.80-7.89 (m, 2H).

Synthesis of compound 18.



To a solution of compound 17 (50 mg, 0.03 mmol) in 10 mL of dichloromethane was added FeCl₃ (0.050 g, 0.31 mmol) (10 equiv) under an argon atmosphere. The resulting mixture was stirred at for 3 hrs. The reaction was quenched by addition of dry methanol (10 mL). The reaction mixture was washed with water (40 mL) and the aqueous layer was extracted with dichloromethane (2 x 10 mL). The combined organic layers dried over anhydrous MgSO₄ and filtered through silica pad. Removal of the solvent in *vacuo* afforded the crude product which was purified by column chromatography and by repeated recrystallization. mp 165-167 °C; ¹H NMR δ (CDCl₃): 0.38-1.52 (m, 41H), 1.96-2.52 (m, 9H), 2.77 (s, 3H), 4.08 (s, 3H), 4.20 (s, 3H), 7.01 (s, 1H), 7.61 (s, 1H), 8.08-8.29 (m, 3H), 8.86 (s, 1H), 8.93 (s, 1H), 9.00 (s, 1H), 9.23 (s, 1H), 10.00 (s, 1H). ¹³C NMR (CDCl₃): 14.15, 14.19, 22.73, 27.19, 29.92, 29.96, 55.35, 55.69, 56.55, 128.41, 128.68, 129.93, 129.49, 130.14, 130.60, 130.68, 133.10, 136.60, 139.99, 142.06, 145.98, 149.11, 150.16, 150.66, 150.91, 198.42.

Crystal structure of compound 17.

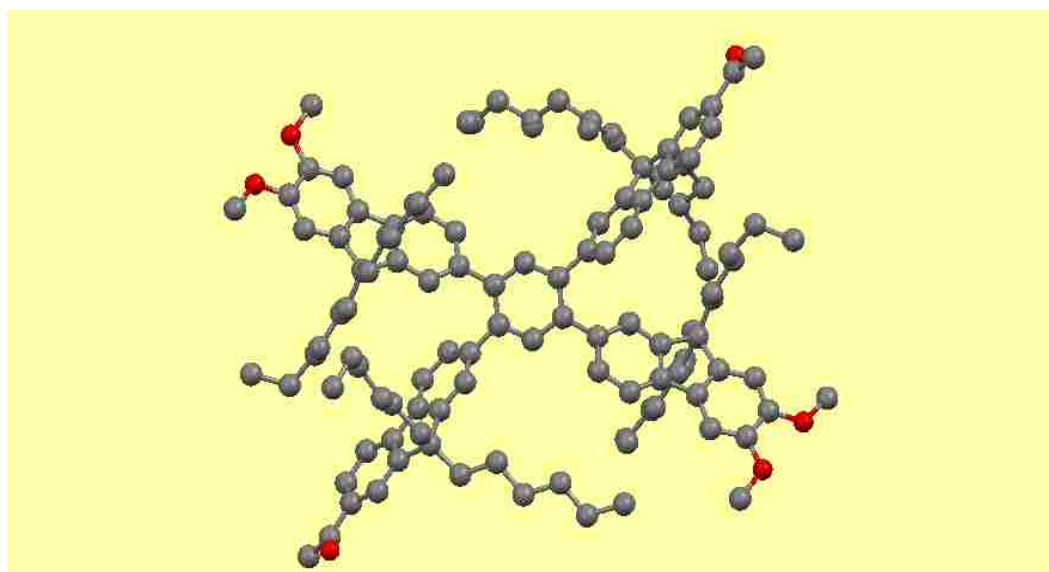
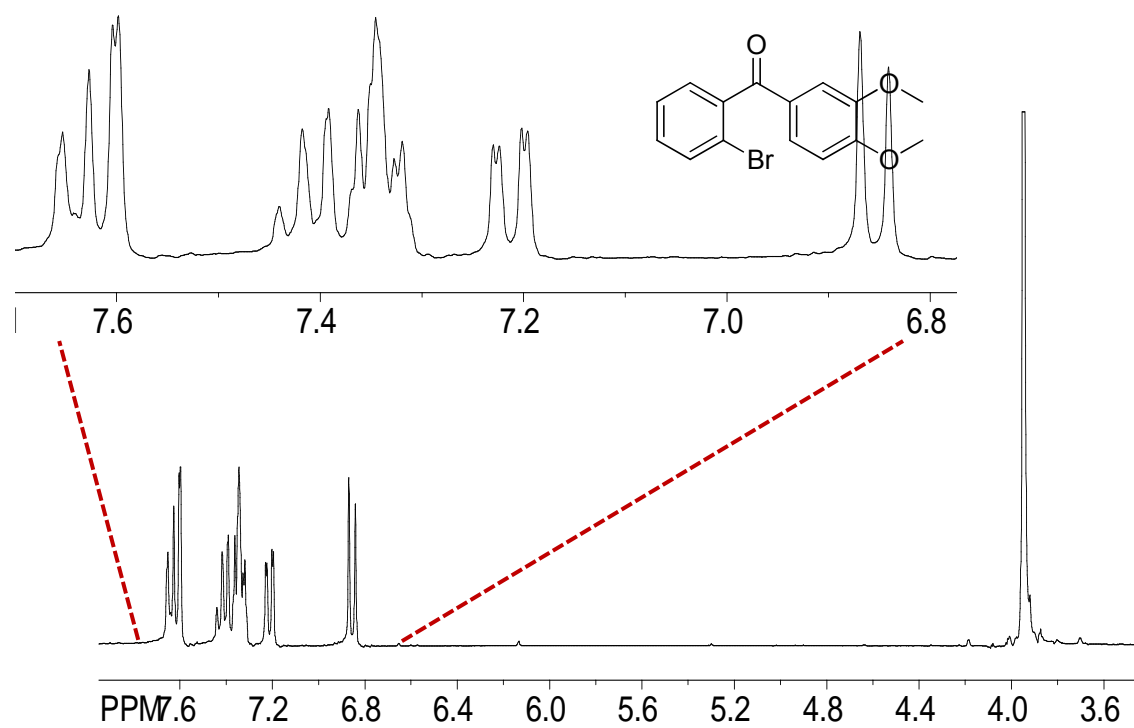


Table 2: Crystal data and structure refinement for raj20k

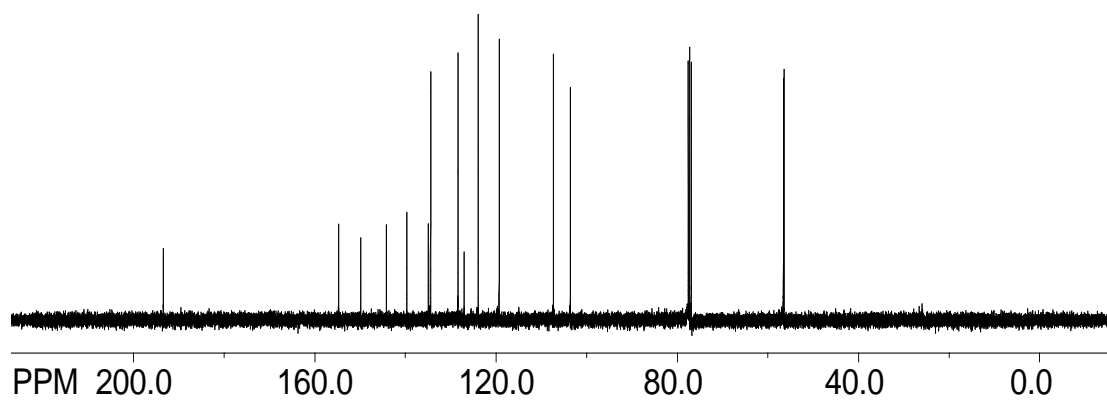
Identification code	raj20k
Empirical formula	$C_{117.48773}H_{155.96722}Cl_{3.9837}O_{7.49588}$
Formula weight	1829.40
Temperature \square/\square K	100.0
Crystal system	triclinic
Space group	P-1
$a/\square\text{\AA}$, $b/\square\text{\AA}$, $c/\square\text{\AA}$	15.6209(4), 18.3883(4), 21.6244(5)
$\alpha/^\circ$, $\beta/^\circ$, $\gamma/^\circ$	68.290(2), 69.329(2), 75.579(2)
Volume $\square/\square\text{\AA}^3$	5349.0(2)

Z	2
ρ_{calc} / mg mm^{-3}	1.136
μ / mm^{-1}	1.413
F(000)	1977
Crystal size / mm^3	$0.23 \times 0.12 \times 0.03$
Theta range for data collection	3.38 to 147.62°
Index ranges	$-19 \leq h \leq 19$, $-22 \leq k \leq 22$, $-26 \leq l \leq 24$
Reflections collected	57996
Independent reflections	21096[R(int) = 0.0305]
Data/restraints/parameters	21096/28/1242
Goodness-of-fit on F^2	1.039
Final R indexes [$I > 2\sigma(I)$]	$R_1 = 0.0782$, $wR_2 = 0.2226$
Final R indexes [all data]	$R_1 = 0.0957$, $wR_2 = 0.2420$
Largest diff. peak/hole / $e \text{ \AA}^{-3}$	1.869/-0.485

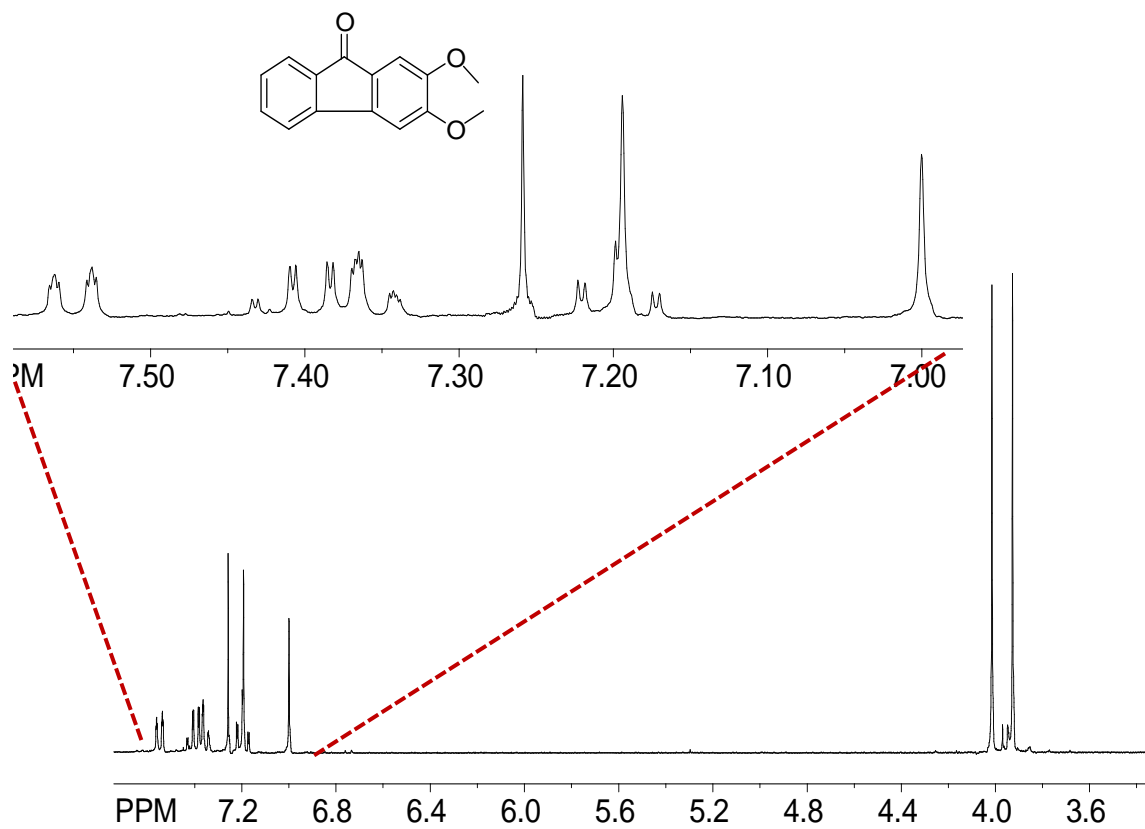
^1H NMR spectrum of (2-Bromo-phenyl)-(3,4-dimethoxy-phenyl)-methanone (2).



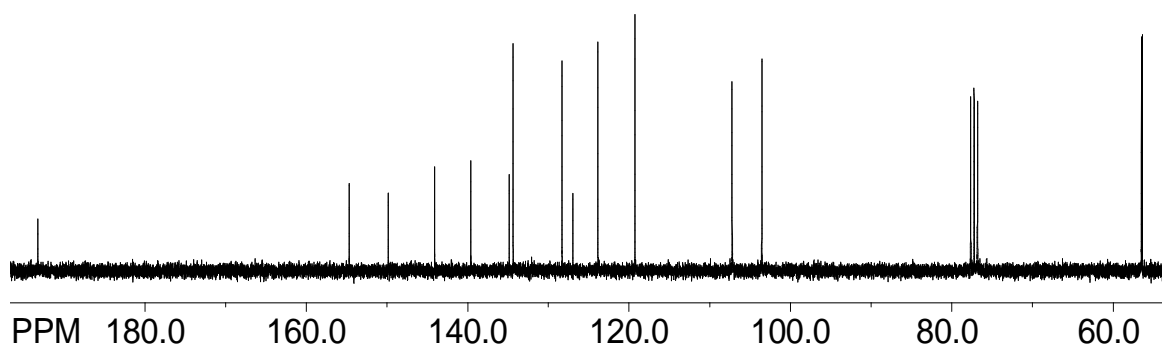
^{13}C NMR spectrum of (2-Bromo-phenyl)-(3,4-dimethoxy-phenyl)-methanone (2).



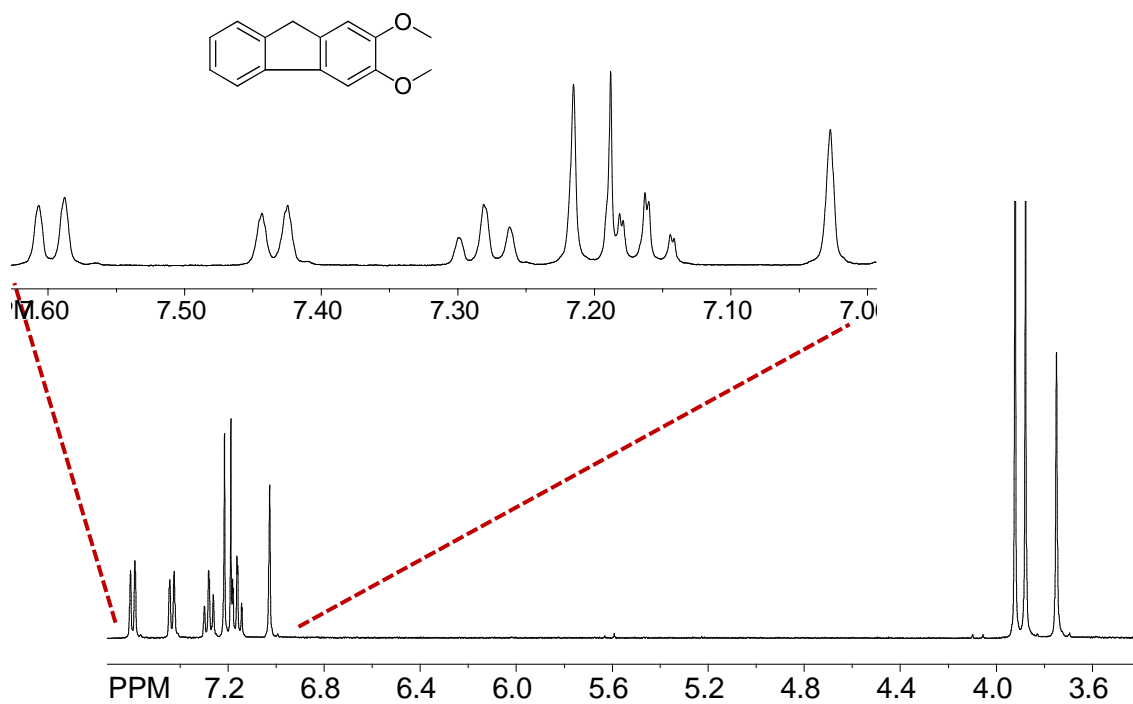
^1H NMR spectrum 2, 3-Dimethoxy-fluoren-9-one (3).



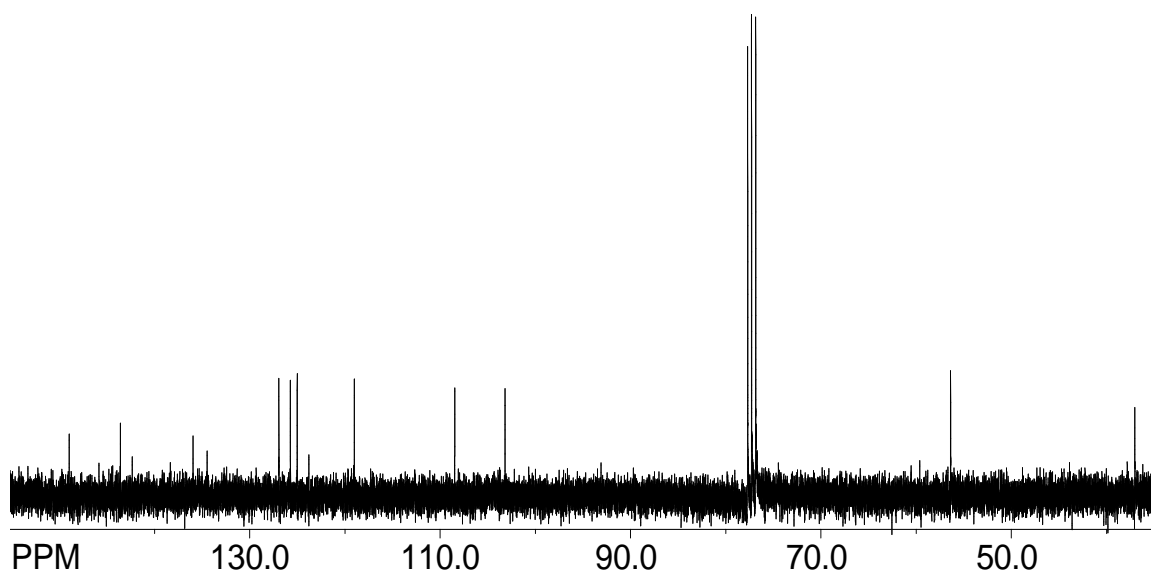
^{13}C NMR spectrum 2, 3-Dimethoxy-fluoren-9-one (3).



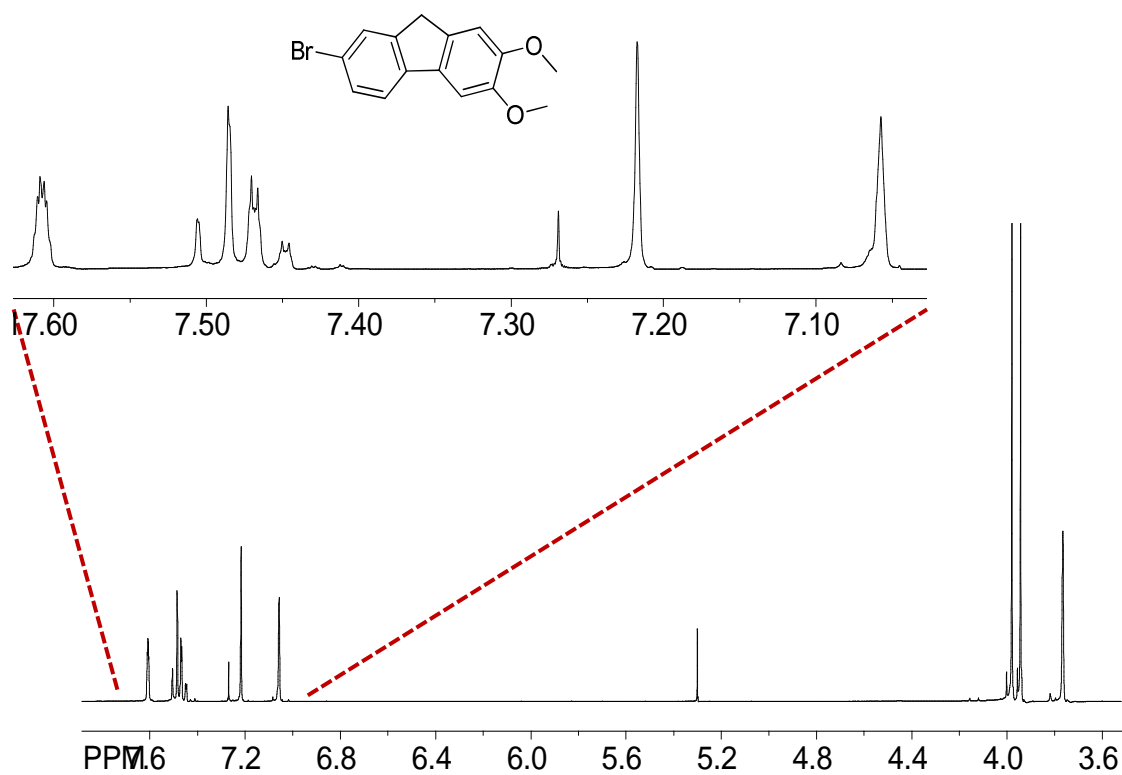
^1H NMR spectrum of 2, 3-Dimethoxy-9H-fluorene (4).



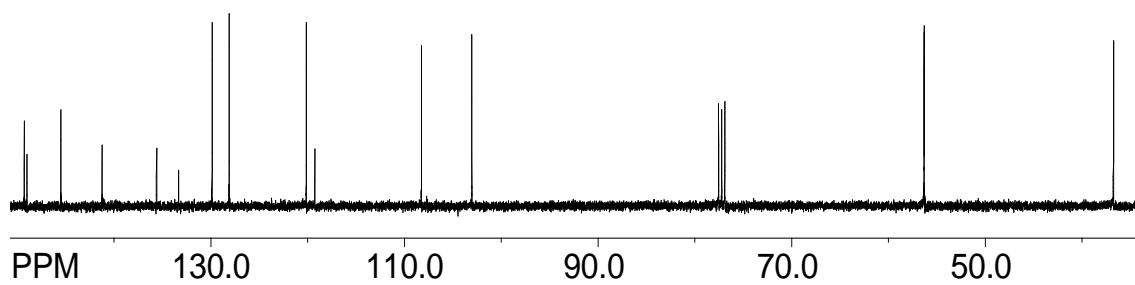
^{13}C NMR spectrum of 2, 3-Dimethoxy-9H-fluorene (4).



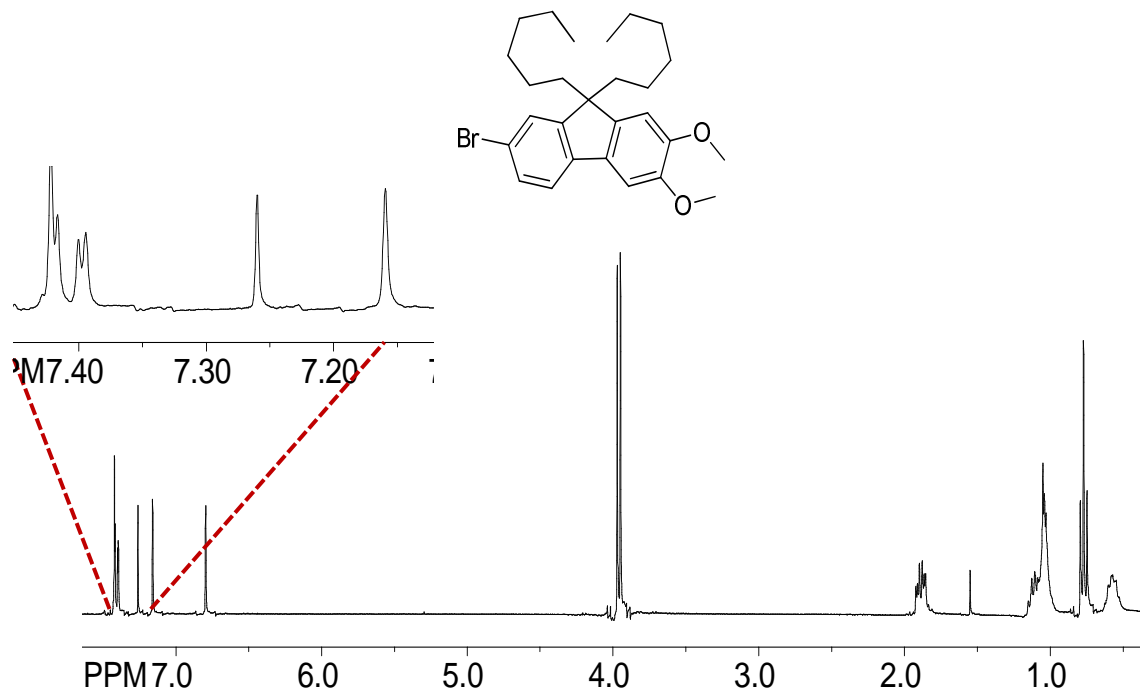
^1H NMR spectrum of 7-Bromo-2,3-dimethoxy-9H-fluorene (5).



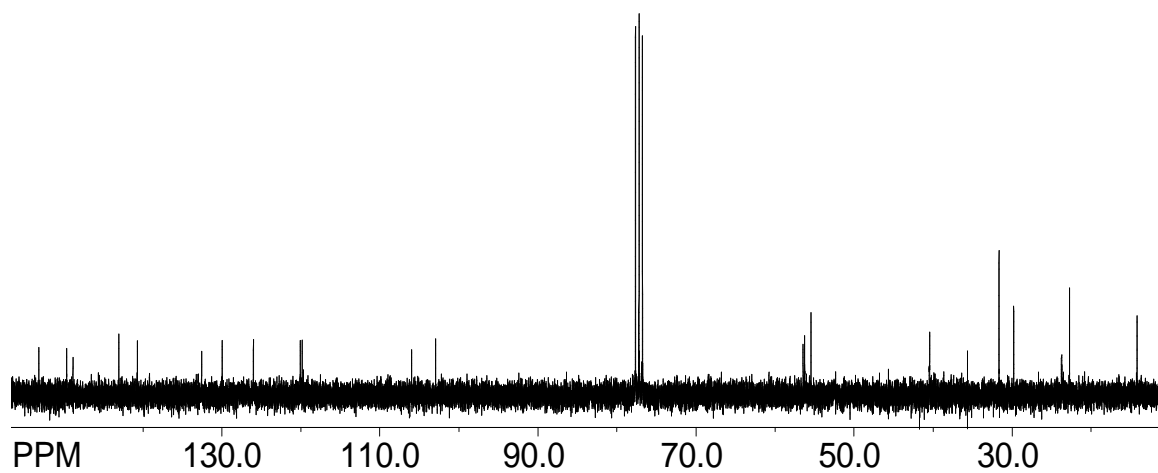
^{13}C NMR spectrum of 7-Bromo-2,3-dimethoxy-9H-fluorene (5).



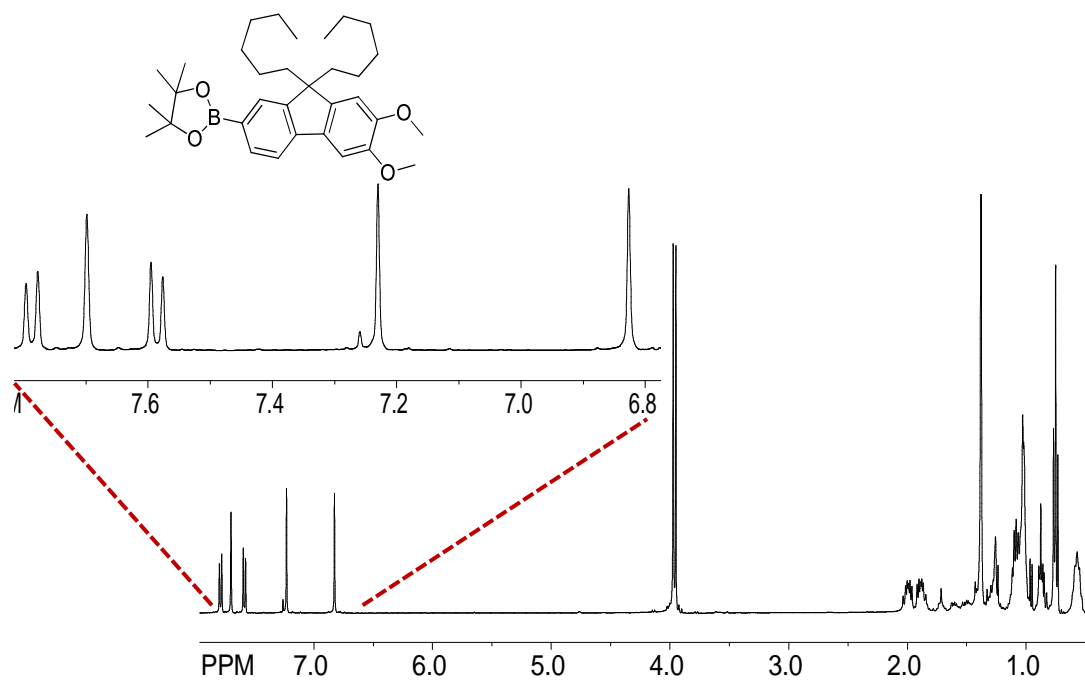
^1H NMR spectrum of 7-Bromo-9,9-dihexyl-2,3-dimethoxy-9H-fluorene (6).



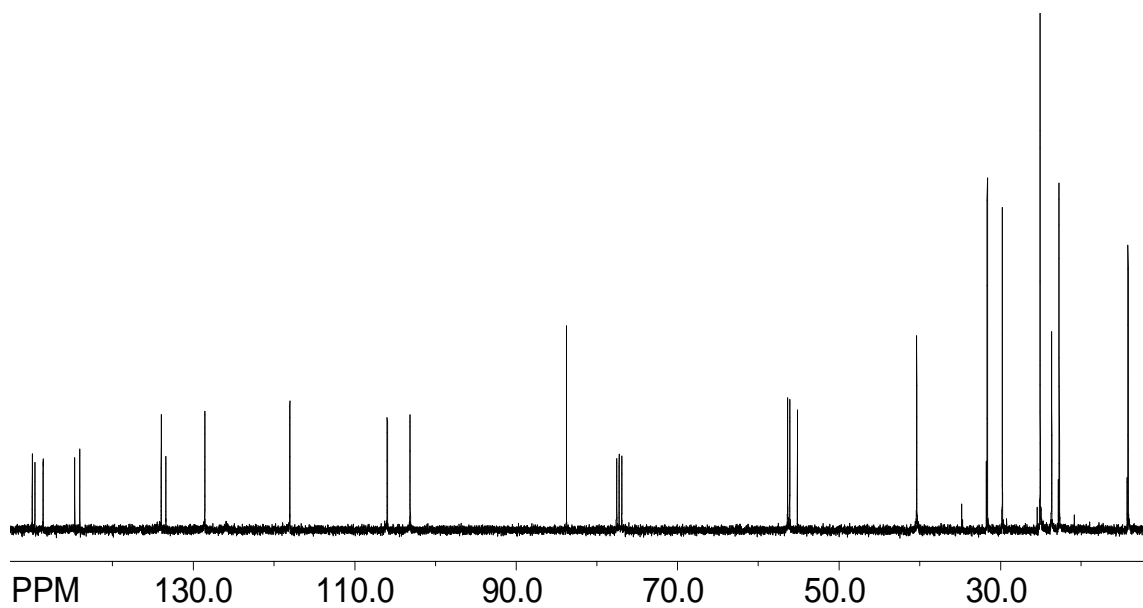
^{13}C NMR spectrum of 7-Bromo-9,9-dihexyl-2,3-dimethoxy-9H-fluorene (6).



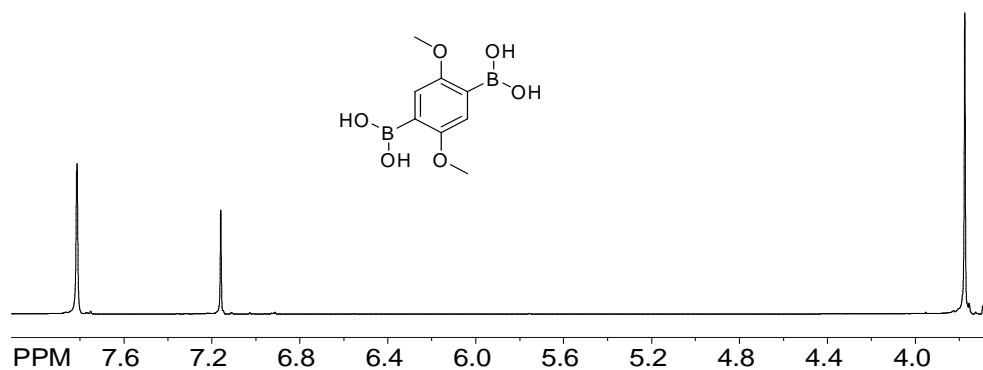
^1H NMR spectrum of (9, 9-Dihexyl-6, 7-dimethoxy-9H-fluorene boronic ester) (8).



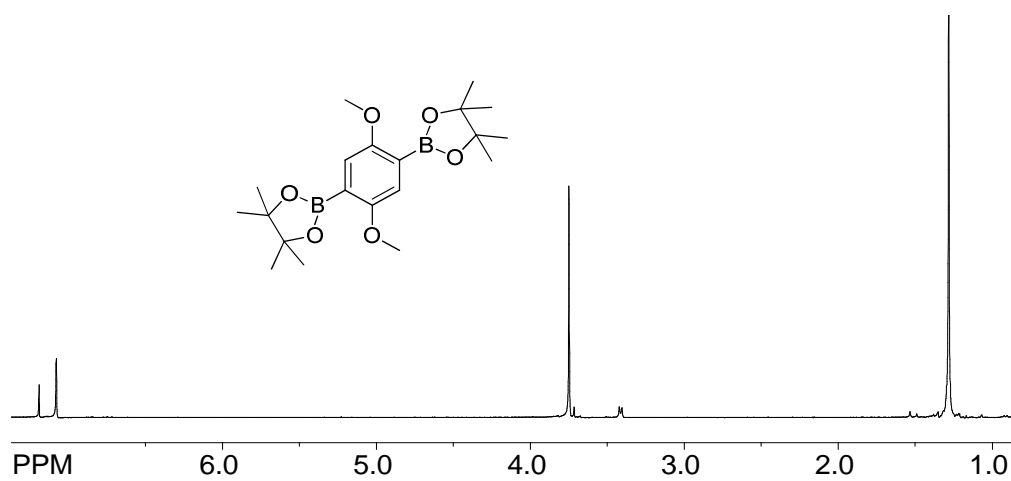
^{13}C NMR spectrum of (9, 9-Dihexyl-6, 7-dimethoxy-9H-fluorene boronic ester) (8).



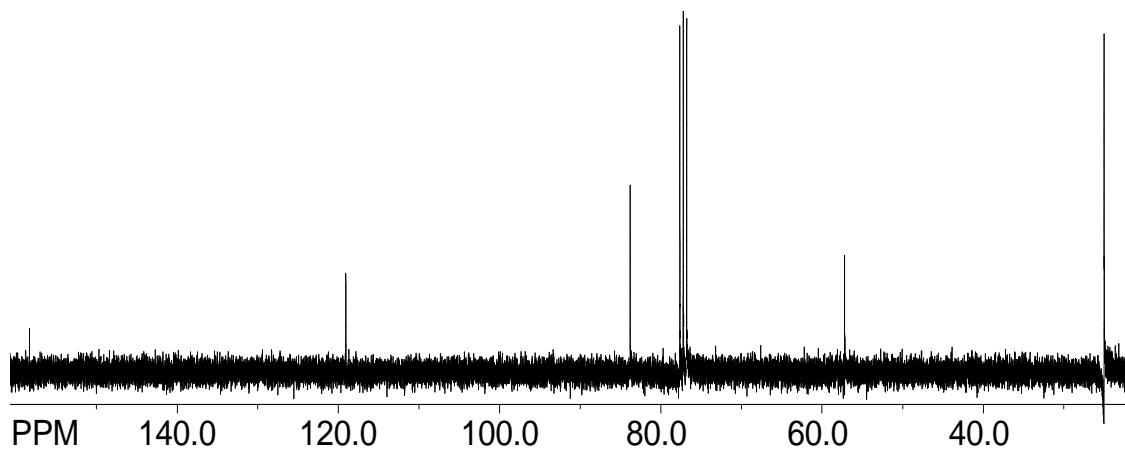
^1H NMR spectrum of boronic acid of dibromo dimethoxy Benjene (10).



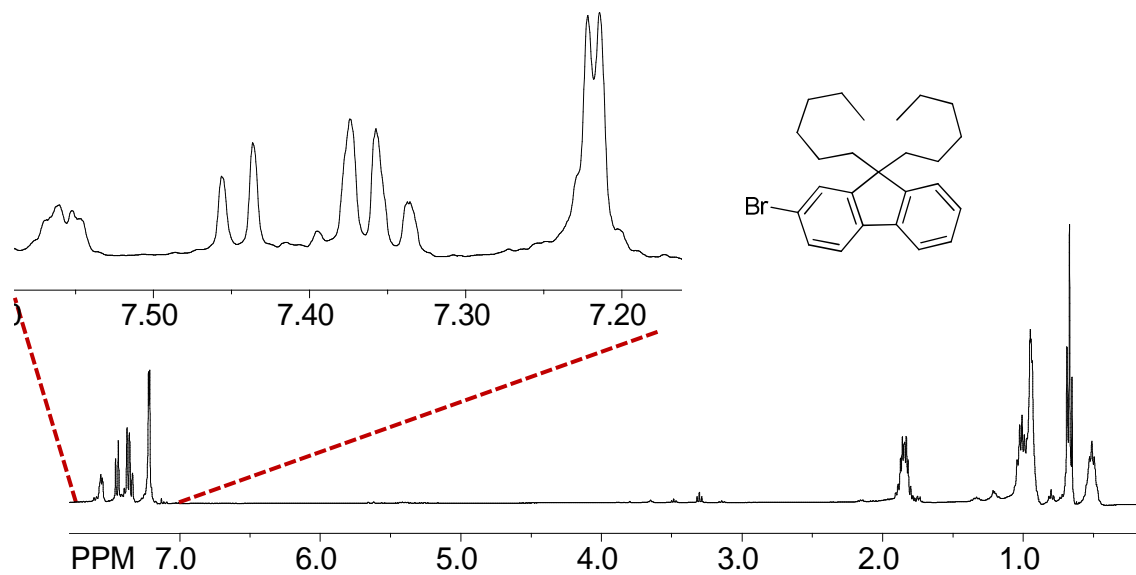
^1H NMR spectrum of boronic ester of dibromo dimethoxy Benjene (11).



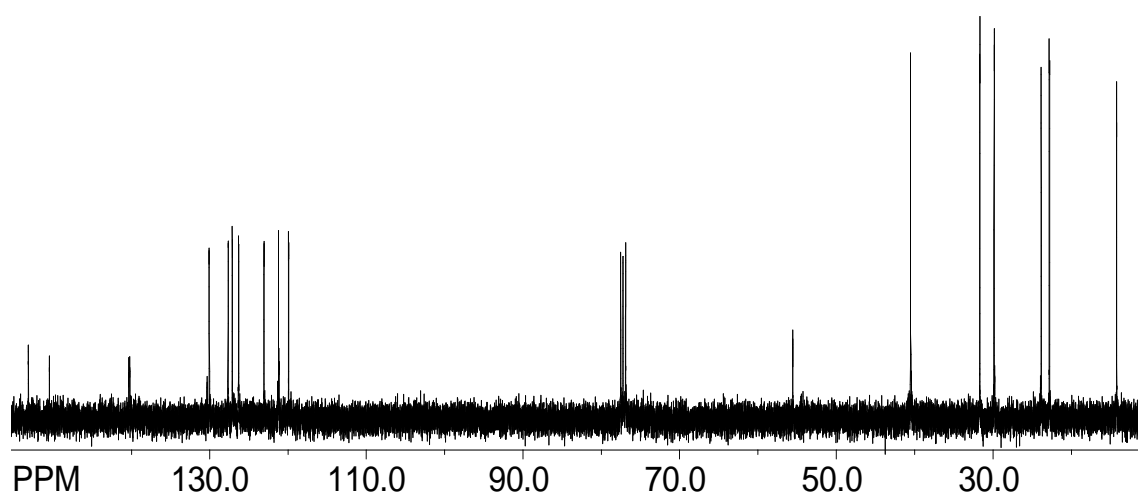
^{13}C NMR spectrum of boronic ester of dibromo dimethoxy Benjene (11).



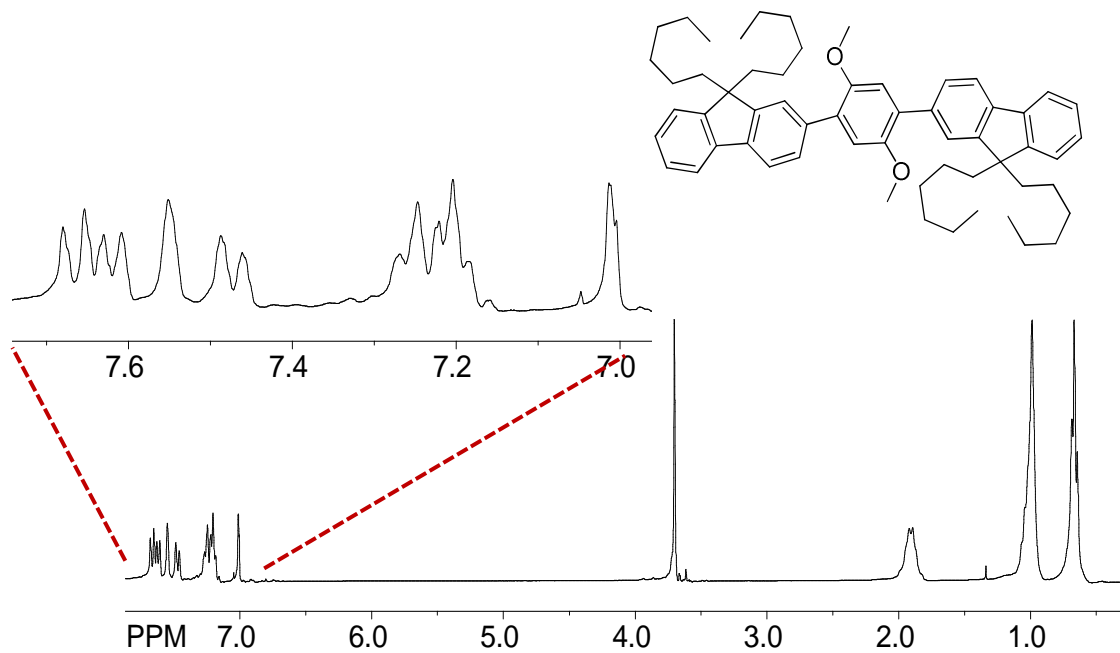
^1H NMR spectrum of 2-Bromo-9,9-dihexyl-9H-fluorene.



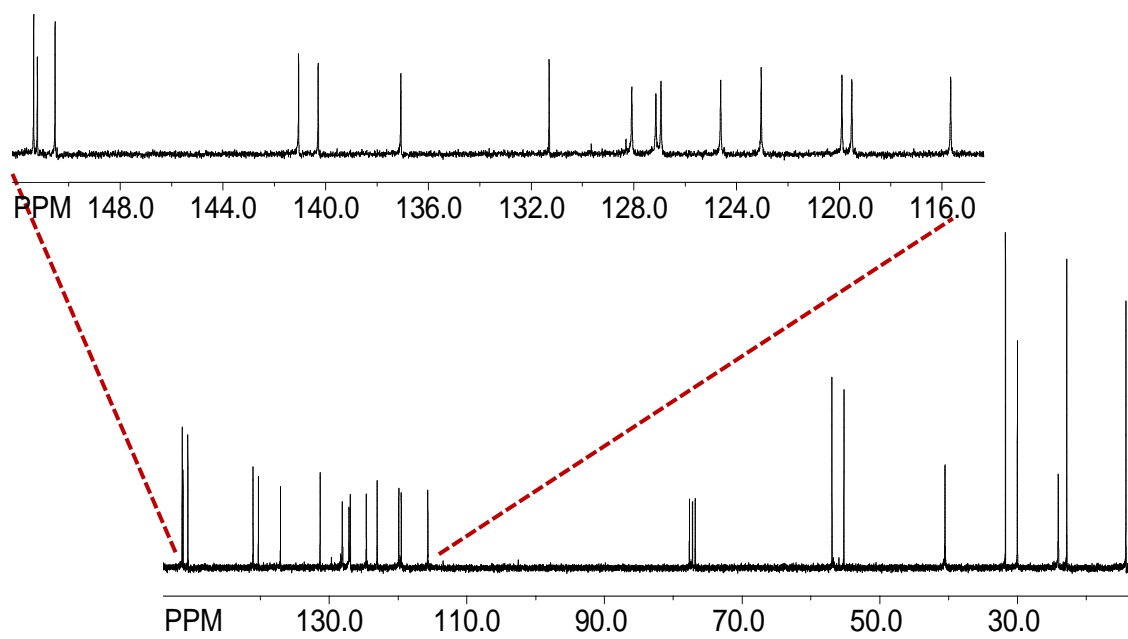
^{13}C NMR spectrum of 2-Bromo-9,9-dihexyl-9H-fluorene.



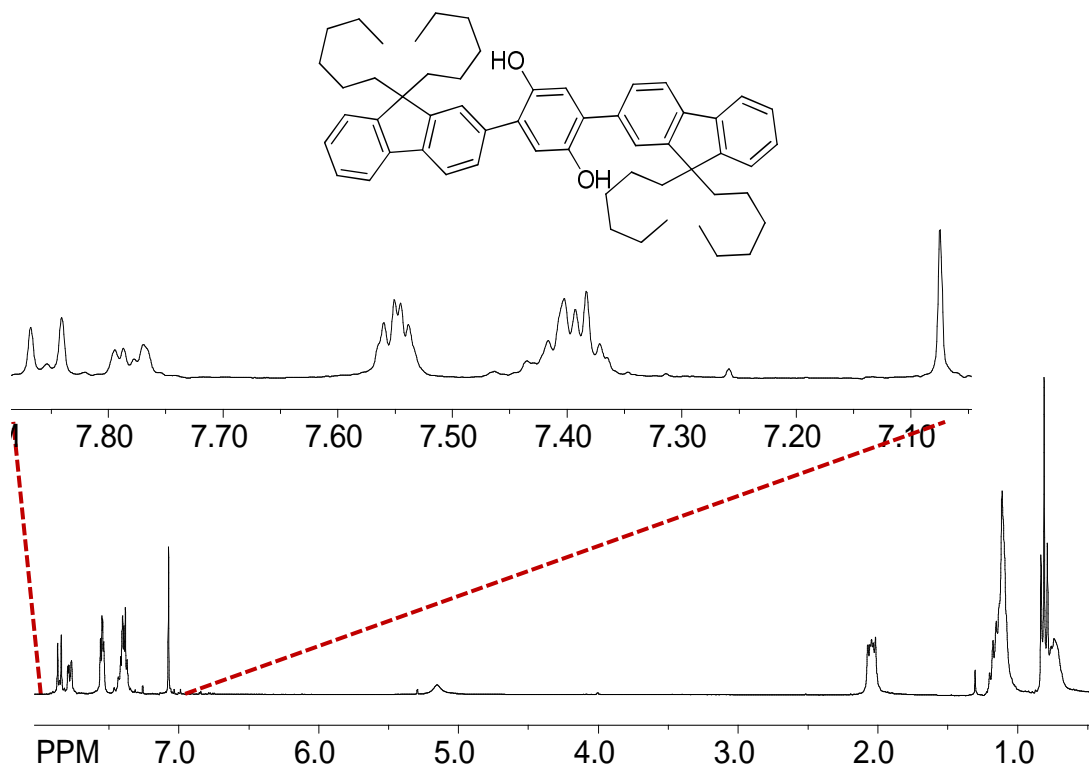
^1H NMR spectrum of compound 12.



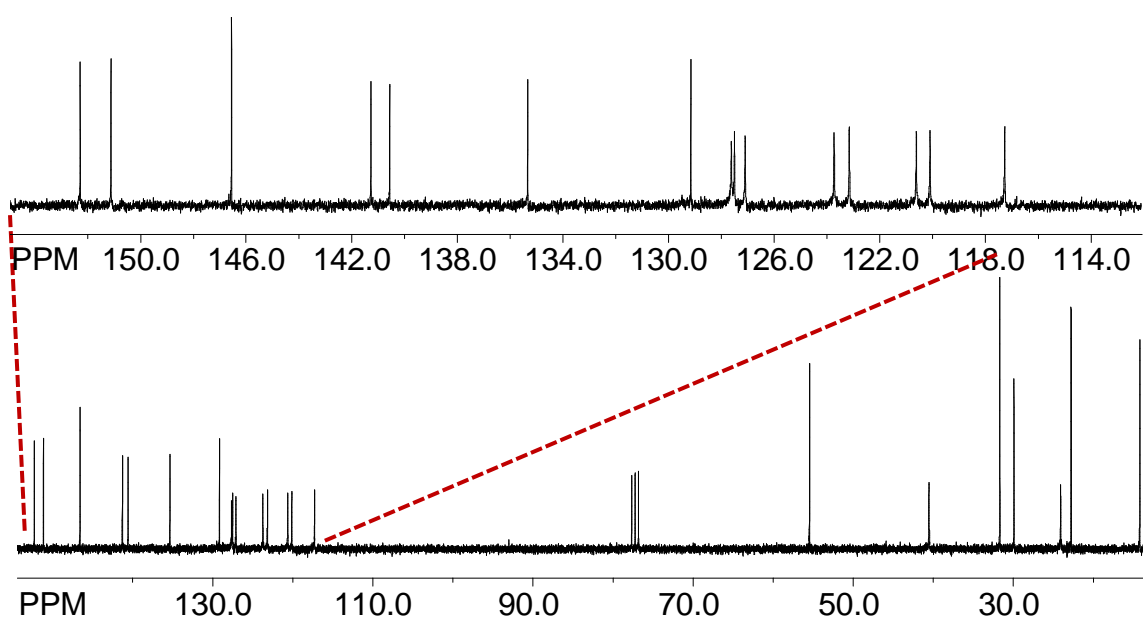
^{13}C NMR spectrum of compound 12.



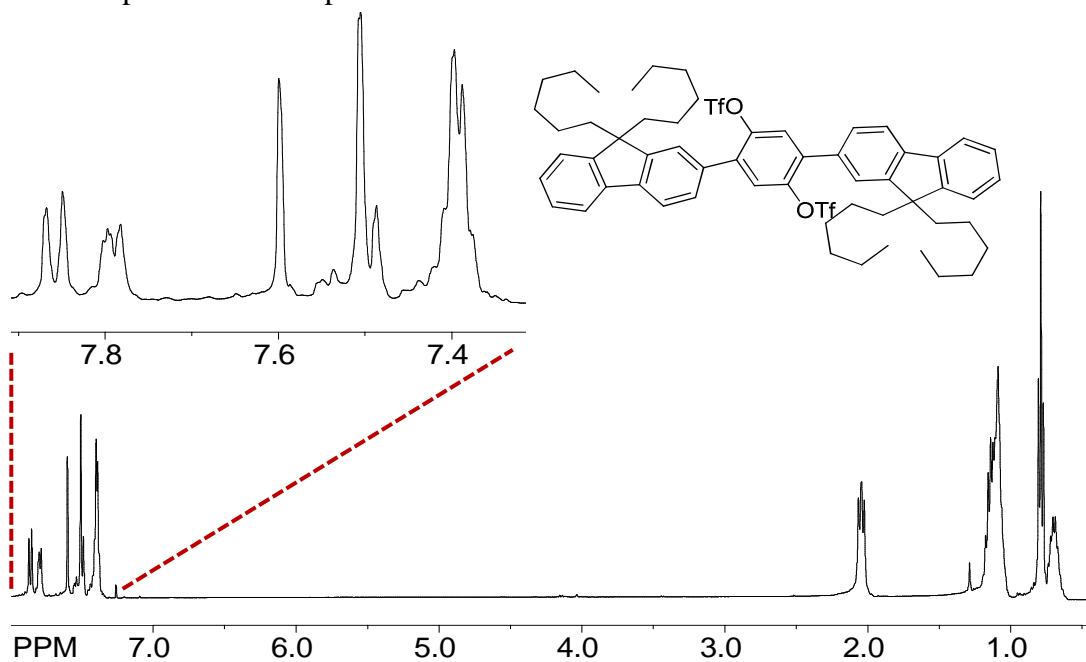
^1H NMR spectrum of compound 13.



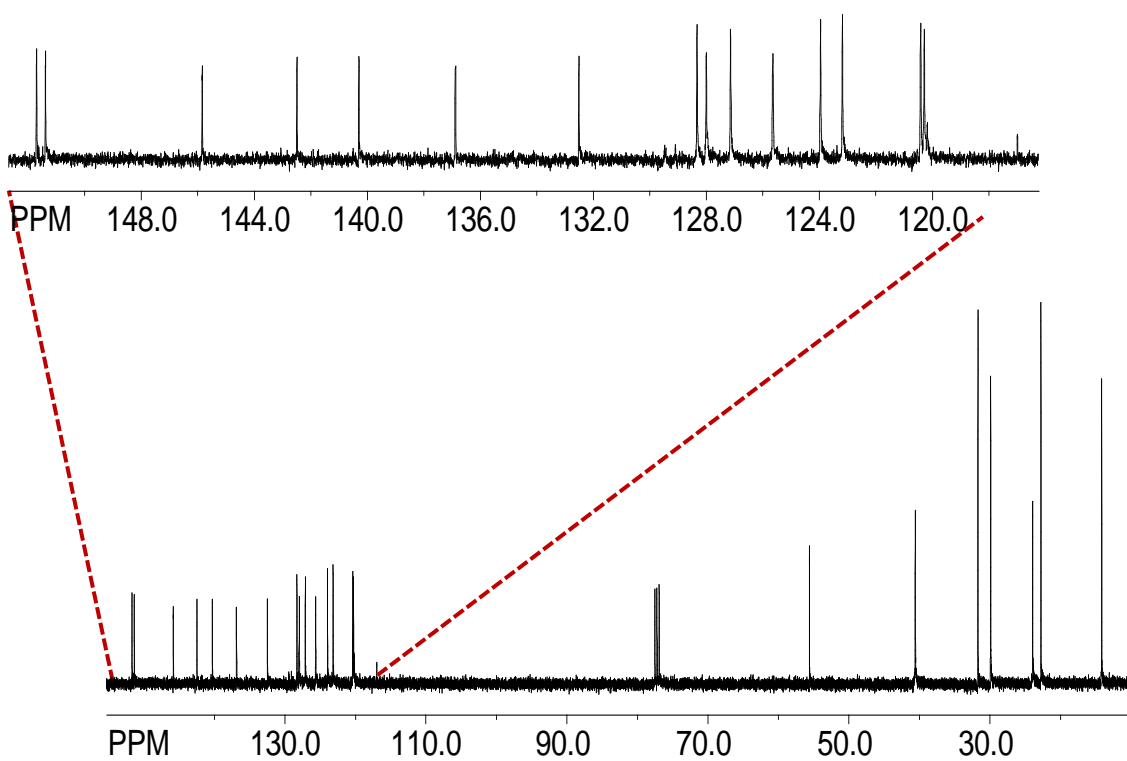
^{13}C NMR spectrum of compound 13.



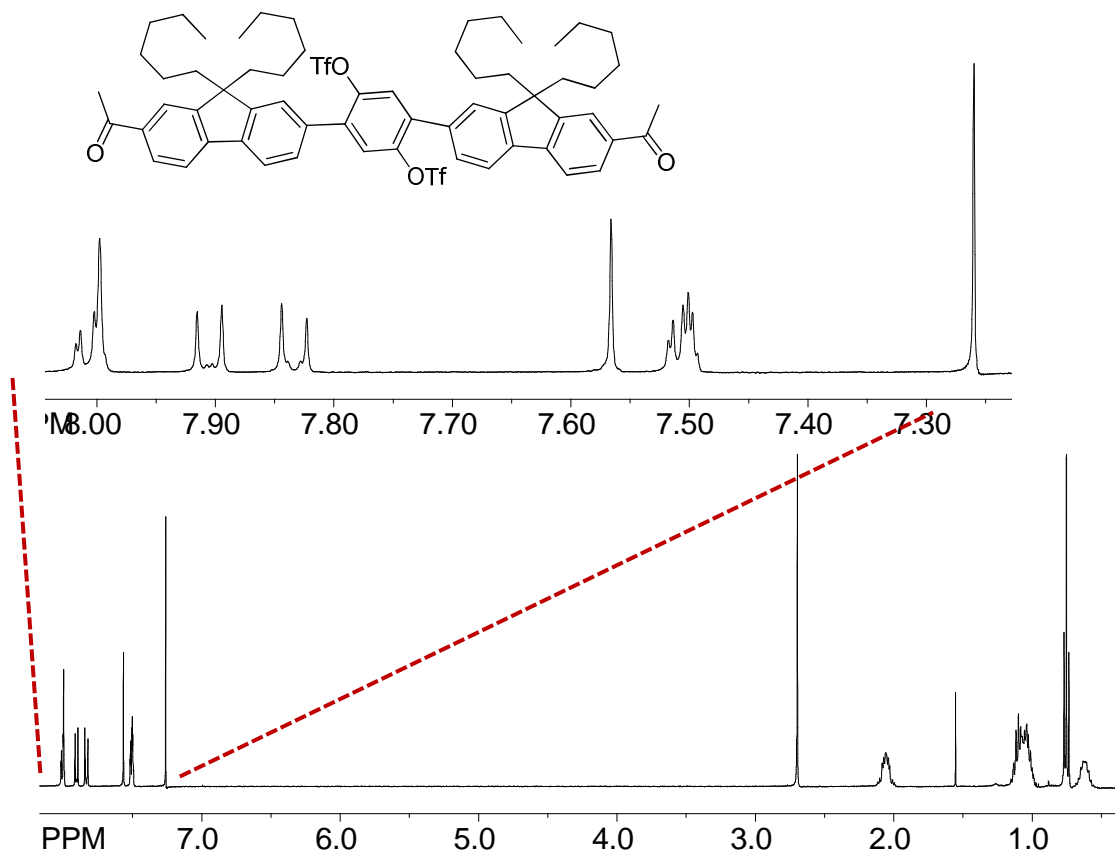
^1H NMR spectrum of compound 14.



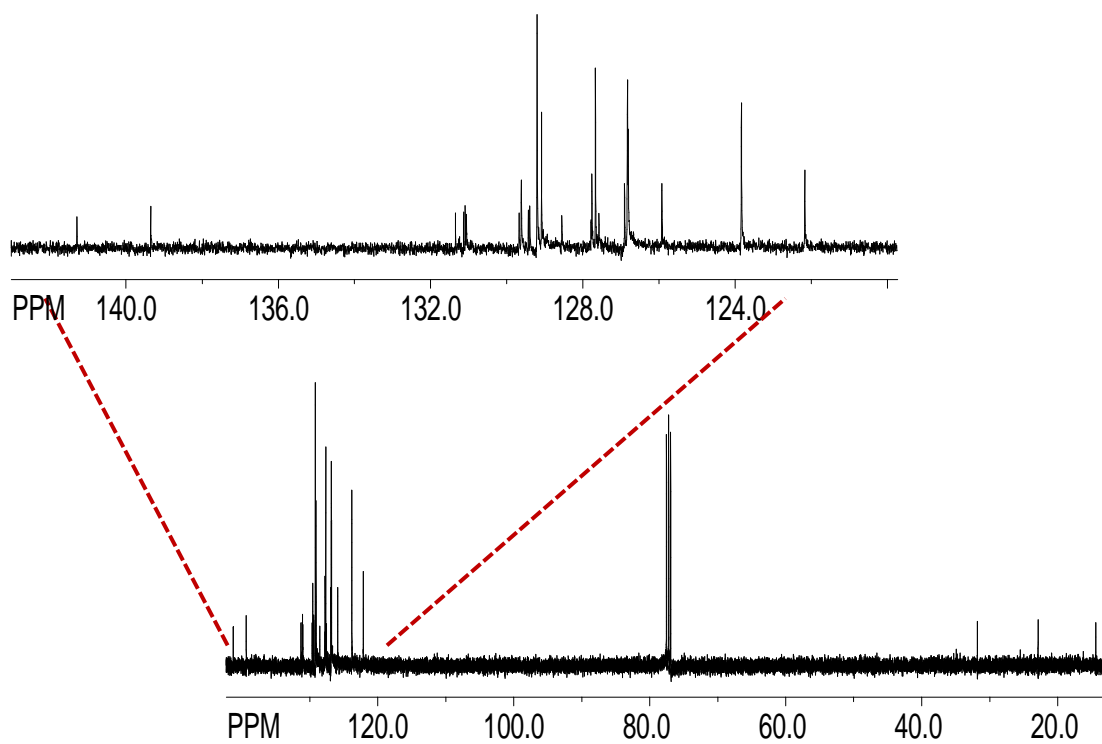
^{13}C NMR spectrum of compound 14.



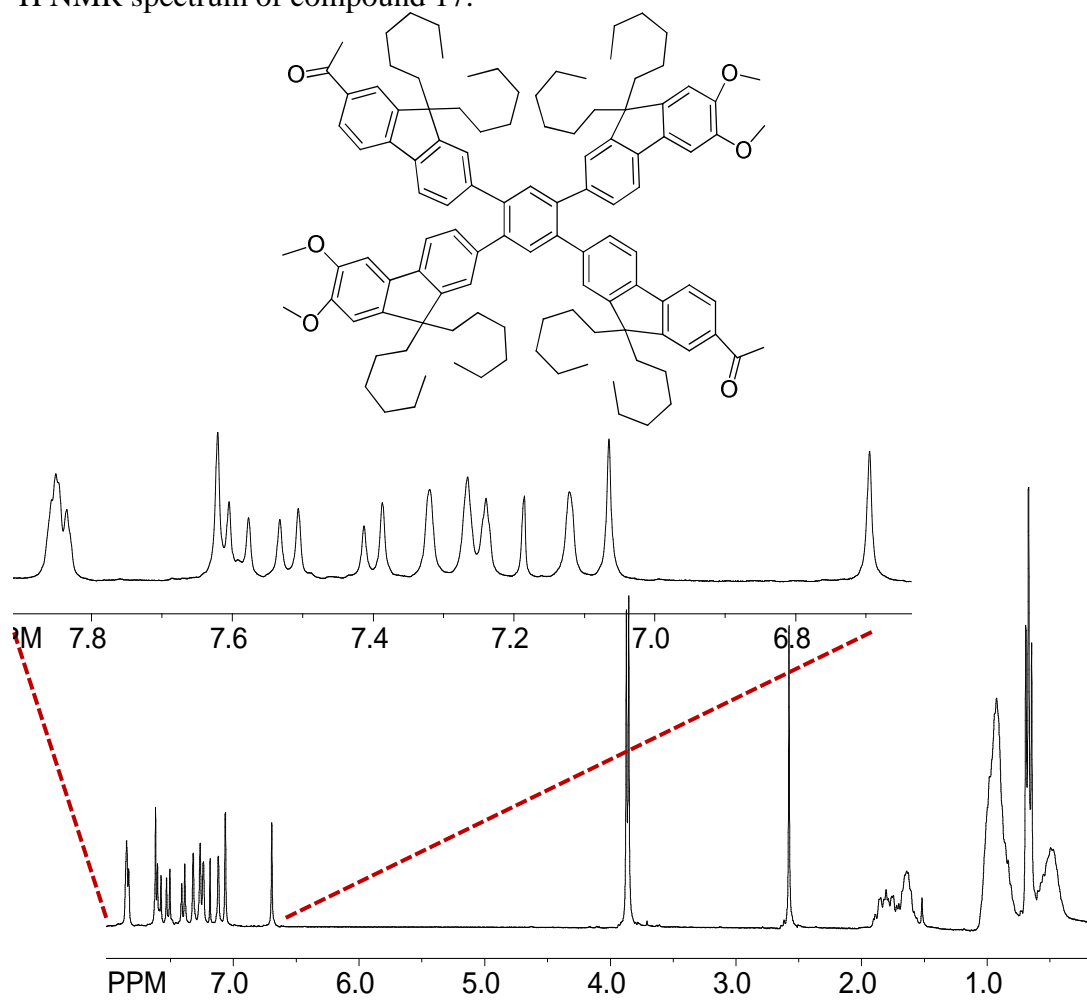
^1H NMR spectrum of compound 15.



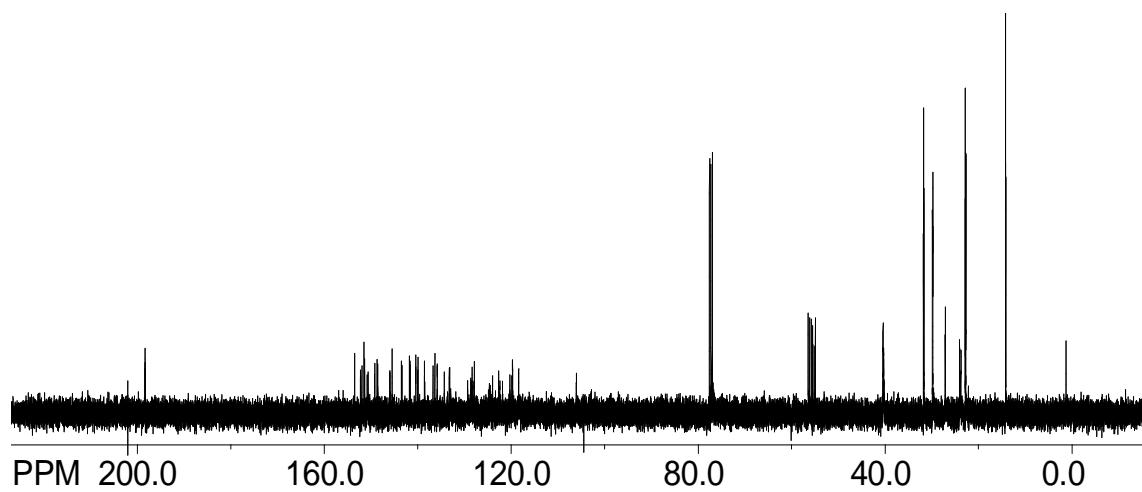
^{13}C NMR spectrum of compound 15.



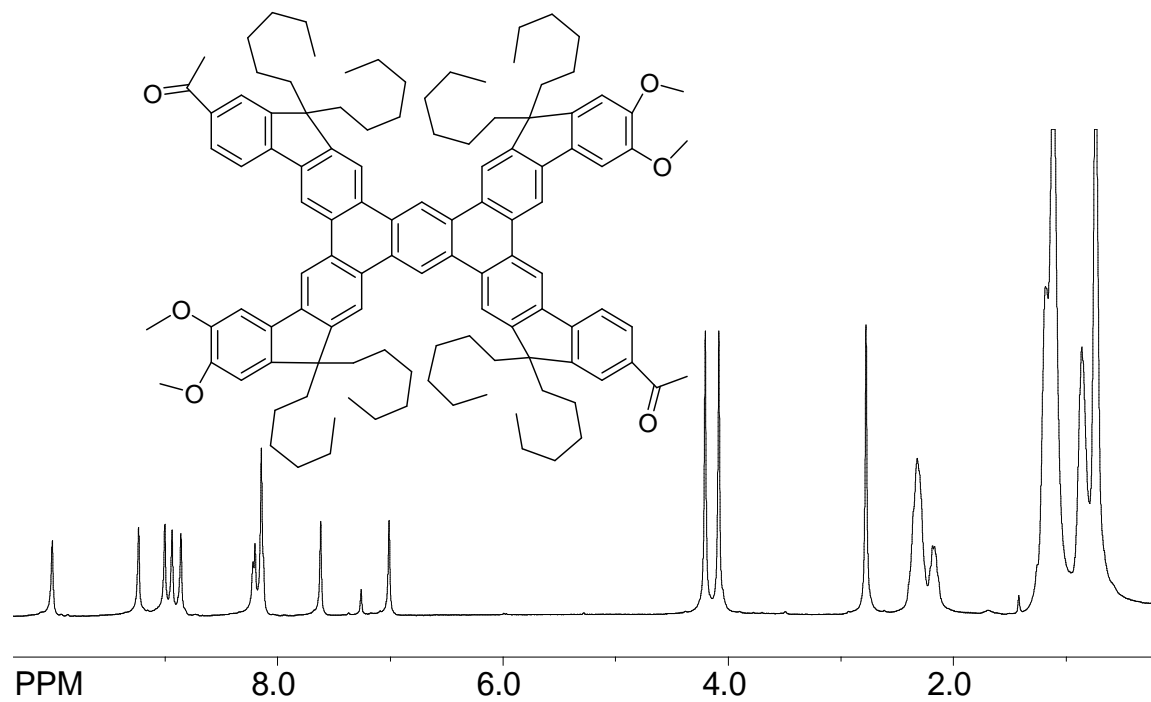
^1H NMR spectrum of compound 17.



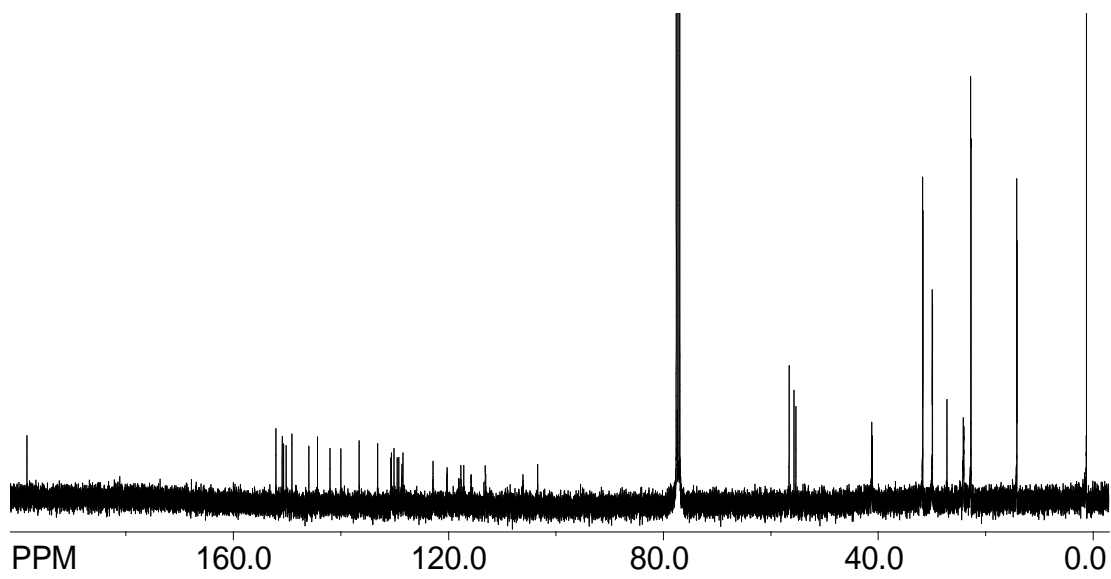
^{13}C NMR spectrum of compound 17.



^1H NMR spectrum of compound 18.



^{13}C NMR spectrum of compound 18.



Chapter-2

Synthesis and Photophysical Properties of Ruthenium and Rhenium Metal Complexes of Fluorene Based Bipyridine ligands

Introduction

Background: Ruthenium polypyridyl complexes have been explored greatly due to their unique combination of luminescence and redox properties.¹⁻² Ru(II)polypyridyl complexes have also contributed greatly to the progress of supramolecular photochemistry, and in particular to photoinduced electron and energy transfer processes within supramolecular assemblies, including luminescent poly-nuclear metal complexes, light active dendrimers, photoinduced charge separation devices.³

In these complexes luminescence is from a metal-to-ligand charge transfer (MLCT) state,⁸ so it is likely to alter the excited state properties such as luminescence wavelength, lifetime, and quantum yield by varying the ligand features. The long lived metal-to-ligand-charge transfer (MLCT) excited states characterizing some transition metal complexes such as tris (2,2'-bipyridine)ruthenium(II) have been widely exploited to design molecular architectures featuring photoinduced electron and energy transfer processes. Numerous studies correlated well the dependence of absorption and luminescence properties to delocalization on the acceptor ligand.

The possibility of combining several ligands with a large range of transition metal ions has made metal-ligand coordination an important method in the field of supramolecular chemistry.⁴⁻⁷ From the large range of transition metal ions, ruthenium(II) represents one of the most favorable ions in synthesizing robust coordination assemblies, because it allows the direct synthesis of both heteroleptic as well as homoleptic systems

Polypyridyl ligands with extended polyaromatic chains have been found to exhibit prolonged excited states. In this context, benzene, anthracene, and pyrene containing polypyridyl complexes were studied with favorable outcome.⁹⁻¹²

The interest in $[\text{Ru}(\text{bpy})_3]^{2+}$ photochemistry arose from its long lived excited states, and bipyridine ligands with extended polyaromatic chains that display more extended excited states. For example, Valenti,¹³ Uno¹⁴ and Mullen¹⁵ have recently synthesized a Ru(bpy)-based complex surrounded by extended polyphenylbenzene chains (see, Figure 1).

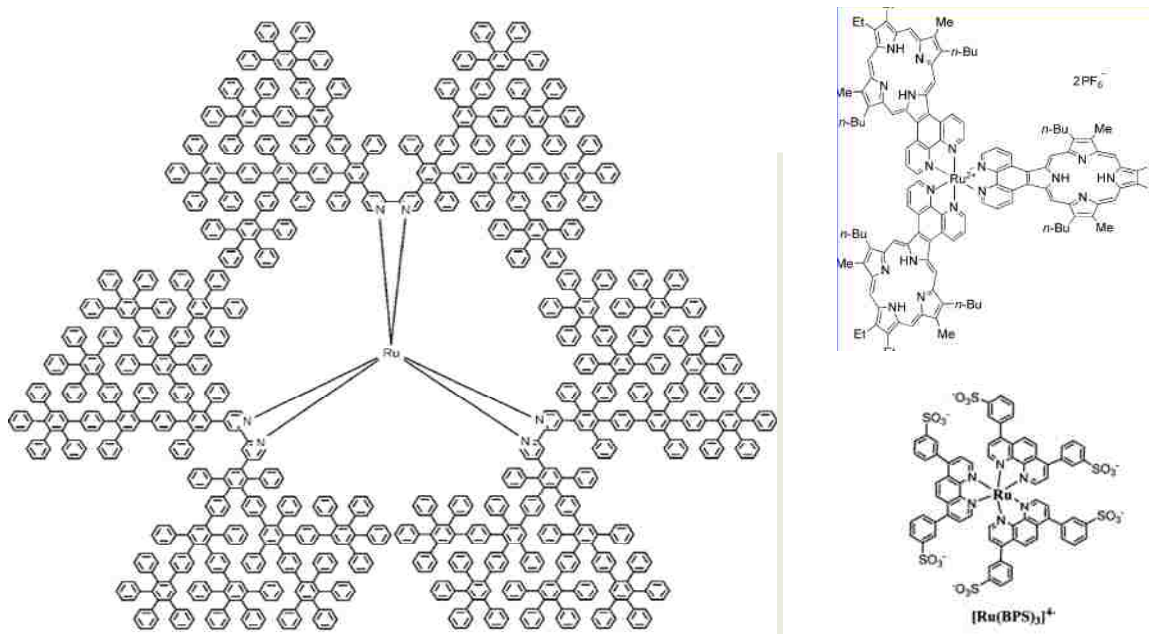


Figure 1. Representative examples of reported Ru (II) –complexes

Fluorene and its derivatives are increasingly used as a constituent in a variety of materials for electro-optic applications due to their strong luminescence, charge delocalization, and thermal stability. Fluorene is a tricyclic aromatic hydrocarbon which

has been extensively utilized for the preparation of a variety of electro-active materials⁶ including the cofacially stacked polyfluorenes¹⁶ (see, Figure 2).

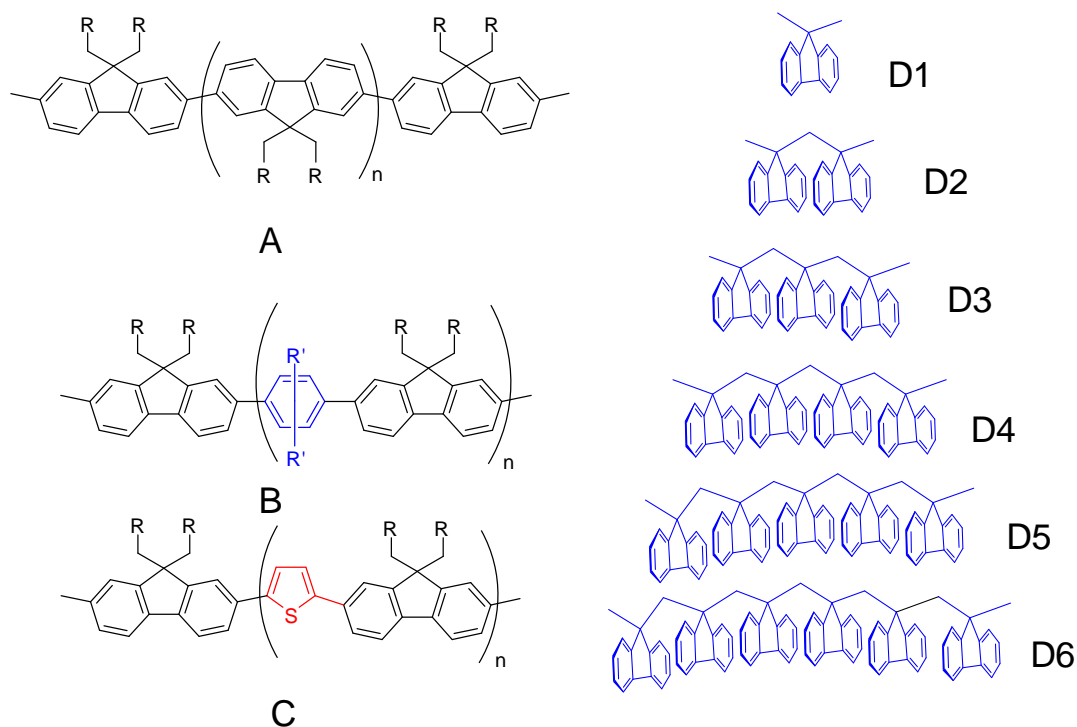


Figure 2. Representative examples of electro-active materials obtained using fluorene framework.^{16,17}

Problem statement: The unique properties of stacked polyfluorenes led us to synthesize stacked polyfluorene-containing bipyridine ligands and their complexes with ruthenium and rhenium metal and to study their photophysical and electrochemical properties. It is surmised that the properties of Ru^{+2} complexes, surrounded by multiple stacked polyfluorene containing ligands, should alter significantly, in comparison to the appropriate model compounds, if there is significant electronic coupling amongst the

polyfluorenes and bipyridine ligand. Accordingly, the synthesis of two such complexes shown in Figure 3 was initiated.

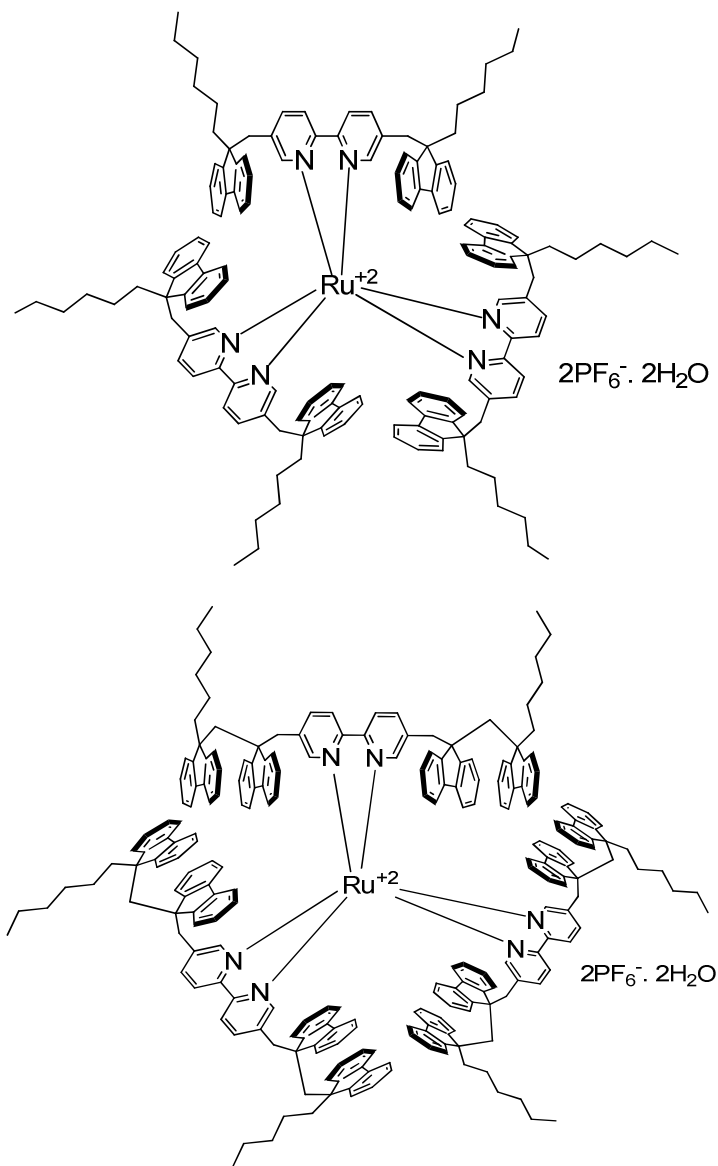
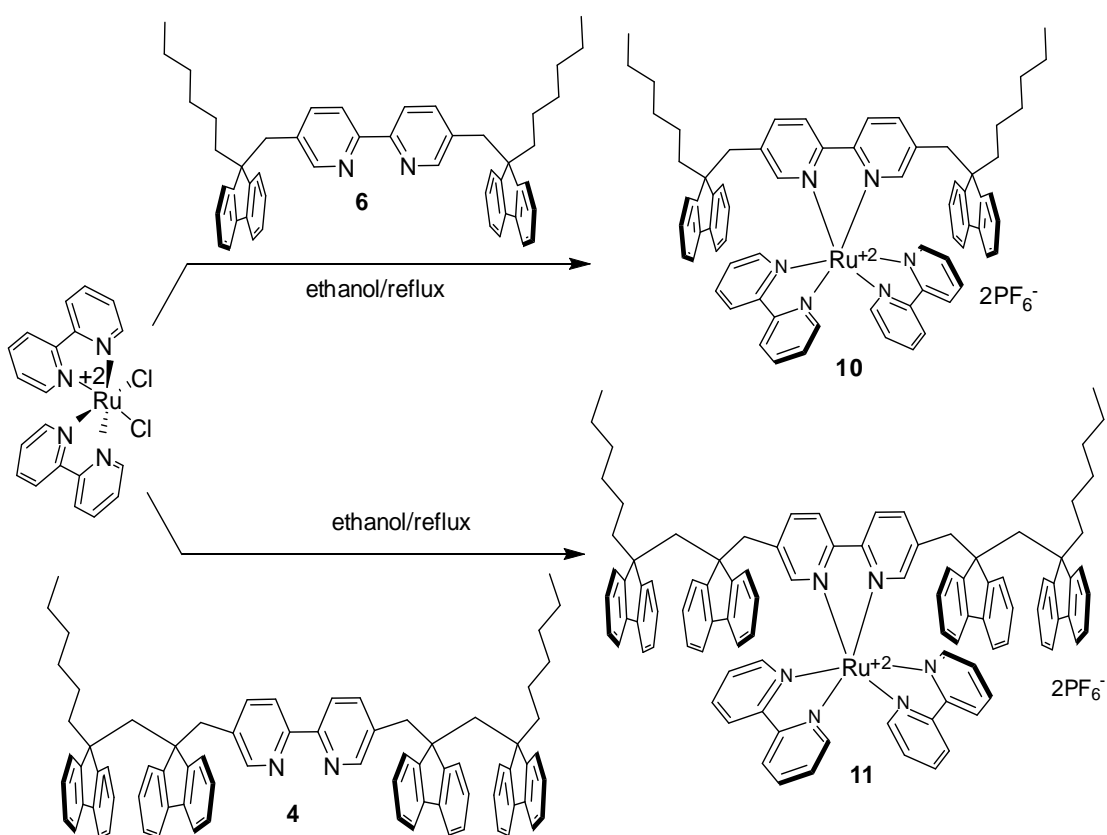


Figure 3. The proposed structure of Ru(II)–complexes based on polyfluorene substituted bipyridine ligands.

Unfortunately, the efforts to put two and three polyfluorene-based bipyridine ligands around ruthenium metal have been unsuccessful. However, ruthenium and rhenium complexes with one polyfluorene-based bipyridine ligand and a pair of

bipyridines were successfully synthesized. Herein, we will discuss the synthesis, photophysical, electrochemical properties and characterization of these new Ru(II) and Rhenium complexes as follows.

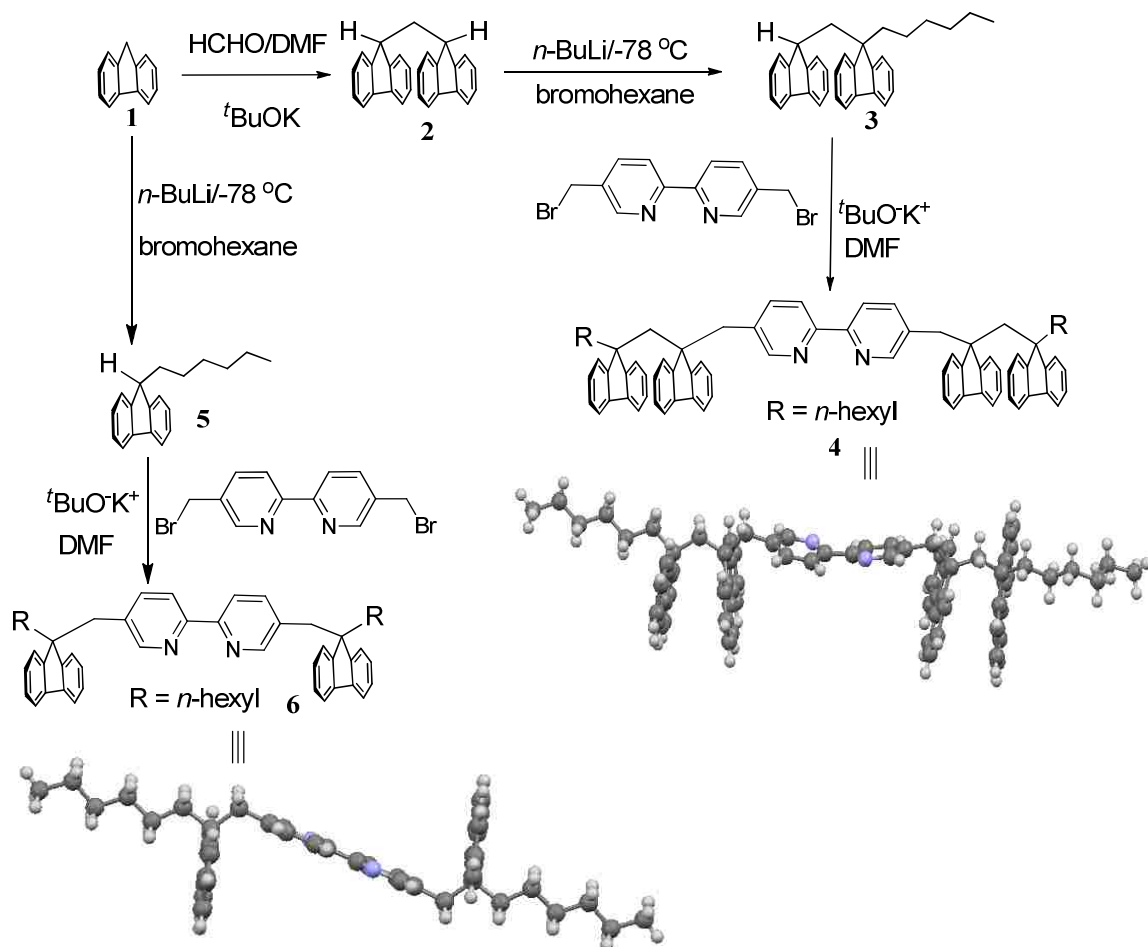
Scheme 1: Schematic representation of the synthesis of Ruthenium metal complexes of fluorene based bipyridine ligands.



Results and discussions

Synthesis of fluorene and difluorene-based bipyridine ligands (4 and 6). The synthesis of the fluorene and difluorene-based ligands (4 and 6) was accomplished by a three-step procedure. Thus, fluorene was coupled with formaldehyde in the presence of potassium *tert*-butoxide in *N,N*-dimethylformamide (DMF) to afford difluoranylmethane 2, which in turn undergoes a monolithiation using *n*-butyllithium in tetrahydrofuran at $-78\text{ }^{\circ}\text{C}$ followed by a reaction with 1-bromohexane to give 9-(9H-fluoren-9-ylmethyl)-9-hexyl-9H-fluorene (3). A deprotonation of 3 by potassium *tert*-butoxide in THF followed by a reaction with 5,5'-bis-bromomethyl-[2,2']bipyridine afforded 5'-bis-[9-(9-hexyl-9H-fluoren-9-ylmethyl)-9H-fluoren-9-ylmethyl]-[2,2']bipyridine (4) in good yield (see Scheme 1). Bifluorene-based bipyridine ligand 4 was purified by crystallization with a mixture of DCM and methanol and its structure was confirmed by X-ray crystallography.

Similarly 5,5'-bis-(9-hexyl-9H-fluoren-9-ylmethyl)-[2,2']bipyridinyl (6) was prepared by monohexylation of fluorene using *n*-butyllithium and 1-bromohexane in tetrahydrofuran at $-78\text{ }^{\circ}\text{C}$ to afford monhexylfluorene 5 in good yield. A deprotonation of 5 with potassium *tert*-butoxide in THF followed by a reaction with 5,5'-bis-bromomethyl-[2,2']bipyridine yielded monofluorene-based bipyridine ligand 6 in good yield. Ligand 6 was purified by crystallization and its structure was confirmed by X-ray crystallography (see Scheme 2). Also, the structures of ligands 4 and 6 were in agreement with their ^1H and ^{13}C NMR spectral data (see Figure 4).

Scheme 2: Synthesis of mono- and bifluorene-based bipyridinyl ligands (4 and 6).

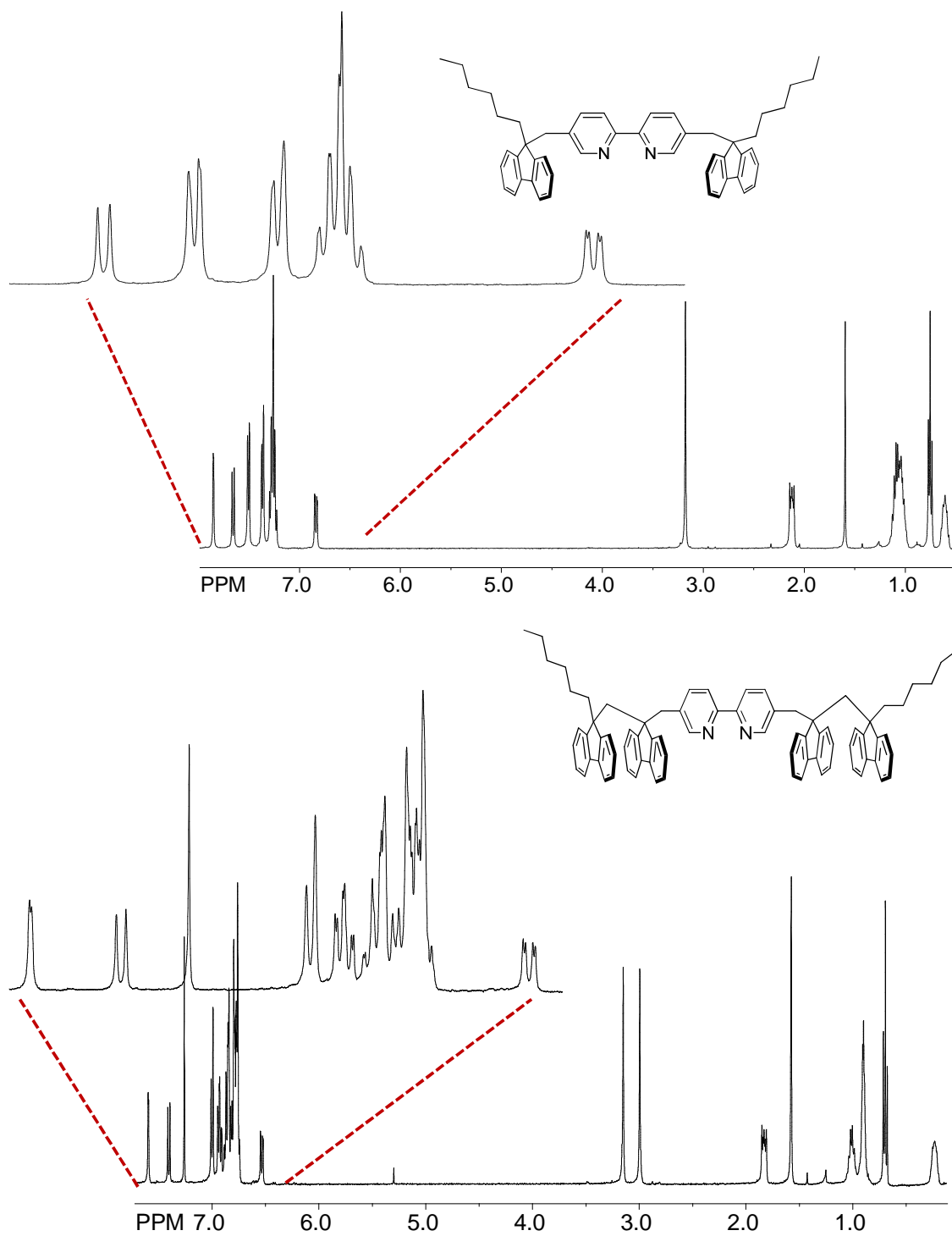
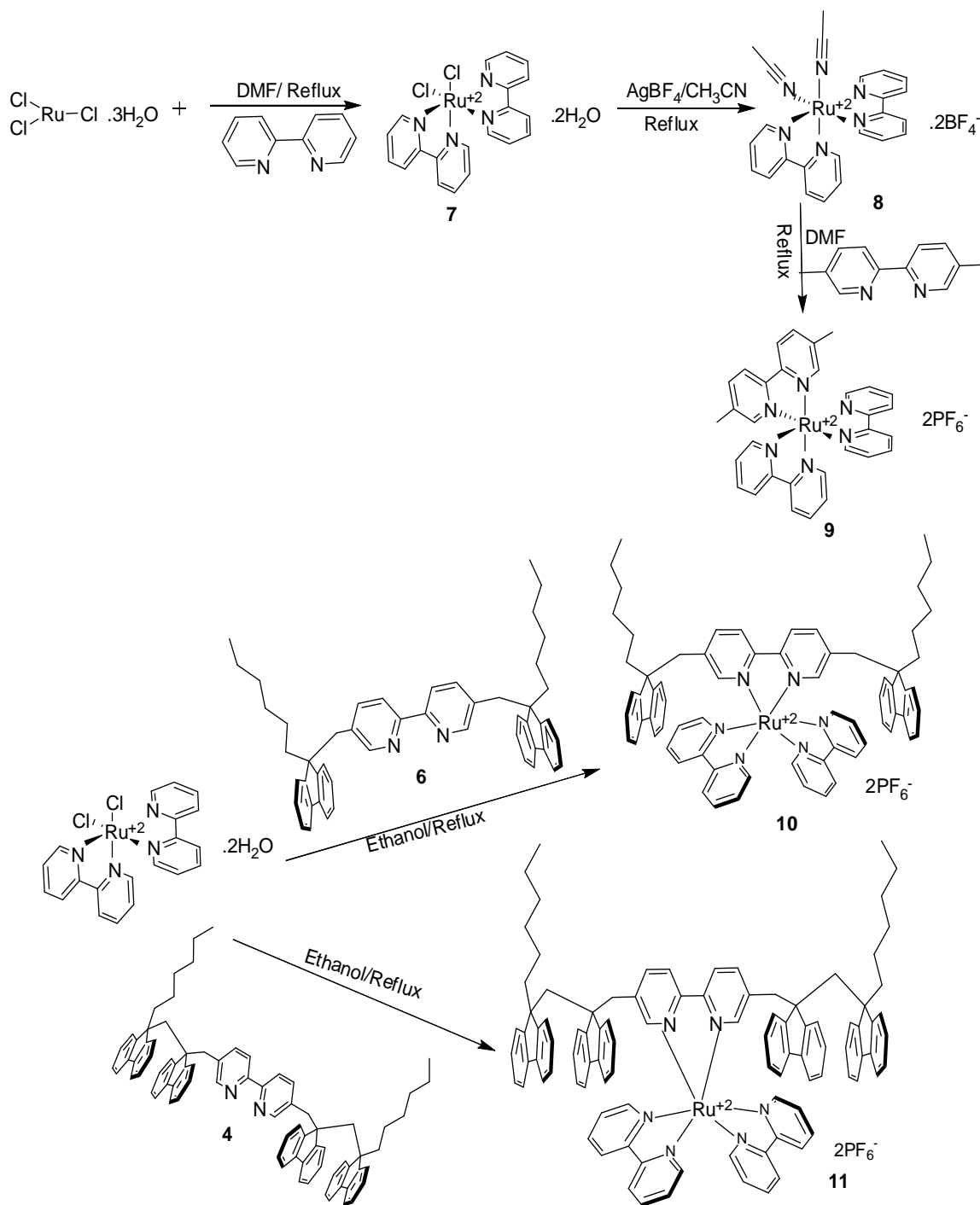


Figure 4. ^1H NMR spectra of ligand 4 and 6 in CDCl_3 at 22°C .

Synthesis and characterization of ruthenium metal complexes of methylbipyridine and fluorene-based bipyridine ligands. Synthesis of $[\text{Ru}(\text{bpy})_2\text{bpyMe}]$ **9** began by treatment of commercially available ruthenium trichloride trihydrate and bipyridine in presence of DMF, at 60 °C for 4 hr to afford the desired compound **7** in excellent yield. It was then treated with silver tetrafluoroborate in acetonitrile and refluxed for 4 hr to furnish compound **8**. Further treatment of the Ru^{II} -complex **8** with methylbipyridine in DMF at 70 °C afforded the complex **9** [i.e. $\text{Ru}(\text{bpy})_2\text{bpyMe}$], which was characterized by ^1H and ^{13}C NMR spectroscopy and by X-ray crystallography (see Scheme 3).

The fluorene-based Ru-complexes were obtained by a reaction of monofluorene and difluorene-based bipyridine ligand with Ru complex **7** synthesized above. Thus, a reaction of **7** with ligand **6** in refluxing ethanol furnished complex **10** [i.e. $\text{Ru}(\text{F}_1\text{bpy})(\text{Bpy})_2$] in 63% yield. Analogous treatment of the Ru-complex **7** with ligand **4** afforded the complex **11** [i.e. $\text{Ru}(\text{F}_2\text{bpy})(\text{Bpy})_2$] in good yield (see Scheme 3). The ruthenium complexes **9**, **10**, and **11** were fully characterized by ^1H and ^{13}C NMR spectroscopy (Figure 5).

Scheme 3: Synthetic schemes for the preparation of ruthenium complexes of methyl bipyridine and mono- and di-fluorene-based bipyridine ligands.



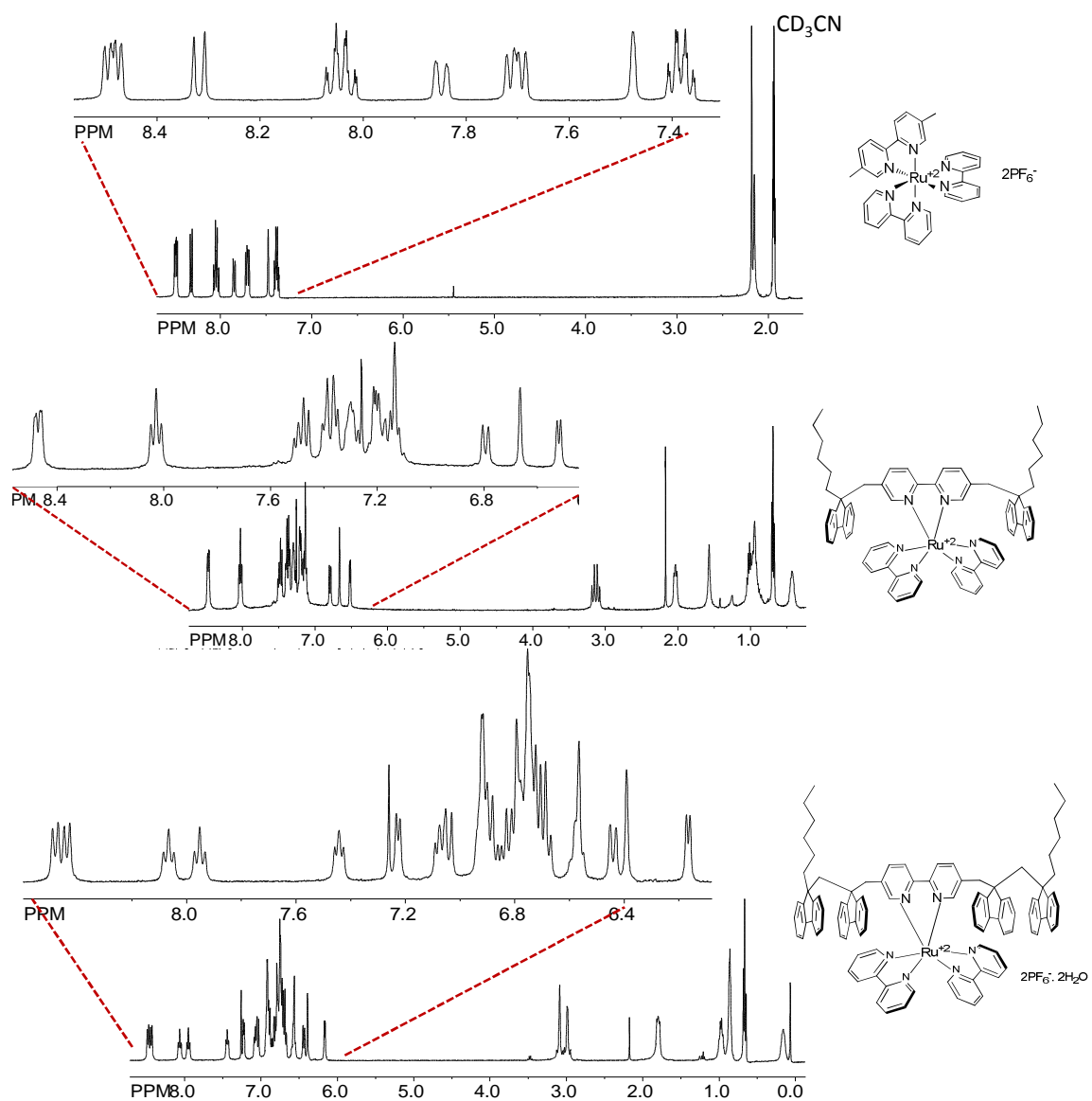
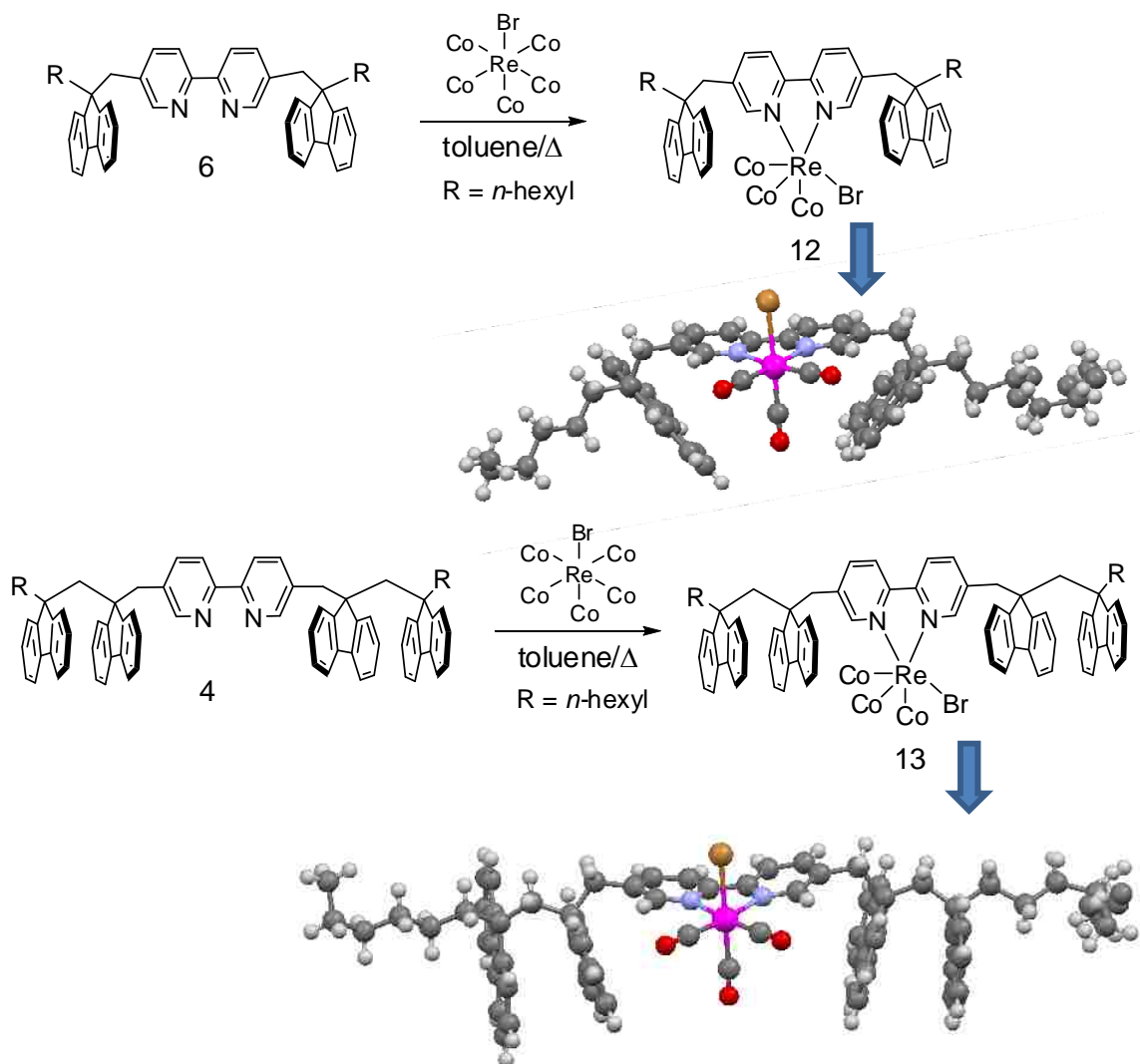


Figure 5. ^1H NMR spectra of ruthenium complexes 9, 10, and 11 in CD_3CN at 22°C .

Synthesis and characterization of Rhenium Metal Complexes of fluorene-based bipyridine ligands. The corresponding rhenium complex 12 [i.e. $\text{Re}(\text{F}_1\text{Bpy})(\text{CO})_3\text{Br}$] was then obtained by a reaction of **6** with $[\text{Re}(\text{CO})_5\text{Br}]$ in refluxing toluene. Similarly a reaction of ligand **4** with $[\text{Re}(\text{CO})_5\text{Br}]$ furnished complex **13** [i.e. $\text{Re}(\text{F}_2\text{Bpy})(\text{CO})_3\text{Br}$] in excellent yield (see Scheme 4). These complexes were characterized by ^1H and ^{13}C NMR spectroscopy (see Figure 6) and their molecular structures were confirmed by X-ray crystallography (Scheme 4).

Scheme 4: Synthesis of rhenium complexes of ligands **4** and **6**.



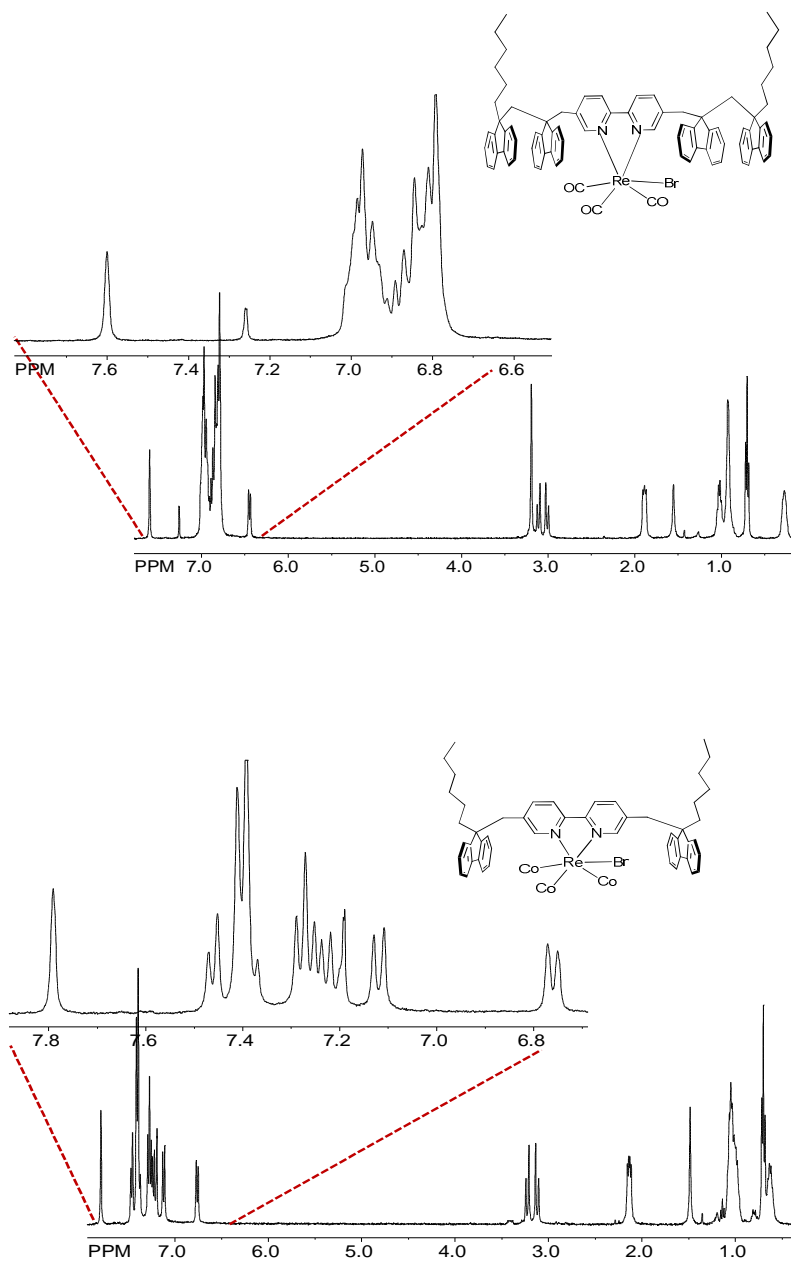


Figure 6. ^1H NMR spectra of Re complexes **12-13** in CDCl_3 at $22\text{ }^\circ\text{C}$.

Electrochemistry. The redox potentials of Ru(BPy)₂.BpyMe (9), Ru(BPy)₂(F1BPy) (10) and Ru(Bpy)₂(F2BPy) (11) were determined by cyclic voltammetry at a platinum electrode in dry MeCN containing 0.2 M *n*-Bu₄NPF₆ as the supporting electrolyte. Cyclic voltammogram of 9, 10 and 11 are compared in Figure 7. The cyclic voltammograms of 9-11 exhibit one reversible metal-based oxidation wave at ~1.3 V and the second oxidation wave in cyclic voltammograms of 10 and 11 originates from the oxidation of mono- and difluorene at 1.8 V and 1.5 V, respectively. Expectedly, several quasi-reversible ligand-centered reduction waves were also observed.

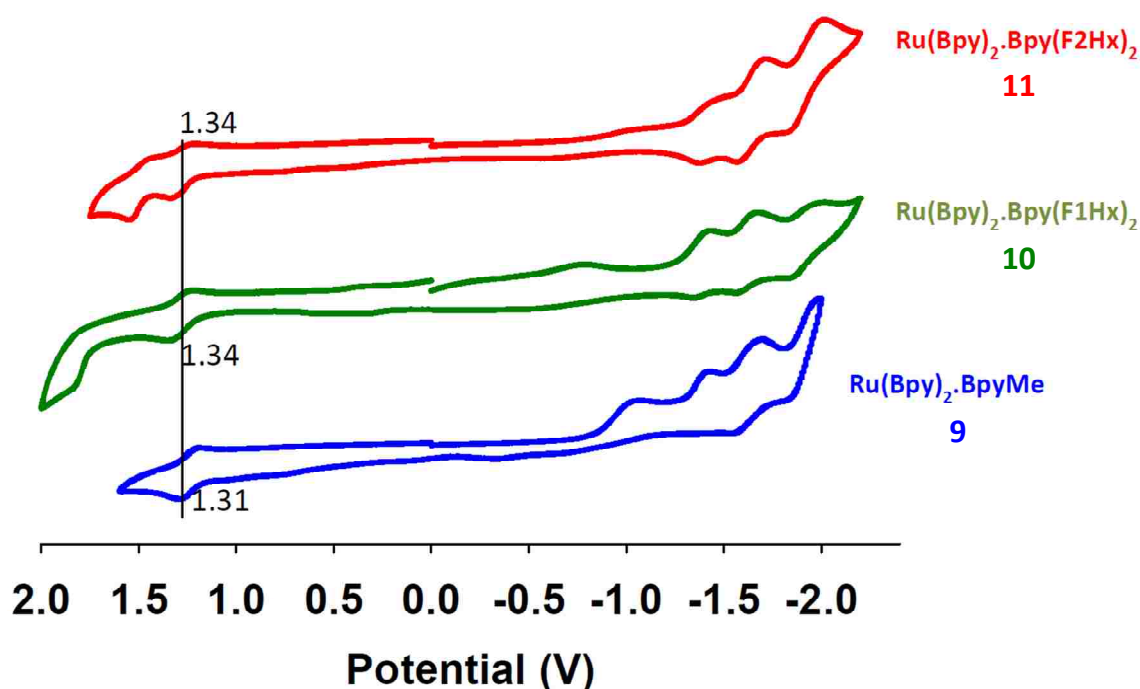


Figure 7. Cyclic voltammograms of **9**, **10**, and **11** (5 mM) in CH₃CN (containing 0.2 M *n*Bu₄NPF₆ as the supporting electrolyte) measured at a scan rate of $\nu = 100 \text{ mV s}^{-1}$ at 22 °C.

Absorption/emission spectroscopy of Ru complexes. The UV-vis and fluorescence spectrum of Ru complexes 9-11 recorded in dry MeCN at 22 °C are compiled in Figure 8. The absorption spectra of 9-11 exhibit the characteristic metal-to-ligand-charge transfer (MLCT) absorption peaks arising from $\text{Ru}(t_{2g}) \rightarrow \text{Bpy}(\pi^*)$ transition at 450 nm. The ligand centered transition from the bpy ligands are observed between 250-290 nm. The invariant emission maxima in 9-11 were observed to occur in visible region at 600 nm. The strong similarity of the absorption and emission spectra of 9-11 indicated that decoration of a bipyridine ligand with fluorene and difluorene substituents did not alter their optoelectronic properties.

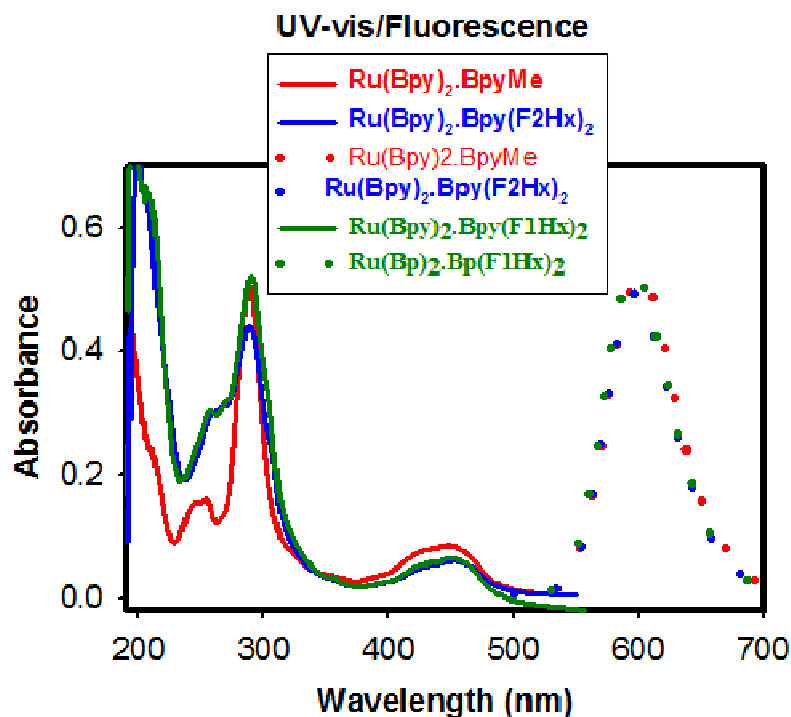


Figure 8: Comparison of the normalized absorption and emission spectra of 9-11. All spectra were recorded at a concentration of 2×10^{-3} M in CH_3CN at 22 °C.

Absorption and Emission Spectra of $\text{Re}(\text{CO})_3\text{Br}(\text{MeBpy})$, $\text{Re}(\text{CO})_3(\text{F1Bpy})$ and $\text{Re}(\text{CO})_3(\text{F2BPy})$. The optical properties of rhenium complexes 12 and 13 and a model compound were evaluated with the aid of UV-vis and emission spectroscopy as follows. The electronic absorption spectra of 12 and 13 and the model compound as 2×10^{-3} M solutions in dry CH_3CN were recorded at 22°C and are displayed in Figure 9a. $\text{Re}(\text{CO})_3\text{Br}(\text{MeBpy})$, $\text{Re}(\text{CO})_3(\text{F1Bpy})$ and $\text{Re}(\text{CO})_3(\text{F2BPy})$ showed structured absorption bands (see Figure 9a) while their emission spectra were rather invariant. As such this observation further confirms that decoration of a bipyridine ligand with fluorene and difluorene substituents does not alter their optoelectronic properties.

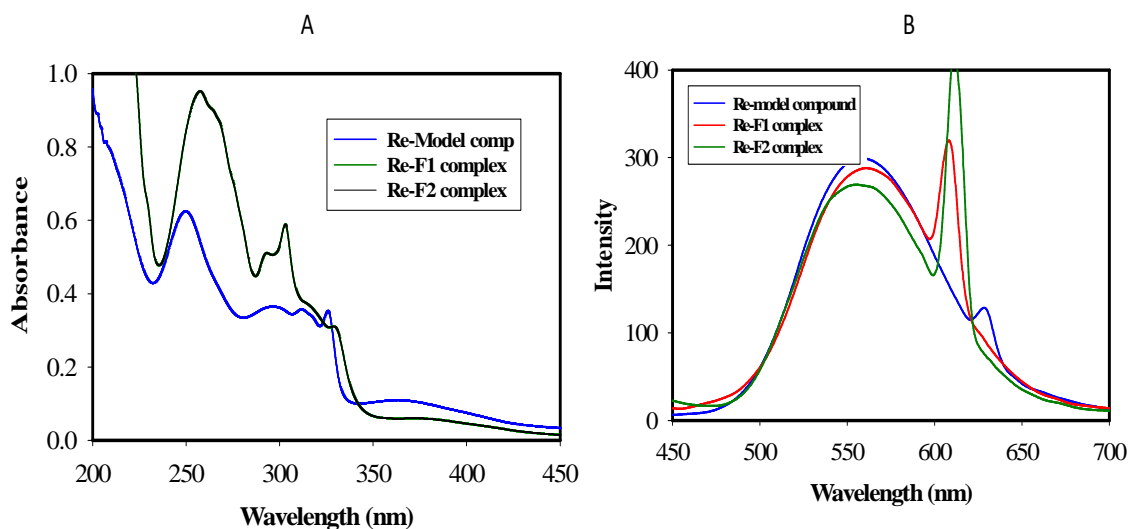


Figure 9: Comparison of the normalized absorption (A) and emission spectra (B) of $\text{Re}(\text{CO})_3\text{Br}(\text{MeBpy})$, $\text{Re}(\text{CO})_3(\text{F1Bpy})$ and $\text{Re}(\text{CO})_3(\text{F2BPy})$. All spectra were recorded at a concentration of 2×10^{-3} in CH_3CN at 22°C .

Summary and Conclusions. In summary, we have successfully synthesized fluorene and difluorene containing bipyridine ligands and synthesized their rhenium and ruthenium complexes. The structures of various complexes were characterized by means of ^1H and ^{13}C NMR spectroscopy and UV-Vis spectroscopy and their electrochemical and photophysical properties were investigated. These studies confirmed that decoration of a bipyridine ligand with fluorene and difluorene substituents does not alter their optoelectronic properties of their metal complexes when compared with the corresponding model compounds.

Experimental Section

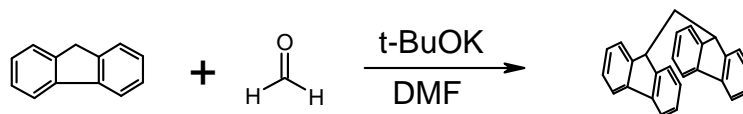
Materials: Fluorene, formaldehyde, 5,5'-bis-bromomethyl-[2,2']bipyridinyl, 1-bromohexane, *n*-butyllithium (2.5 M in hexanes), methanol, hexanes, toluene, potassium *tert*-butoxide, *N,N*-dimethylformamide (DMF), tetrahydrofuran (THF), and ethyl acetate were commercially available and were used as received unless otherwise specified.

Anhydrous tetrahydrofuran (THF) was prepared by refluxing the commercial tetrahydrofuran (Aldrich) over lithium tetrahydroaluminate under an argon atmosphere for 24 hours followed by distillation. It was stored under an argon atmosphere in a Schlenk flask equipped with a Teflon valve fitted with Viton O-rings. Dichloromethane (Aldrich) was repeatedly stirred with fresh aliquots of concentrated sulfuric acid (~10% by volume) until the acid layer remained colorless. After separation it was washed successively with water, aqueous sodium bicarbonate, water, and saturated aqueous sodium chloride and dried over anhydrous calcium chloride. The dichloromethane was distilled twice from P_2O_5 under an argon atmosphere and stored in a Schlenk flask

equipped with a Teflon valve fitted with Viton O-rings. The hexanes and toluene were distilled from P₂O₅ under an argon atmosphere and then refluxed over calcium hydride (~12 hrs). After distillation from CaH₂, the solvents were stored in Schlenk flasks under argon atmosphere.

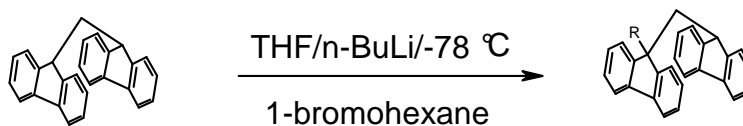
Cyclic Voltammetry (CV). The CV cell was of an air-tight design with high vacuum Teflon valves and Viton O-ring seals to allow an inert atmosphere to be maintained without contamination by grease. The working electrode consisted of an adjustable platinum disk embedded in a glass seal to allow periodic polishing (with a fine emery cloth) without changing the surface area (~1 mm²) significantly. The reference SCE electrode (saturated calomel electrode) and its salt bridge were separated from the catholyte by a sintered glass frit. The counter electrode consisted of platinum gauze that was separated from the working electrode by ~3 mm. The CV measurements were carried out in a solution of 0.1 to 0.2 M supporting electrolyte (tetra-*n*-butylammonium hexafluorophosphate, TBAH) and the substrate in dry dichloromethane under an argon atmosphere. All the cyclic voltammograms were recorded at a sweep rate of 200 mV sec⁻¹, unless otherwise specified and were IR compensated. The oxidation potentials ($E_{1/2}$) were referenced to SCE, which was calibrated with added (equimolar) ferrocene ($E_{1/2} = 0.450$ V vs. SCE). The $E_{1/2}$ values were calculated by taking the average of anodic and cathodic peak potentials in reversible cyclic voltammograms or directly from square-wave voltammograms in irreversible cyclic voltammograms.

Synthesis of 9, 9'-methylenebis-9H-fluorene (2).



To a solution of fluorene (8.3 g, 50 mmol) in DMF (75 mL) under argon atmosphere at room temperature, potassium *tert*-butoxide (0.28 g, 2.5 mmol) was added. After 5 min of stirring, formaldehyde (0.75 g, 25 mmol) was added and the mixture was stirred for an additional 10 min. Resulting reaction mixture was poured onto 200 mL aqueous HCl (5%) solution and the precipitate thus formed was filtered and recrystallized using dichloromethane/methanol mixture to afford 9,9'-methylenebis-9H-fluorene as colorless crystals. Yield: 7.2 g, 83%; mp 202-203 °C. ¹H NMR (CDCl₃) δ: 2.23 (t, 2H, *J* = 7.65 Hz), 4.41 (t, 2H, *J* = 7.65 Hz), 7.25 (d, 4H, *J* = 7.65), 7.28 (t, 4H, *J* = 7.38 Hz), 7.40 (t, 4H, *J* = 7.38 Hz), 7.55 (d, 4H, *J* = 7.38), 7.82 (d, 4H, *J* = 7.65 Hz); ¹³C NMR (CDCl₃) δ: 39.09, 46.10, 120.34, 125.26, 127.23, 127.51, 141.22, 147.70.

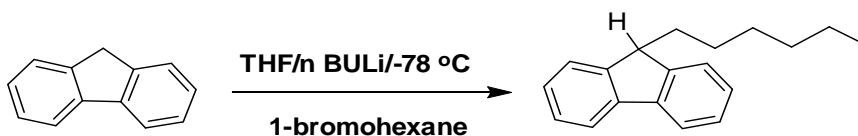
Synthesis of 9-(9H-fluoren-9-ylmethyl)-9-hexyl-9H-fluorene (3).



To a solution of 2 (6.79 g, 19.7 mmol) in anhydrous tetrahydrofuran (90 mL) at -78 °C under argon atmosphere, *n*-butyllithium (2.5 M in hexanes, 7.9 mL) was added dropwise. The resulting dark-red solution of difluoranyl anion was stirred for 10 min and after which time 1-bromohexane (2.77 mL, 19.7 mmol) was added and the mixture was stirred for an additional 15 min. The cooling bath was removed and the reaction mixture

was stirred for 30 min at room temperature. The reaction mixture was then poured onto water (100 mL) and extracted with dichloromethane (3 x 50 mL). The combined dichloromethane extracts were dried over anhydrous MgSO_4 , filtered, and evaporated under reduced pressure to afford a white crude product which was recrystallized using a dichloromethane/methanol mixture to afford 9-(9H-fluoren-9-ylmethyl)-9-hexyl-9H-fluorene as colorless crystals. Yield: 6.7 g, 80%; mp 122-123 °C; ^1H NMR (CDCl_3) δ : 0.66 (m, 2H), 0.76 (t, 3H), 1.00 ~ 1.16 (m, 6H), 2.10 (p, 2H), 2.66 (d, 2H, $J = 4.75$ Hz), 3.10 (t, 1H, $J = 4.75$ Hz), 6.60 (d, 2H, $J = 7.48$ Hz), 7.03 (t, 2H, $J = 7.57$ Hz), 7.18 (t, 2H, $J = 7.57$ Hz), 7.40 (m, 4H), 7.54 (m, 4H), 7.77 (m, 2H); ^{13}C NMR (CDCl_3) δ : 14.28, 22.84, 24.11, 29.93, 31.75, 41.10, 44.55, 45.66, 55.59, 119.44, 120.49, 124.26, 125.06, 126.72, 126.90, 127.54, 127.71, 140.64, 141.82, 149.20, 149.97.

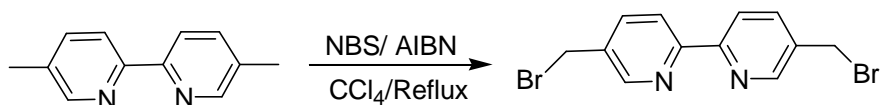
Synthesis of 9-hexyl-9H-fluorene (5).



To a solution of fluorene (4 g, 24.06 mmol) in anhydrous tetrahydrofuran (50 mL) at -78 °C under argon atmosphere, *n*-butyllithium (2.5 M in hexanes, 9.6 mL) was added drop wise. The resulting dark-red solution of difluoranyl anion was stirred for 10 min and after that bromohexane (3.38 mL, 24.06 mmol) was added and the mixture was stirred for an additional 15 min. The cooling bath was removed and the reaction mixture was stirred for 30 min at room temperature. The reaction mixture was then poured onto water (100 mL) and extracted with dichloromethane (3 x 50 mL). The combined dichloromethane

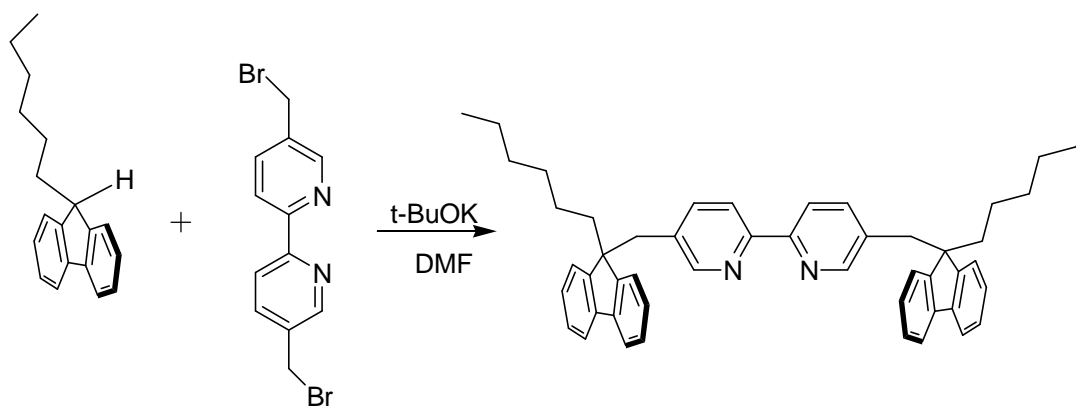
extracts were dried over anhydrous MgSO_4 , filtered, and evaporated under reduced pressure to afford the product. This was purified via flash chromatography on silica gel using hexanes as an eluent to afford the product. Yield: 4.1 g, 66%; ^1H NMR (CDCl_3) δ : 0.79 (t, 3H, $J = 7.05\text{Hz}$), 1.14 (m, 8H), 1.89 (m, 2H), 3.85 (t, 1H, $J = 6.08$), 7.22 (m, 4H, $J = 7.36\text{Hz}$), 7.40 (d, 2H, $J = 7.68\text{Hz}$), 7.63 (d, 2H, $J = 7.68\text{Hz}$); ^{13}C NMR (CDCl_3) δ : 14.28, 22.85, 25.87, 29.86, 31.85, 33.29, 47.64, 119.90, 124.42, 126.89, 126.96, 141.27, 147.72.

Synthesis of 5,5'-bis-bromomethyl-[2,2']bipyridinyl.



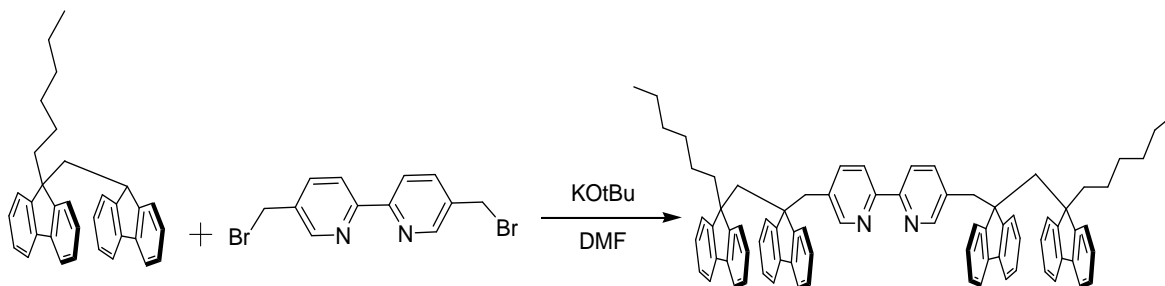
A solution of (1.0 g, 5.42 mmol), NBS (1.93 g, 10.8 mmol), and AIBN (0.32 g, 1.94 mmol) in CCl_4 (40 mL) was refluxed under argon for 22 min and the precipitated succinimide was removed immediately from the hot mixture by filtration. The precipitate was washed with CCl_4 and the combined CCl_4 phases were evaporated. The remaining solid was dissolved in CH_2Cl_2 (100 mL) and washed with water. The crude product was recrystallized from CH_2Cl_2 . Yield: 0.500 g, 28%; mp 193–194 °C. ^1H NMR (CDCl_3): 4.53 (s, 4H), 7.85 (2H, dd, $J = 8.24$ Hz), 8.39 (d, 2H, $J = 8.11\text{Hz}$), 8.68 (d, 2H, $J = 2.18\text{Hz}$). ^{13}C NMR (CDCl_3): 29.77, 121.36, 134.09, 137.83, 149.59, 155.63.

Synthesis of 5,5'-bis-(9-hexyl-9H-fluoren-9-ylmethyl)-[2,2']bipyridinyl (6).

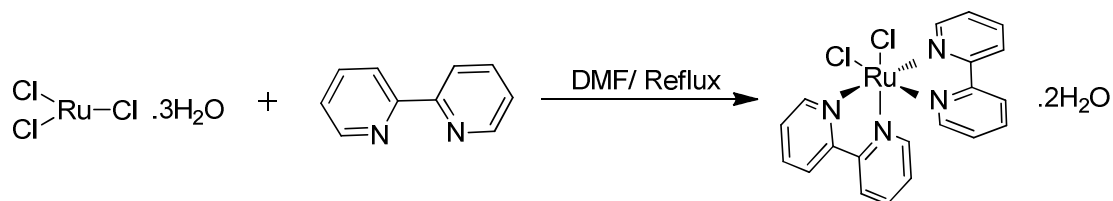


To a solution of monohexylated fluorene (0.89 g, 3.566 mmol) in 20 mL DMF at 0 °C under argon atmosphere, potassium *tert*-butoxide (0.420 g, 3.7 mmol) was added. After 20 min. of stirring, 5,5-bis(bromomethyl)-2,2'-bipyridine (0.61 g, 1.78 mmol) was added at room temperature and the resulting mixture was stirred for 24 h. The reaction mixture was then poured onto water and extracted with dichloromethane (3 x 50 mL). The combined organic extracts were dried over anhydrous MgSO₄, filtered and evaporated under reduced pressure to afford a yellow product which was purified via flash chromatography on silica gel using 0.5% ethyl acetate in hexanes as an eluent to afford a solid. A pure sample of **6** was obtained by recrystallization with a mixture of dichloromethane/methanol. Yield: 360 mg, 30%; mp 161-163 °C. ¹H NMR (CDCl₃) δ: 0.55-0.66 (m, 4H), 0.75 (t, 6H, *J* = 7.64Hz), 0.96-1.17 (m, 12H), 2.07-2.17 (m, 4H), 3.17 (s, 4H), 6.83 (dd, 2H, *J* = 6.47Hz), 7.20-7.32 (m, 8H), 7.36 (d, 4H), 7.50 (d, 4H), 7.65 (d, 2H), 7.85 (s, 2H). ¹³C NMR (CDCl₃) δ: 14.18, 22.76, 23.91, 29.83, 31.65, 39.48, 43.79, 55.95, 119.55, 120.18, 123.53, 127.16, 127.42, 132.73, 138.12, 141.17, 148.73, 150.44, 153.88.

Synthesis of 5,5'-bis-[9-(9-hexyl-9H-fluoren-9-ylmethyl)-9H-fluoren-9-ylmethyl]-[2,2']bipyridinyl (4).

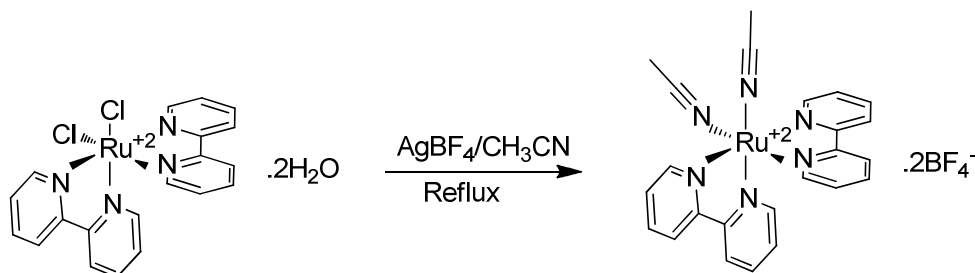


To a solution of mono-hexylated difluorene (1.25 g, 2.92 mmol) in 20 mL DMF at 0 °C under argon atmosphere, potassium *tert*-butoxide (0.34 g, 3.06 mmol) was added. After 20 min of stirring, 5,5-bis(bromomethyl)-2,2'-bipyridine (0.50 g, 1.46 mmol) was added at room temperature and the resulting mixture was stirred for 24 hr. The reaction mixture was cooled at -40 °C and then filtered, precipitate was washed with water multiple times, and then dried under vacuum. The filtrate was also poured onto water and extracted with dichloromethane (3 x 50 mL). The combined extracts were dried over anhydrous MgSO₄, filtered and evaporated under reduced pressure to afford a yellow crude product which was purified by recrystallization with a mixture of DCM/methanol. Yield: 800 mg, 53%; mp 238-240 °C. ¹H NMR (CDCl₃) δ: 0.15-0.31 (m, 4H), 0.69 (t, 6H, *J* = 7.70 Hz), 0.80-1.80 (m, 12H), 1.75-1.89 (m, 4H), 2.99 (s, 4H), 3.15 (s, 4H), 6.53 (dd, 2H, *J* = 8.19 Hz), 6.70-6.96 (m, 28H), 6.97-7.05 (m, 4H), 7.40 (d, 2H, *J* = 8.35 Hz), 7.60 (s, 2H). ¹³C NMR (CDCl₃) δ: 13.95, 22.50, 29.41, 31.28, 42.55, 45.24, 48.34, 53.24, 54.03, 118.77, 119.02, 119.13, 123.35, 123.93, 125.54, 125.66, 125.74, 126.10, 131.65, 137.84, 140.48, 140.74, 146.54, 148.31, 150.10.

Synthesis of 7.

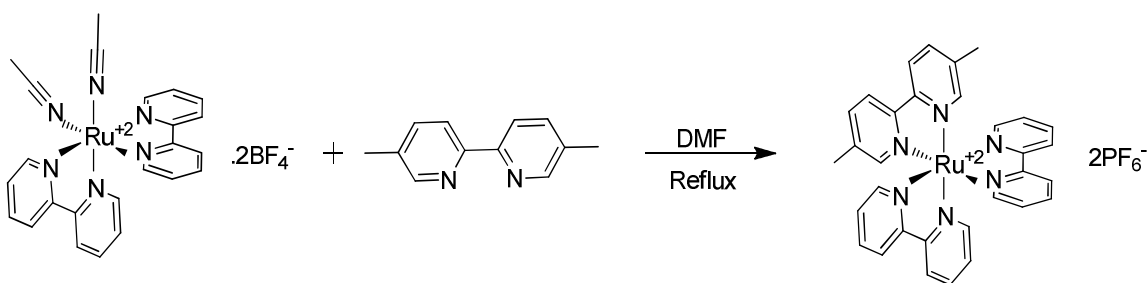
RuCl₃·3H₂O (1.56 g, 5.97 mmol) was dissolved in dimethylformamide (10 mL), lithium chloride (1.48 g, 34.9 mmol) and 2,2-bipyridine (1.87 g, 12 mmol) were then added and the resulting mixture was de-aerated with argon for 5 min. The resulting solution was refluxed for 6 h. After this time, the heating mantle was removed and while the reaction was hot, 50 ml of acetone was added and the resultant solution was stirred at room temperature for an additional ½ h. A simple filtration yielded a dark violet-black crystalline solid that was washed with 5 mL of cold H₂O, and then dried using a suction pump. Yield: 2.26 g, 73%; ¹H NMR (DMSO) δ: 6.21 (t, 2H, *J* = 6.48 Hz), 6.62 (d, 2H, *J* = 5.50 Hz), 6.79 (t, 2H, *J* = 5.50 Hz), 6.88 (t, 2H, *J* = 6.15 Hz), 7.18 (t, 2H, *J* = 7.77 Hz), 7.59 (d, 2H, *J* = 8.10 Hz), 7.75 (d, 2H, *J* = 8.42 Hz), 9.08 (d, 2H, *J* = 5.83 Hz).

Synthesis of 8.



A solution of cis-(bpy)₂RuCl₂·2H₂O (0.38 g, 0.73 mmol) and silver tetrafluoro borate (0.280 g, 1.46 mmol) in dry acetonitrile (40ml) was refluxed for 12 hr. After completion, the reaction mixture was filtered through cannula filtration and filtrate was evaporated under reduced pressure to afford an orange solid. Yield: 0.41 g, 84%; ¹H NMR (CD₃CN) δ: 7.25 (t, 2H, *J* = 6.86 Hz), 7.58 (d, 2H, *J* = 5.77 Hz), 7.84 (t, 2H, *J* = 7.22 Hz), 7.93 (t, 2H, *J* = 8.30 Hz), 8.26 (t, 2H, *J* = 8.30 Hz), 8.37 (d, 2H, *J* = 8.30 Hz), 8.52 (d, 2H, *J* = 7.94 Hz), 9.31 (d, 2H, *J* = 5.77 Hz).

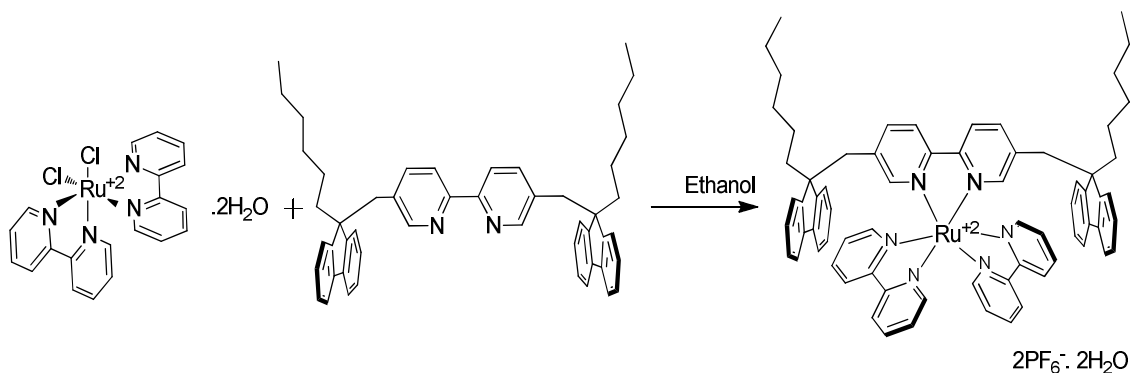
Synthesis of [Ru(bpy)₂.bpyMe] (9).



A mixture of cis-[Ru(bpy)₂(CH₃CN)₂](BF₄) (0.36 g, 0.54 mmol) and 5,5-dimethyl-2,2'-bipyridine (0.10 g, 0.54 mmol) in DMF (20 mL) was refluxed for 6h. After the mixture was cooled, the crude product was precipitated as its PF₆⁻ salt by addition of a methanolic solution of NH₄PF₆ (2 g) in MeOH (50 mL) followed by water. The solid product was

filtered, washed with water and Et₂O. Recrystallization from CH₃CN/toluene yielded 9 (395 mg, 94%) as an orange solid; mp 300 °C. ¹H NMR (CD₃CN) δ: 2.18(s, 6H), 7.35-7.41 (m, 4H), 7.47 (s, 2H), 7.67-7.73 (m, 4H), 7.84 (d, 2H, *J* = 8.41 Hz), 8.00-8.08 (m, 4H), 8.31 (d, 2H, *J* = 8.41 Hz), 8.45-8.51 (m, 4H). ¹³C NMR (CD₃CN) δ: 18.47, 124.12, 125.16, 125.18, 128.30, 128.44, 138.54, 139.21, 139.27, 152.36, 152.51, 152.58, 155.33, 157.96, 158.05.

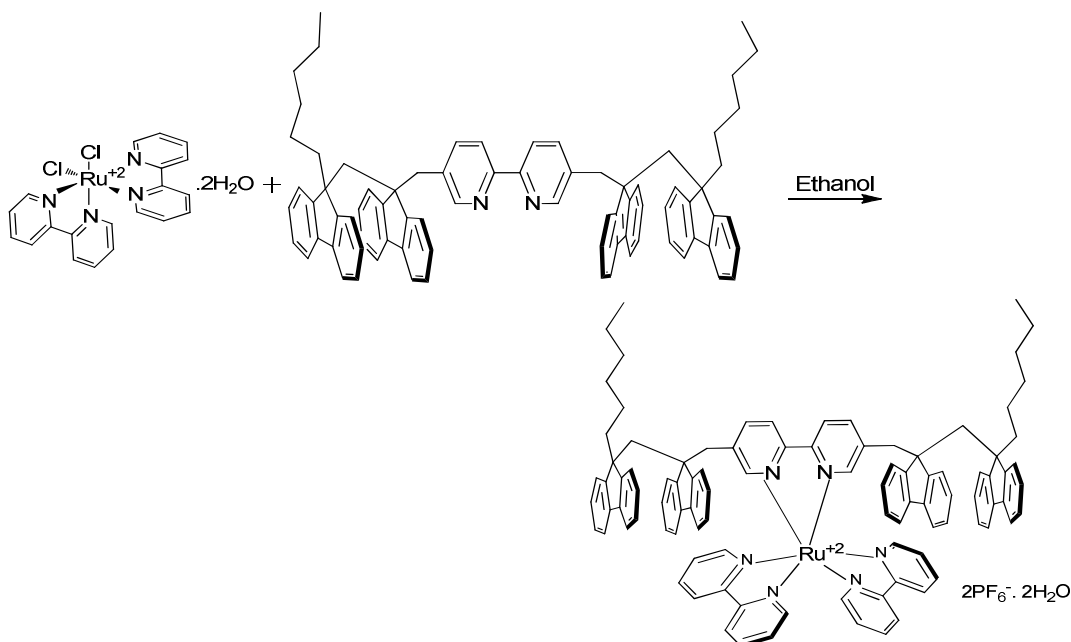
Synthesis of [Ru(F1bpy)(Bpy)₂] (10).



An ethanol solution (20 mL) of F1bpy (70 mg, 0.10 mmol) and Ru(bpy)₂Cl₂·2H₂O (53 mg, 0.10 mmol) was refluxed for 12 h. The resulting red solution was cooled, and a saturated aqueous solution of NH₄-PF₆ was added. Orange precipitate formed immediately; it was filtered, washed successively with water (10 mL) and diethyl ether (20 mL), and finally dried in vacuo. It was further purified by recrystallization from acetone/diethyl ether. Yield: 100 mg, 63%; mp 120-122 °C. ¹H NMR (CDCl₃) δ: 0.36-0.48 (m, 4H), 0.69 (t, 6H, *J* = 7.37 Hz), 0.85-1.08 (m, 12H), 1.97-2.08 (m, 4H), 3.13 (q, 4H, *J* = 16.15 Hz), 6.51 (d, 2H, *J* = 5.64 Hz), 6.66 (s, 2H), 6.79 (d, 2H, *J* = 8.37 Hz),

7.10-7.22 (m, 10H), 7.26-7.32 (m, 4H), 7.33-7.42 (m, 6H), 7.44-7.52 (m, 4H), 8.02 (t, 4H, $J = 7.63$ Hz), 8.47 (d, 4H, $J = 8.07$ Hz).

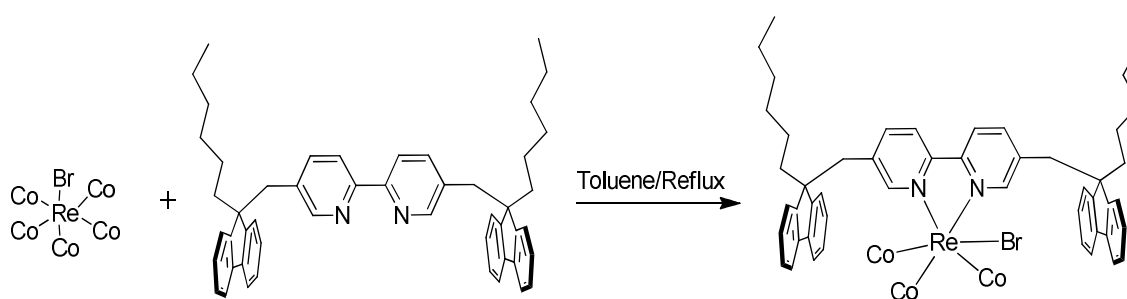
Synthesis of $[\text{Ru}(\text{F}_2\text{bpy})(\text{Bpy})_2]$ (11).



An ethanol solution (20 mL) of ligand F2bpy (100 mg, 0.096 mmol) and $\text{Ru}(\text{bpy})_2\text{Cl}_2 \cdot 2\text{H}_2\text{O}$ (50 mg, 0.096 mmol) was refluxed for 12 h. The resulting red solution was cooled, and a saturated aqueous solution of $\text{NH}_4\text{-PF}_6$ was added. A red precipitate formed immediately; it was filtered, washed successively with water (10 mL) and diethyl ether (20 mL), and finally dried in vacuo. It was further purified by recrystallization from acetone/diethyl ether. Yield: 136 mg, 95%; mp 196-198 °C. ^1H NMR (CDCl_3) δ : 0.10-0.21 (m, 4H), 0.66 (t, 6H, $J = 7.70$ Hz), 0.80- 1.0 (m, 12H), 1.75-1.85(m, 4H), 2.93-3.14 (m, 8H), 6.16(d, 2H, $J = 5.36$ Hz), 6.39(s, 2H), 6.44 (d, 2H, $J = 8.71$ Hz), 6.52-6.61 (m, 4H), 6.65-6.85 (m, 20H), 6.85-6.95(m, 8H), 7.01-7.10 (m, 4H), 7.22 (d, 2H, $J = 5.02$ Hz),

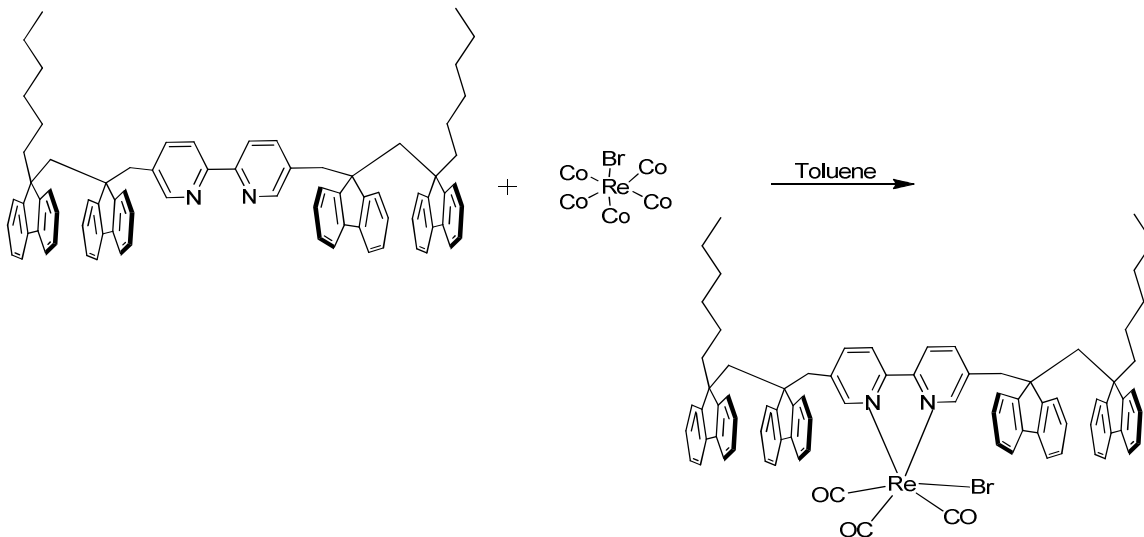
7.44 (t, 2H, $J = 6.70$ Hz), 7.95 (t, 2H, $J = 8.04$ Hz), 8.06 (t, 2H, $J = 7.70$ Hz), 8.45 (dd, 4H, $J = 17.09$ Hz). ^{13}C NMR (CDCl_3) δ : 14.10, 22.61, 29.44, 31.41, 42.37, 44.20, 48.31, 53.29, 54.65, 118.95, 119.90, 119.16, 121.02, 123.52, 123.91, 123.98, 124.76, 124.87, 126.02, 126.21, 126.30, 126.81, 127.03, 127.74, 127.83, 136.78, 137.88, 138.10, 138.29, 140.24, 140.57, 140.68, 140.76, 145.54, 145.90, 148.05, 148.22, 150.56, 151.27, 151.40, 153.36, 156.34, 156.53.

Synthesis of $[\text{Re}(\text{F}_1\text{bpy})(\text{CO})_3\text{Br}]$ (12).



A solution of F1bpy (100 mg, 0.146 mmol) and $\text{Re}(\text{CO})_5\text{Br}$ (59 mg, 0.146 mmol) in toluene (15 mL) was heated at 60°C for 8 h. The yellow precipitate thus formed was filtered, washed with ether, and dried in vacuo to yield 98 mg (65%) of a yellow solid, mp $>300^\circ\text{C}$. ^1H NMR (CDCl_3) δ : 0.56-0.66 (m, 4H), 0.70 (t, 6H, $J = 7.24$ Hz), 0.92-0.11 (m, 12H), 2.08-2.17 (m, 4H), 3.12 (d, 2H, $J = 12.99$ Hz), 3.23 (d, 2H, $J = 12.99$ Hz), 6.75 (d, 2H, $J = 7.99$ Hz), 7.11 (d, 2H, $J = 8.74$ Hz), 7.17-7.30 (m, 8H), 7.37-7.43 (m, 8H), 7.46 (d, 2H, $J = 7.49$ Hz), 7.79 (s, 2H). ^{13}C NMR (CDCl_3) δ : 14.16, 22.69, 24.05, 29.72, 31.58, 38.99, 43.99, 56.31, 120.41, 120.49, 120.60, 123.08, 123.32, 127.41, 127.84, 128.10, 128.36, 136.33, 139.03, 140.83, 141.23, 147.07, 147.42, 152.45, 153.55, 188.26, 196.79.

Synthesis of $[\text{Re}(\text{F}_2\text{bpy})(\text{CO})_3\text{Br}]$ (13).



A solution of F2bpy (300 mg, 0.289 mmol) and $\text{Re}(\text{CO})_5\text{Br}$ (0.117 mg, 0.289 mmol) in toluene (30 mL) was heated at 60 °C for 8 h. The yellow precipitate thus formed was filtered, washed with ether, and dried in vacuo to yield 319 mg (80%) of a yellow solid; mp >300 °C. ^1H NMR (CDCl_3) δ : 0.20-0.33 (m, 4H), 0.70 (t, 6H, $J = 7.42$ Hz), 0.84-1.07 (m, 12H), 1.84- 1.93 (m, 4H), 3.00 (d, 2H, $J = 12.64$ Hz), 3.11 (d, 2H, $J = 12.92$ Hz), 3.19 (s, 4H), 6.44 (d, 2H, $J = 8.24$ Hz), 6.73-7.03 (m, 34H), 7.60 (s, 2H). ^{13}C NMR (CDCl_3) δ : 14.21, 22.76, 29.67, 31.56, 42.61, 45.22, 48.29, 53.56, 54.68, 119.08, 119.16, 119.55, 119.69, 120.17, 123.66, 123.85, 123.89, 123.97, 125.97, 126.03, 126.09, 126.25, 126.70, 126.80, 127.36, 135.35, 138.94, 140.32, 140.87, 140.99, 141.11, 145.54, 145.63, 148.23, 148.58, 152.21, 153.62, 187.99, 196.92.

Crystal structure of ligand (6)

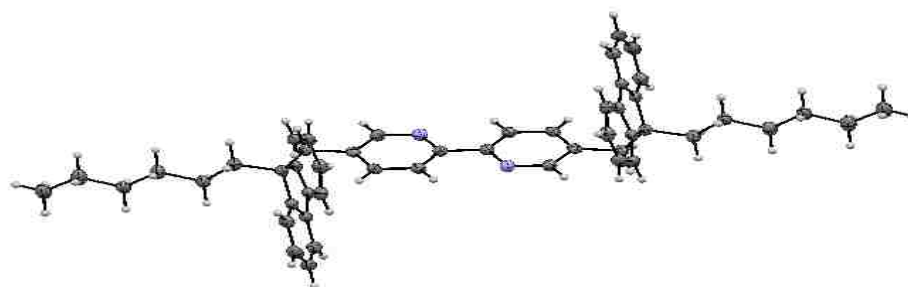


Table 1: Crystal data and structure refinement for raj19z

Identification code	raj19z
Empirical formula	C ₅₀ H ₅₂ N ₂
Formula weight	680.94
Temperature □/□K	100.0
Crystal system	triclinic
Space group	P-1
a □/□Å, b □/□Å, c □/□Å	10.6063(4), 12.0092(5), 15.5501(9)
α/°, β/°, γ/°	89.648(4), 80.272(4), 89.861(4)
Volume □/□Å ³	1952.14(17)
Z	2
ρ _{calc} □/□mg mm ⁻³	1.158
μ □/□mm ⁻¹	0.499
F(000)	732
Crystal size □/□mm ³	0.16 × 0.12 × 0.08
Theta range for data collection	3.6776 to 147.5344°
Index ranges	-13 ≤ h ≤ 13, -14 ≤ k ≤ 14, -15 ≤ l ≤ 18
Reflections collected	15461
Independent reflections	6890[R(int) = 0.0247]
Data/restraints/parameters	6890/0/471
Goodness-of-fit on F ²	1.039
Final R indexes [I > 2σ (I)]	R ₁ = 0.0410, wR ₂ = 0.1044
Final R indexes [all data]	R ₁ = 0.0547, wR ₂ = 0.1140
Largest diff. peak/hole □/□e Å ⁻³	0.247/-0.239

Crystal structure of 5, 5'-Bis-[9-(9-hexyl-9H-fluoren-9-ylmethyl)-9H-fluoren-9-ylmethyl]-[2, 2'] bipyridinyl ligand (4)

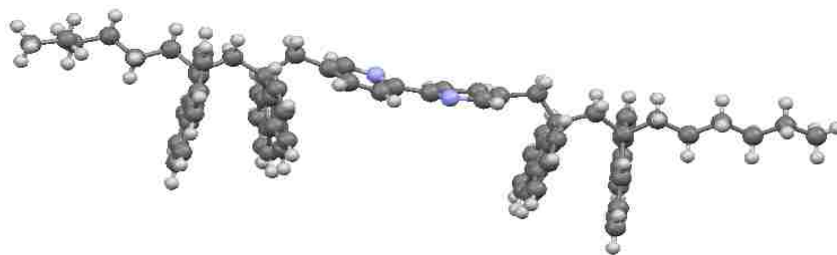


Table 2: Crystal data and structure refinement for raj19u

Identification code	raj19u
Empirical formula	C ₇₈ H ₇₂ N ₂
Formula weight	1037.38
Temperature □/□ K	100
Crystal system	triclinic
Space group	P-1
a □/□ Å, b □/□ Å, c □/□ Å	10.3935(6), 16.8183(9), 17.5870(9)
α /°, β /°, γ /°	108.025(5), 91.150(5), 98.353(5)
Volume □/□ Å ³	2885.4(3)
Z	2
ρ_{calc} □/□ mg mm ⁻³	1.194
μ □/□ mm ⁻¹	0.513
F(000)	1108

Crystal size □/□mm ³	.35 × .25 × .04
Theta range for data collection	4.3061 to 142.2256°
Index ranges	-12 ≤ h ≤ 11, -20 ≤ k ≤ 20, -21 ≤ l ≤ 21
Reflections collected	30898
Independent reflections	10860[R(int) = 0.0403]
Data/restraints/parameters	10860/0/723
Goodness-of-fit on F²	1.035
Final R indexes [I > 2σ (I)]	R ₁ = 0.0524, wR ₂ = 0.1370
Final R indexes [all data]	R ₁ = 0.0706, wR ₂ = 0.1515
Largest diff. peak/hole □/□e Å ⁻³	0.378/-0.319

Crystal structure of Ruthenium metal complex of methyl bipyridine (9)

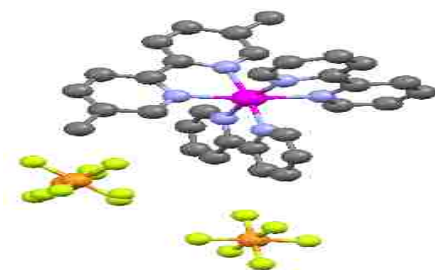


Table 3: Crystal data and structure refinement for raj20e5

Identification code	raj20e5
Empirical formula	C ₃₉ H ₃₆ F ₁₂ N ₆ P ₂ Ru
Formula weight	979.75
Temperature □/□ K	100.0
Crystal system	triclinic
Space group	P-1
a □/□ Å, b □/□ Å, c □/□ Å	11.5644(2), 13.3675(3), 13.8019(3)
α/°, β/°, γ/°	106.806(2), 96.8089(19), 99.4648(19)
Volume □/□ Å ³	1983.26(8)
Z	2
ρ _{calc} □/□ mg mm ⁻³	1.641

μ/mm^{-1}	4.821
F(000)	988
Crystal size mm^3	$0.3353 \times 0.2073 \times 0.0272$
Theta range for data collection	3.3959 to 147.347°
Index ranges	$-13 \leq h \leq 14$, $-14 \leq k \leq 16$, $-17 \leq l \leq 17$
Reflections collected	13712
Independent reflections	13712[R(int) = 0.0000]
Data/restraints/parameters	13712/246/596
Goodness-of-fit on F^2	1.066
Final R indexes [$I > 2\sigma(I)$]	$R_1 = 0.0765$, $wR_2 = 0.2002$
Final R indexes [all data]	$R_1 = 0.0821$, $wR_2 = 0.2058$
Largest diff. peak/hole e \AA^{-3}	1.646/-0.937

Crystal structure of Rhenium metal complex of fluorene based ligand (12)

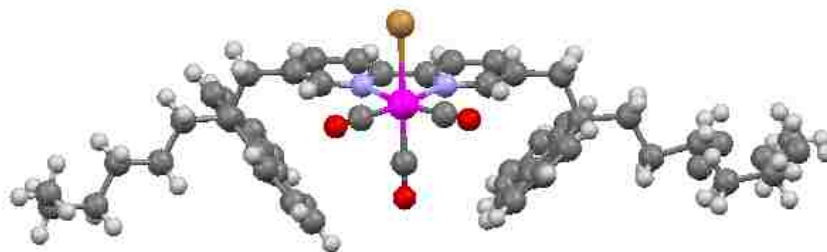


Table 4 : Crystal data and structure refinement for raj20h

Identification code	raj20h
Empirical formula	C ₅₃ H ₅₂ BrN ₂ O _{3.17671} Re
Formula weight	1033.90
Temperature □/□ K	100.0
Crystal system	triclinic
Space group	P-1
a □/□ Å, b □/□ Å, c □/□ Å	13.3720(3), 14.0798(3), 14.9965(3)
α /°, β /°, γ /°	82.0755(15), 68.0002(17), 62.228(2)
Volume □/□ Å ³	2314.00(8)
Z	2
ρ_{calc} □/□ mg mm ⁻³	1.484
μ □/□ mm ⁻¹	3.534
F(000)	1039
Crystal size □/□ mm ³	0.2447 × 0.1784 × 0.0603
Theta range for data collection	3.42 to 59.14°

Index ranges	$-18 \leq h \leq 18, -19 \leq k \leq 18, -19 \leq l \leq 20$
---------------------	--

Reflections collected	52329
Independent reflections	11850[R(int) = 0.0335]
Data/restraints/parameters	11850/5/591
Goodness-of-fit on F^2	1.055
Final R indexes [$I > 2\sigma(I)$]	$R_1 = 0.0279, wR_2 = 0.0586$
Final R indexes [all data]	$R_1 = 0.0338, wR_2 = 0.0611$
Largest diff. peak/hole $\square/\square e \text{ \AA}^{-3}$	1.527/-0.841

Crystal structure of Rhenium metal complex of fluorene based ligand (13)

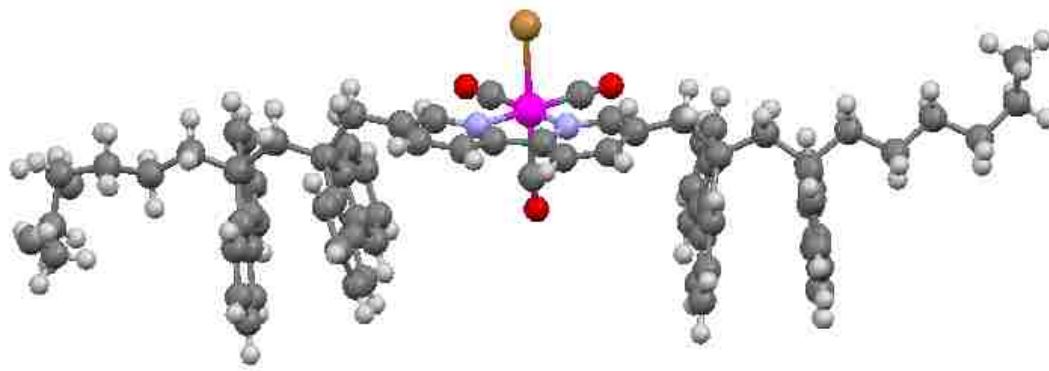


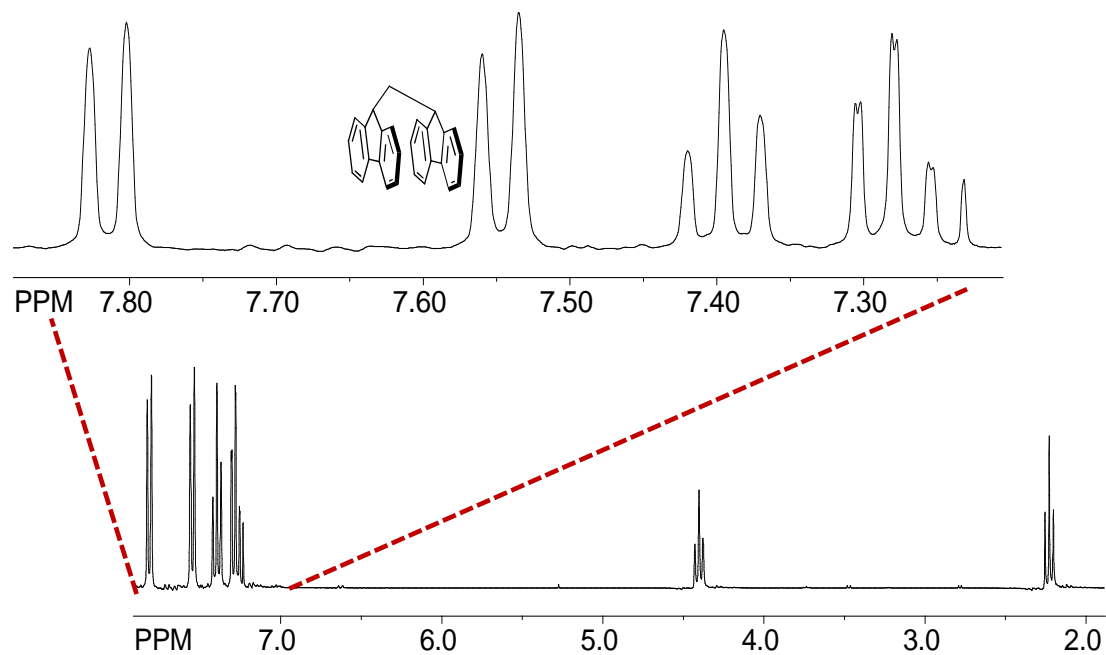
Table 5: Crystal data and structure refinement for raj20g5

Identification code	raj20g5
Empirical formula	C ₈₁ H ₇₂ N ₂ O ₃ BrRe
Formula weight	1387.52
Temperature □/□ K	100
Crystal system	triclinic
Space group	P-1
a □/□ Å, b □/□ Å, c □/□ Å	9.54041(17), 12.4332(3), 27.1606(5)
α /°, β /°, γ /°	91.7364(16), 98.8902(15), 98.7635(17)
Volume □/□ Å ³	3141.08(11)
Z	2
ρ_{calc} □/□ mg mm ⁻³	1.467
μ □/□ mm ⁻¹	4.940
F(000)	1412

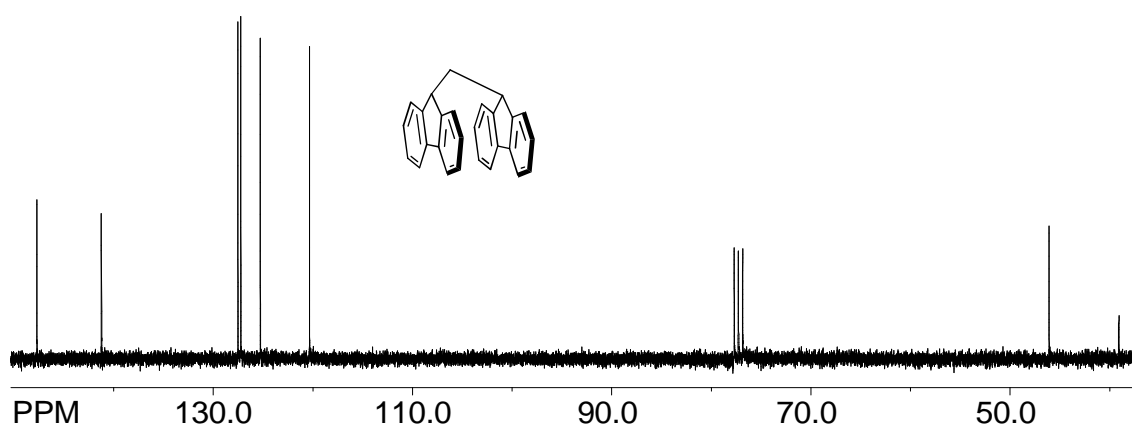
Crystal size □/□mm ³	0.4984 × 0.1398 × 0.0273
--	--------------------------

Theta range for data collection	3.30 to 147.78°
Index ranges	-11 ≤ h ≤ 11, -15 ≤ k ≤ 15, -33 ≤ l ≤ 33
Reflections collected	20060
Independent reflections	20060[R(int) = 0.0000]
Data/restraints/parameters	20060/0/824
Goodness-of-fit on F²	1.151
Final R indexes [I > 2σ (I)]	R ₁ = 0.0505, wR ₂ = 0.1379
Final R indexes [all data]	R ₁ = 0.0537, wR ₂ = 0.1394
Largest diff. peak/hole □/□ e Å ⁻³	2.366/-1.655

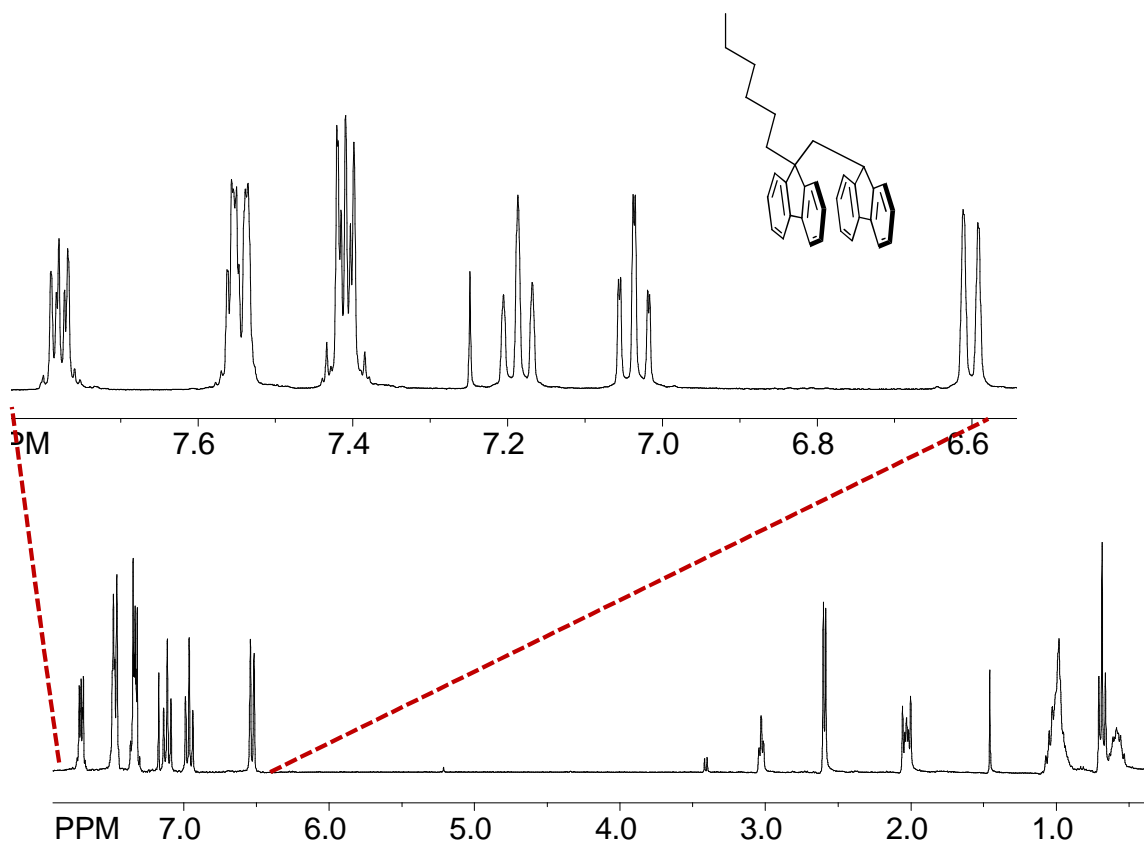
^1H NMR spectrum of 9, 9'-Methylenebis-9H-fluorene (2).



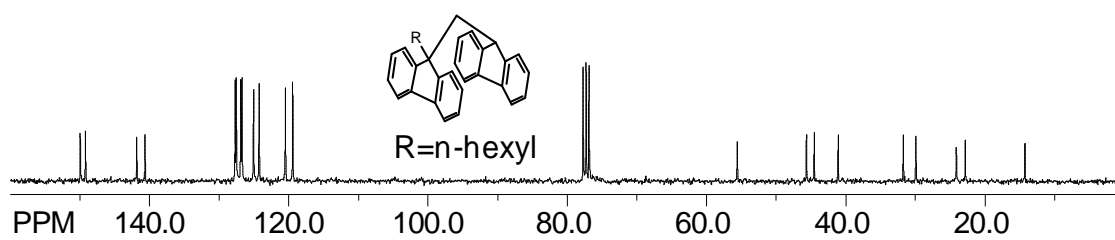
^{13}C NMR spectrum of 9, 9'-Methylenebis-9H-fluorene (2).



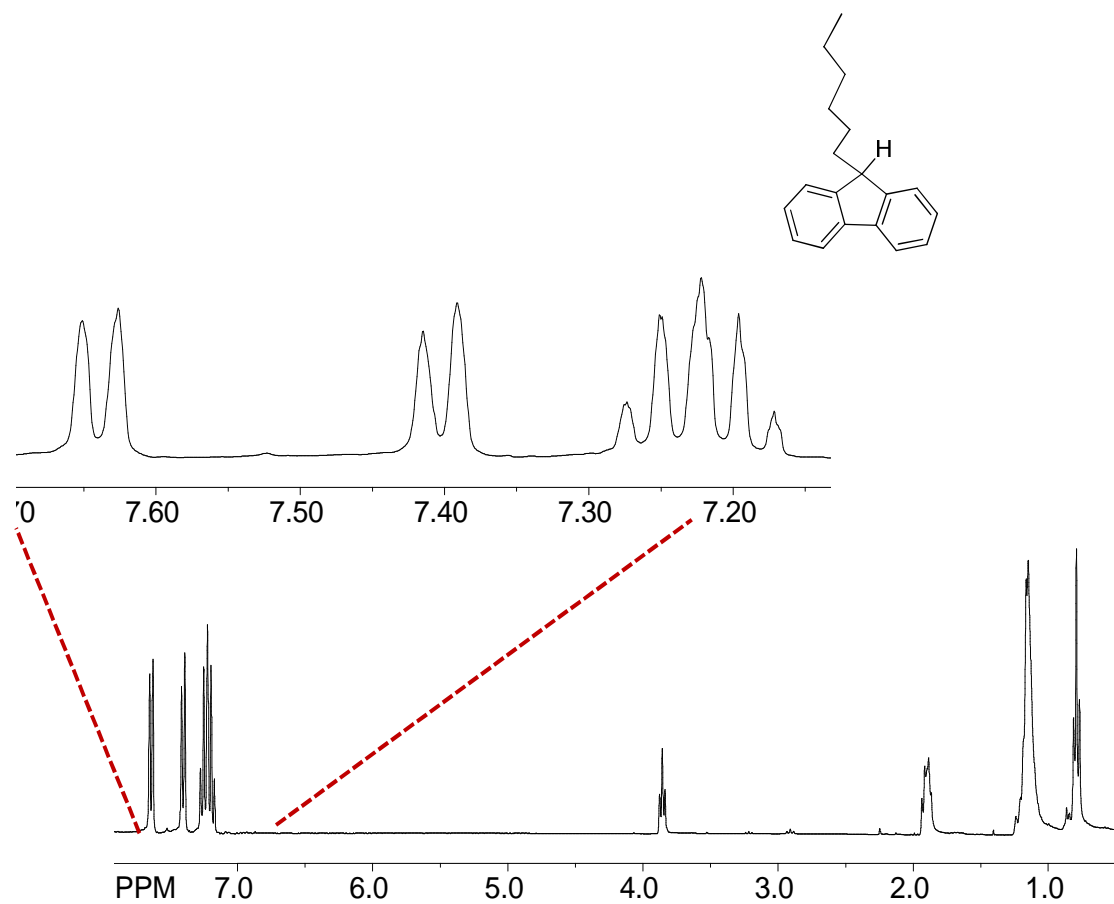
^1H NMR spectrum of 9-(9H-fluoren-9-ylmethyl)-9-hexyl-9H-fluorene (3).



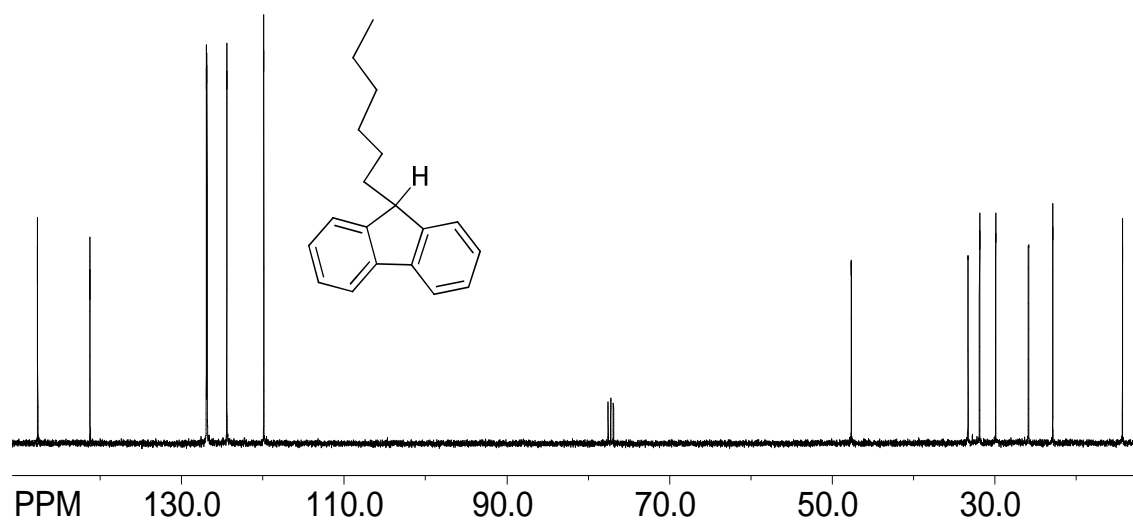
^{13}C NMR spectrum of 9-(9H-fluoren-9-ylmethyl)-9-hexyl-9H-fluorene (3).



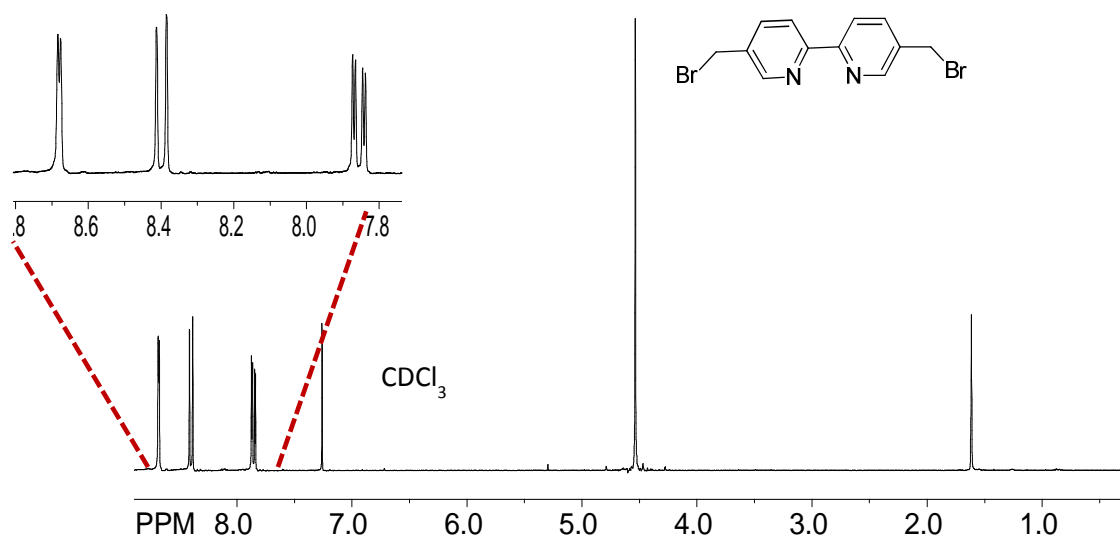
^1H NMR spectrum of 9-Hexyl-9H-fluorene (5).



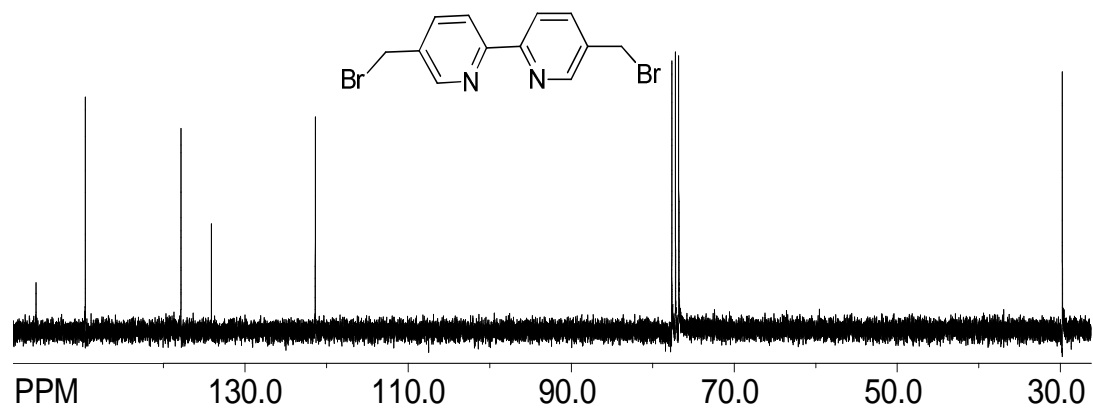
^{13}C NMR spectrum of 9-Hexyl-9H-fluorene (5).



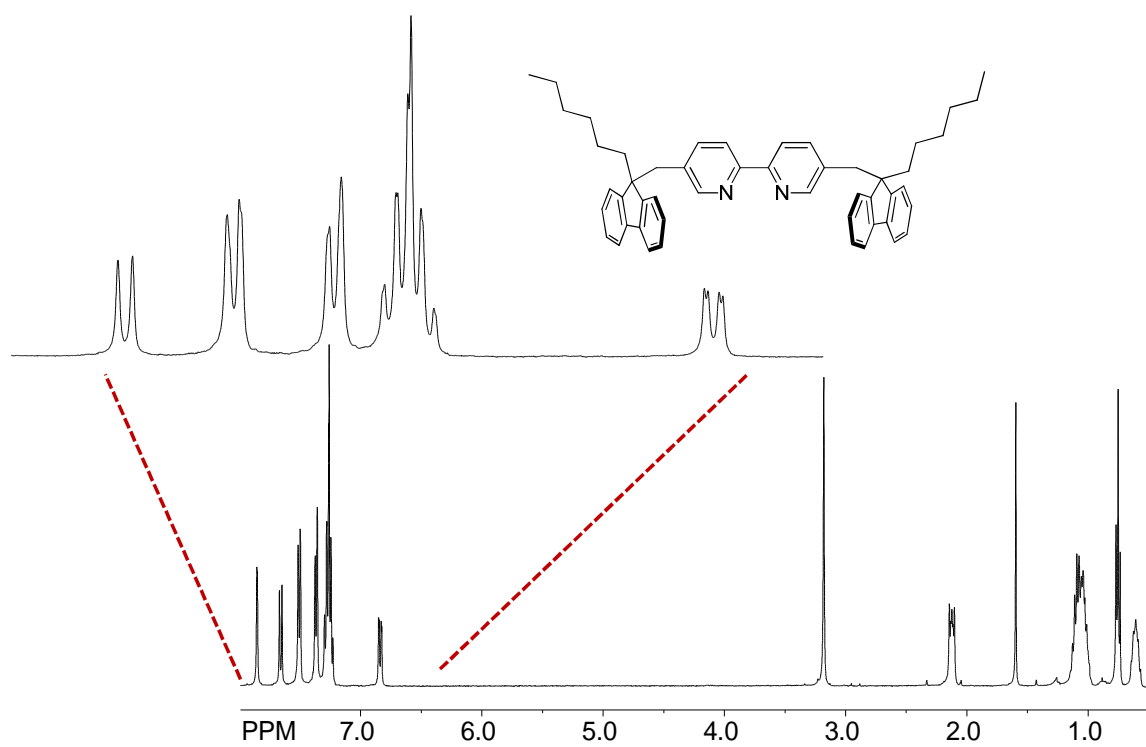
^1H NMR spectrum of 5, 5'-Bis-bromomethyl-[2,2']bipyridinyl.



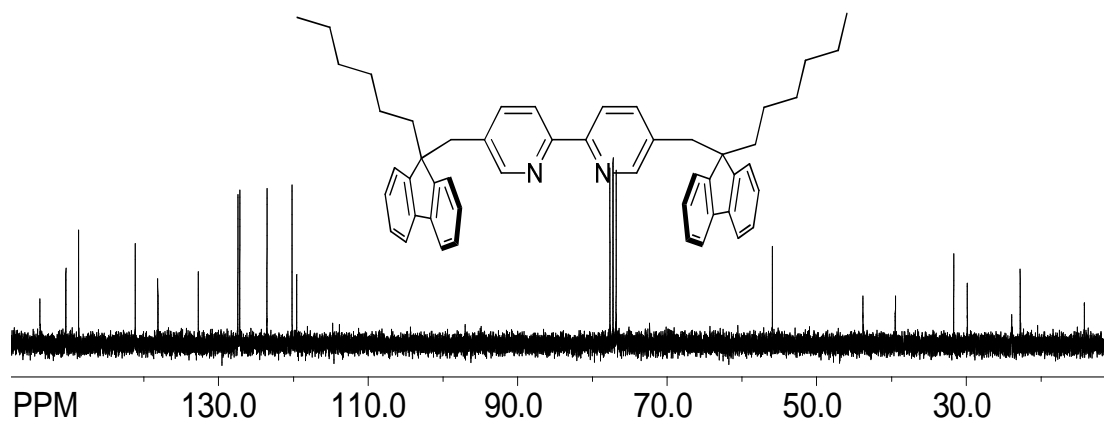
^{13}C NMR spectrum of 5, 5'-Bis-bromomethyl-[2, 2']bipyridinyl.



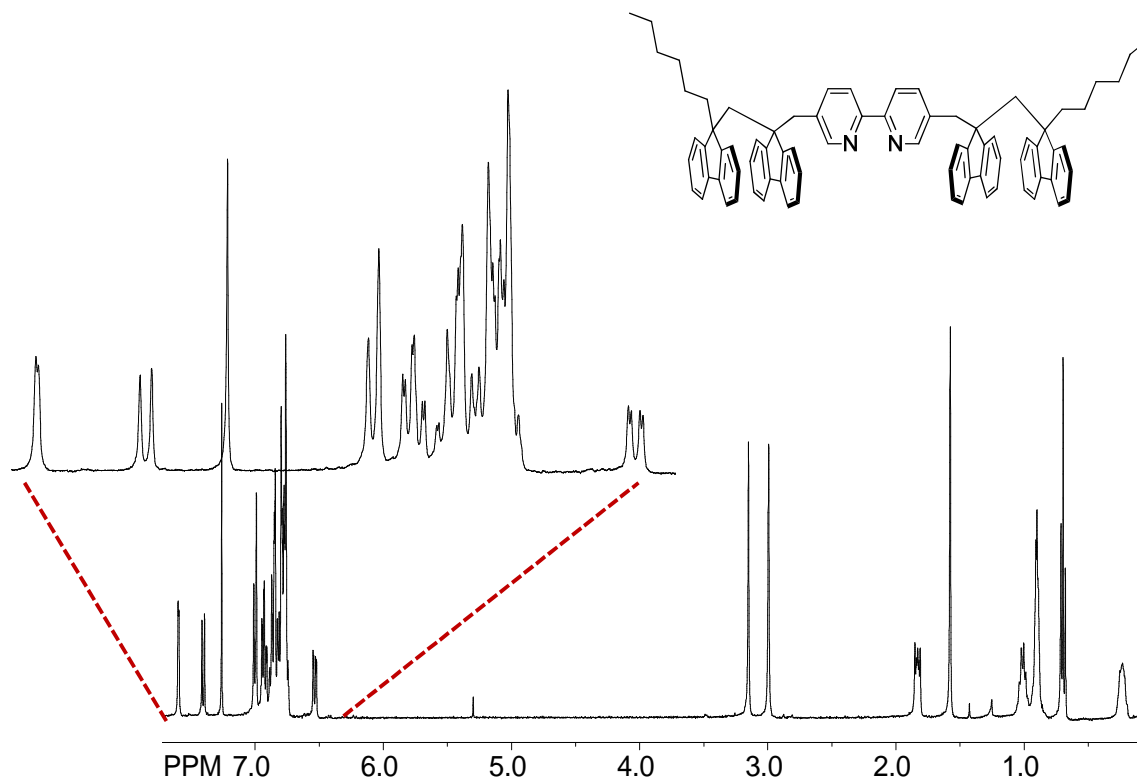
^1H NMR spectrum of 5, 5'-Bis-(9-hexyl-9H-fluoren-9-ylmethyl)-[2,2']bipyridinyl (6).



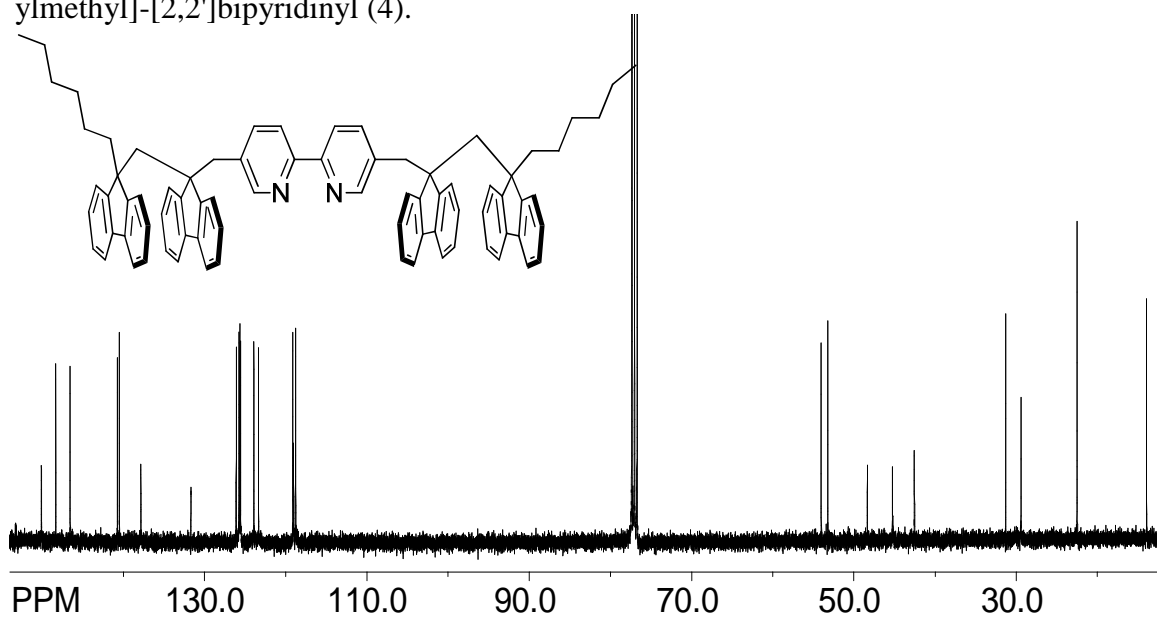
^{13}C NMR spectrum of 5, 5'-Bis-(9-hexyl-9H-fluoren-9-ylmethyl)-[2, 2']bipyridinyl (6).



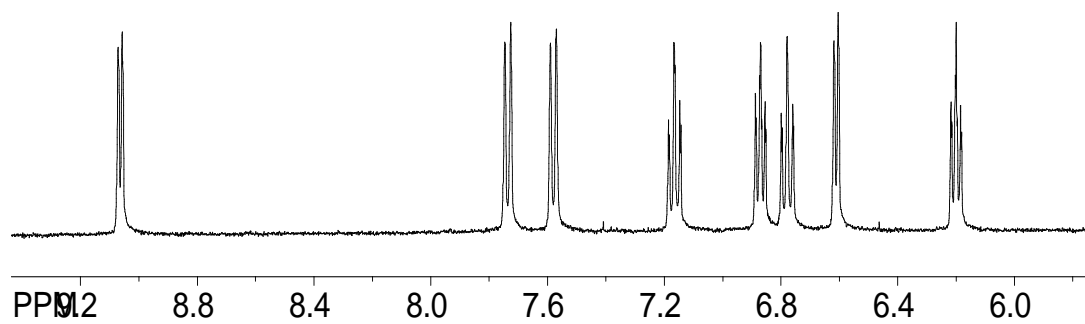
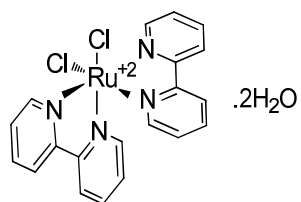
^1H NMR spectrum of 5,5'-Bis-[9-(9-hexyl-9H-fluoren-9-ylmethyl)-9H-fluoren-9-ylmethyl]-[2,2']bipyridinyl (4).



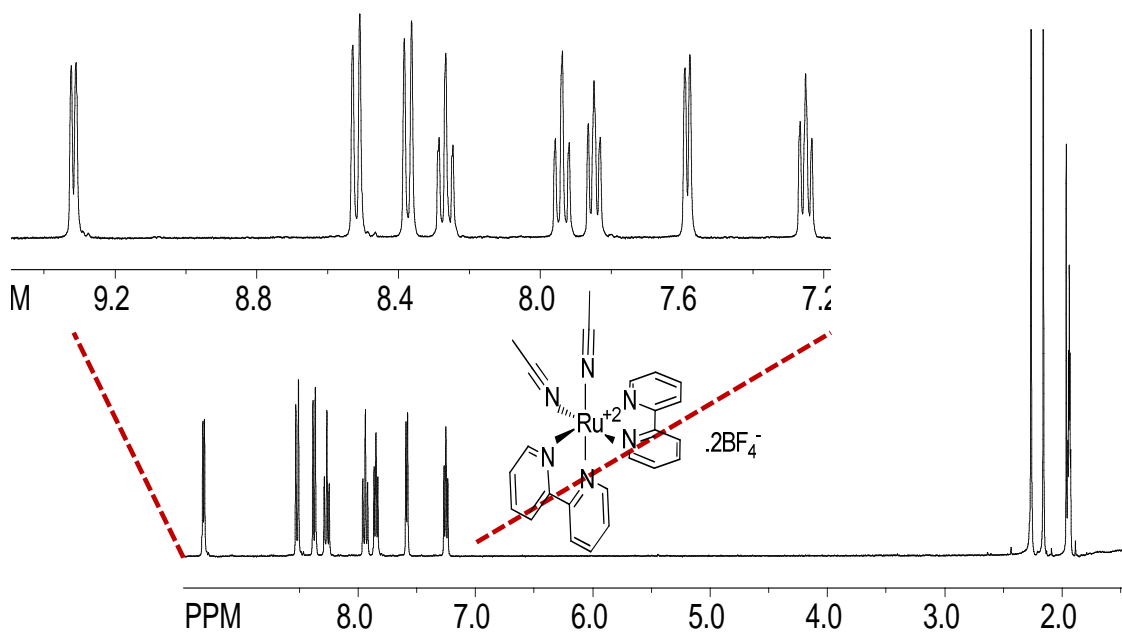
^{13}C NMR spectrum of 5,5'-Bis-[9-(9-hexyl-9H-fluoren-9-ylmethyl)-9H-fluoren-9-ylmethyl]-[2,2']bipyridinyl (4).



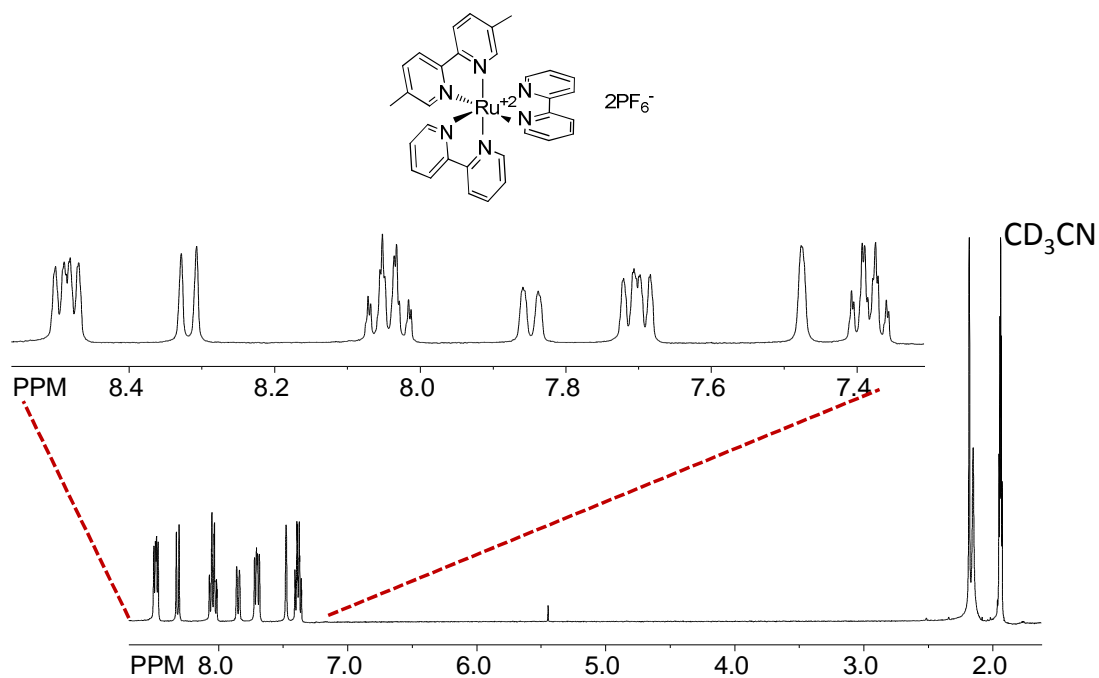
^1H NMR spectrum of 7.



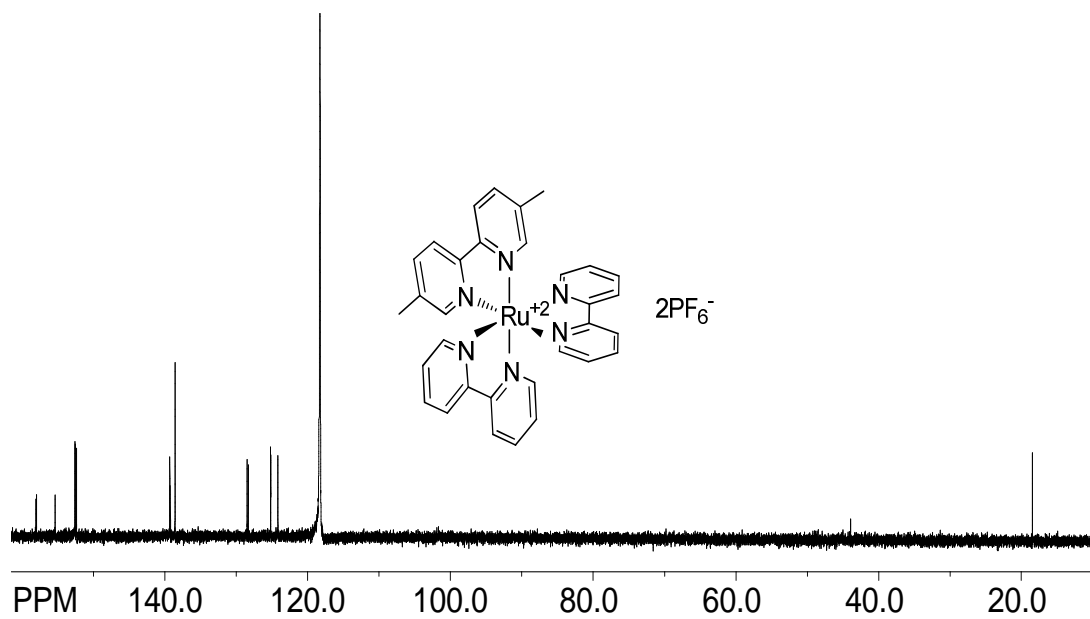
^1H NMR spectrum of 8.



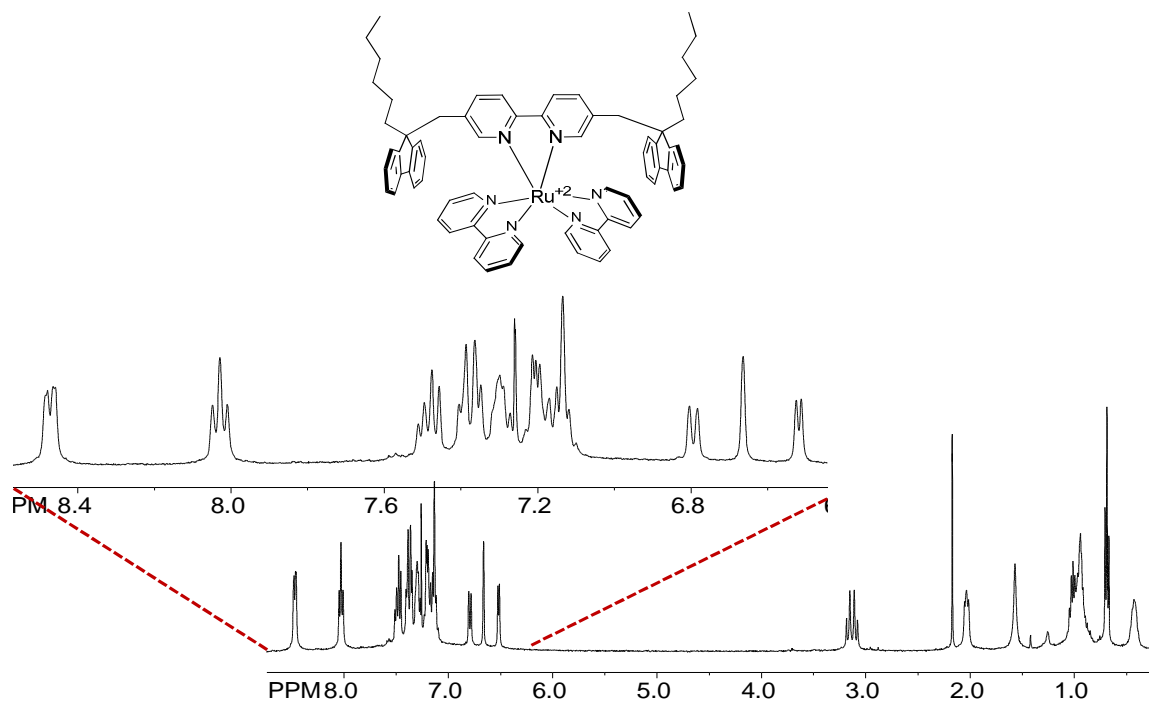
^1H NMR spectrum of $[\text{Ru}(\text{bpy})_2.\text{bpyMe}]$ (9).



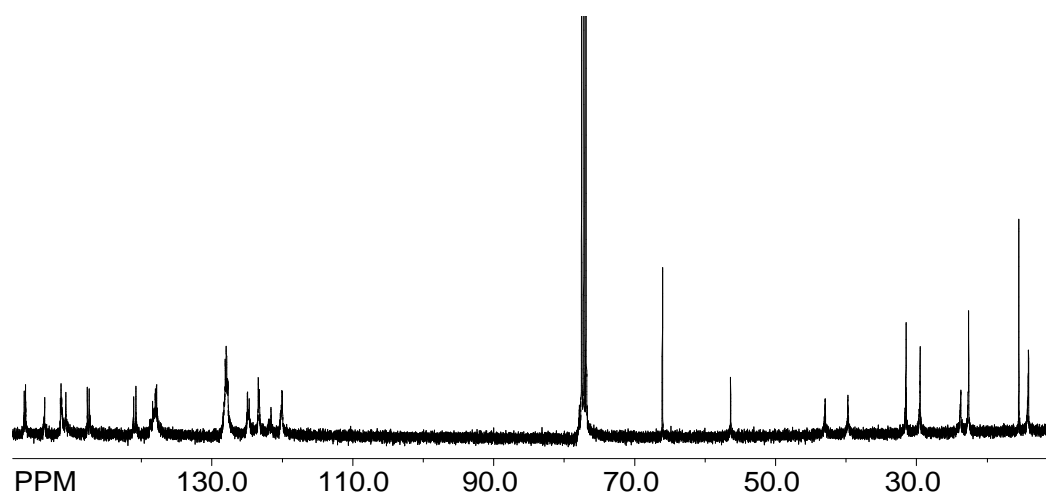
^{13}C NMR spectrum of $[\text{Ru}(\text{bpy})_2.\text{bpyMe}]$ (9).



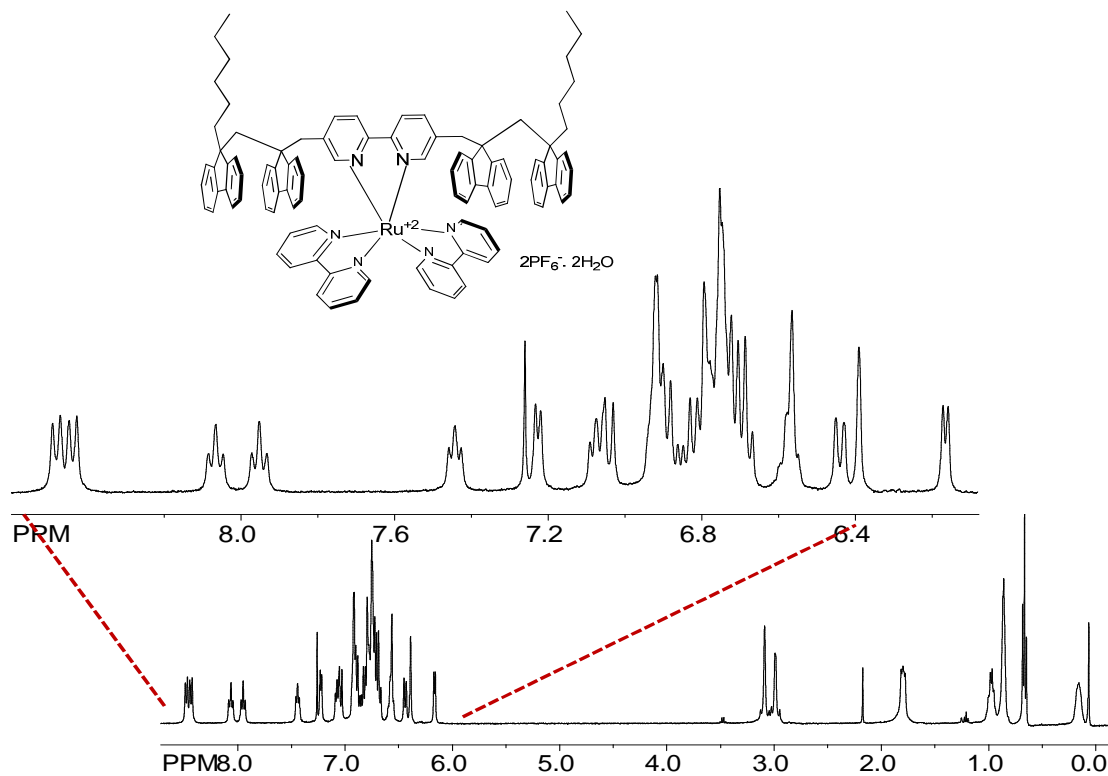
^1H NMR spectrum of $[\text{Ru}(\text{F}_1\text{bpy})(\text{Bpy})_2]$ (10).



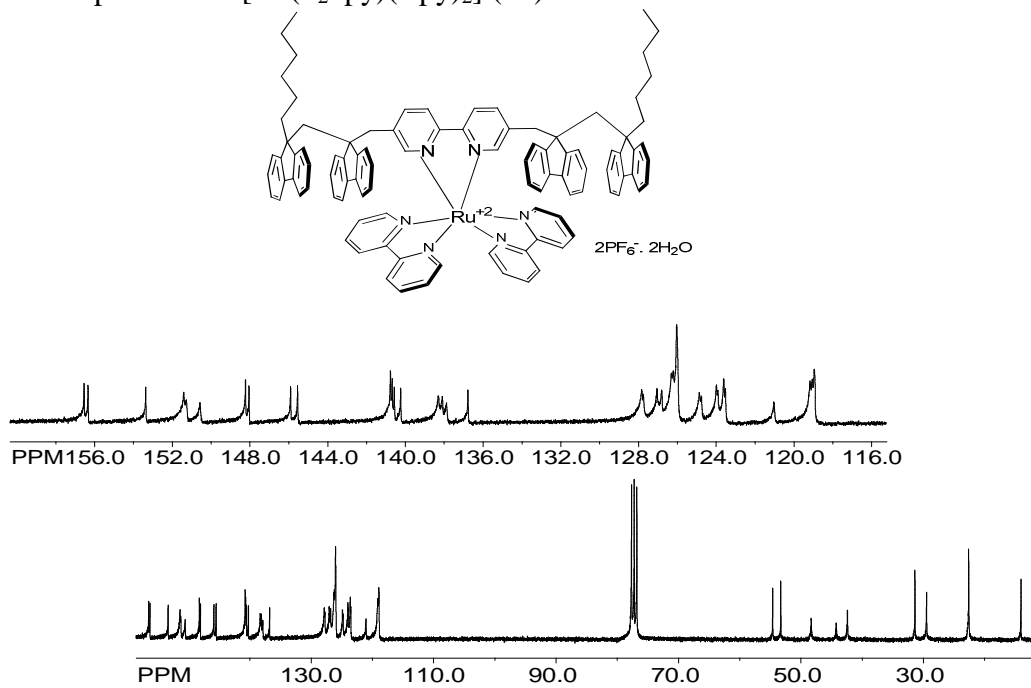
^{13}C NMR spectrum of $[\text{Ru}(\text{F}_1\text{bpy})(\text{Bpy})_2]$ (10).



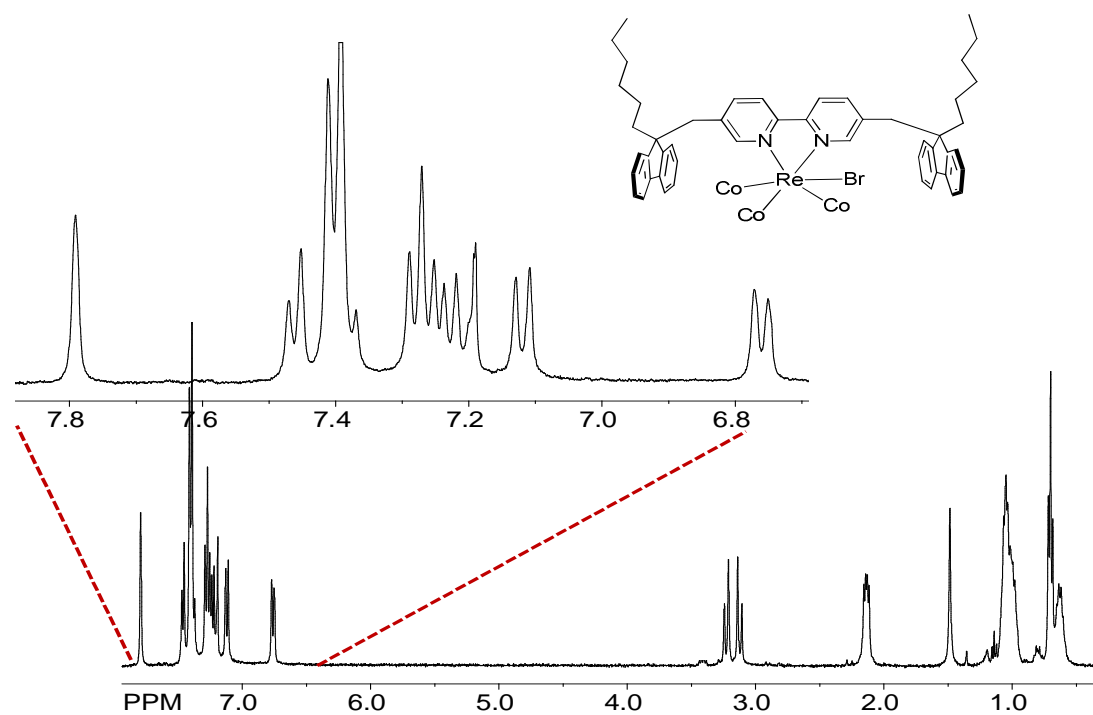
^1H NMR spectrum of $[\text{Ru}(\text{F}_2\text{bpy})(\text{Bpy})_2]$ (11).



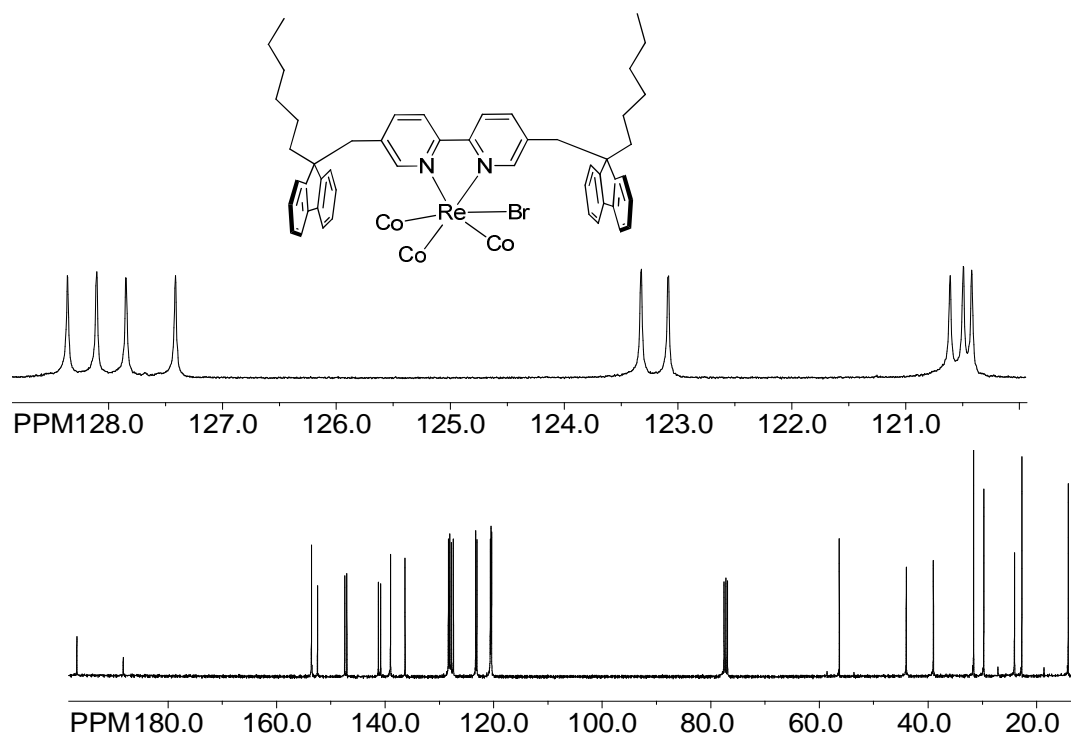
^{13}C NMR spectrum of $[\text{Ru}(\text{F}_2\text{bpy})(\text{Bpy})_2]$ (11).



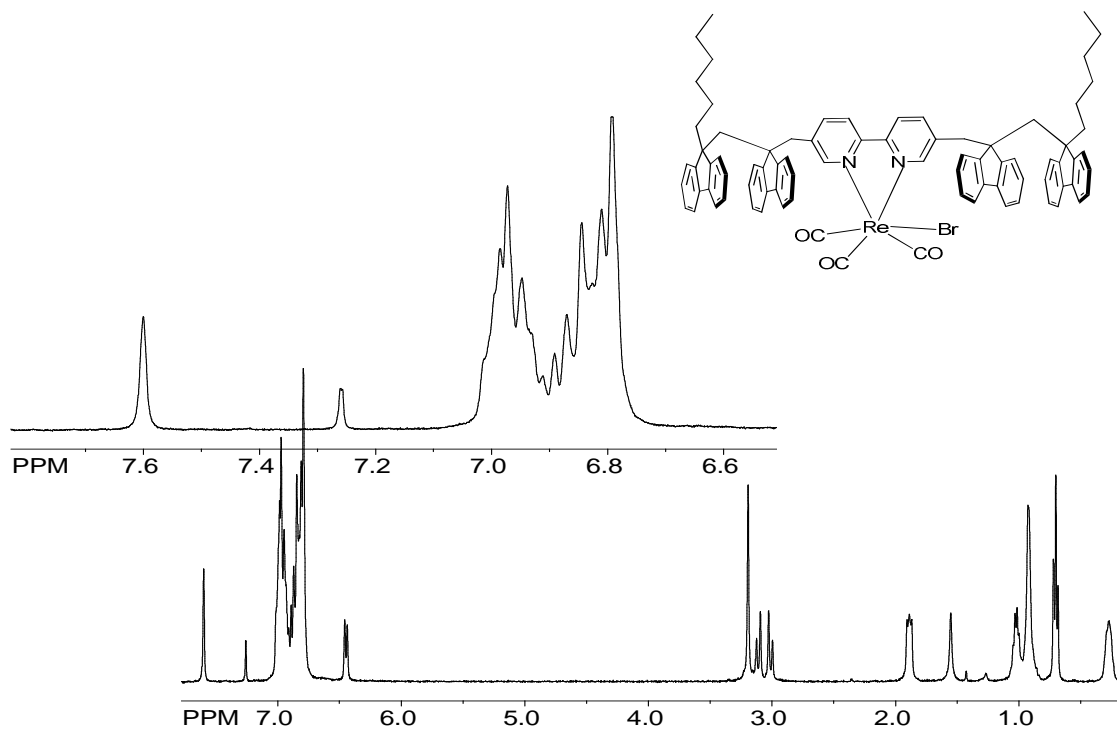
^1H NMR spectrum of $[\text{Re}(\text{F}_1\text{bpy})(\text{Co})_3\text{Br}]$ (12).



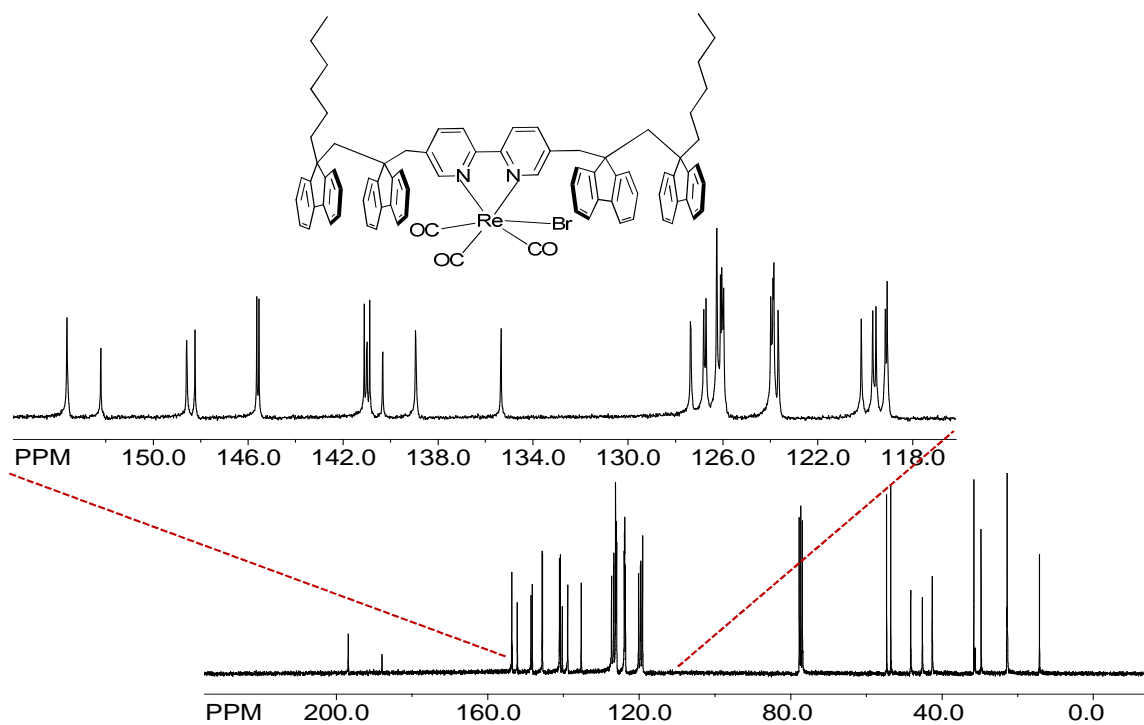
^{13}C NMR spectrum of $[\text{Re}(\text{F}_1\text{bpy})(\text{Co})_3\text{Br}]$ (12).



^1H NMR spectrum of $[\text{Re}(\text{F}_2\text{bpy})(\text{Co})_3\text{Br}]$ (13).



^{13}C NMR spectrum of $[\text{Re}(\text{F}_2\text{bpy})(\text{Co})_3\text{Br}]$ (13).



REFERENCES AND FOOTNOTES

Chapter 1

1. Scholl, R.; Mansfeld, J. *Ber. Dtsch. Chem. Ges.* **1910**, *43*, 1734-1746. Kovacic, P.; Jones, M. B. *Chem. Rev.* **1987**, *87*, 357.
2. Zuccherro, A. J.; McGrier, P. L.; Bunz, U. H. F. *Acc. Of Chem. Res.* **2010**, *43*, 397-408.
3. Wilson, J. N.; Smith, M. D.; Enkelmann, V.; Bunz, U. H. *Chem. Commun. (Camb)* **2004**, 1700-1. Klare, J. E.; Tulevski, G. S.; Sugo, K.; de Picciotto, A.; White, K. A.; Nuckolls, C. *J. Am. Chem. Soc.* **2003**, *125*, 6030-6031.
4. Wilson, J. N.; Bunz, U. H. F. *J Am Chem Soc* **2005**, *127*, 4124-4125.
5. Zuccherro, A. J.; Wilson, J. N.; Bunz, U. H. F. *J Am Chem Soc* **2006**, *128*, 11872-11881.
6. Wilson, J. N.; Bunz, U. H. *J. Am. Chem. Soc.* **2005**, *127*, 4124-5.
7. Tolosa, J.; Zuccherro, A. J.; Bunz, U. H. *J. Am. Chem. Soc.* **2008**, *130*, 6498-506.
8. Wilson Enkelmann, V.; Bunz, U. H. *Chem. Commun. (Camb)* **2004**, 1700-1.
9. Paras L. McGrier, Kyril M. Solntsev, Shaobin Miao, Laren M. Tolbert, Oscar R. Miranda, Vincent M. Rotello, Uwe H.F. Bunz *Chem. Eur.J.* **2008**, *14*, 4503-4510.
10. McGrier P., Solntsev K.M., Brombosz S.M., Tolbert L.M. Bunz U.H. *Chem. Commun.* **2007**, 2127-2129.
11. Hauck, M.; Schonhaber, J.; Zuccherro, A. J.; Hardcastle, K. I.; Muller, T. J.; Bunz, U. H. *J. Org. Chem.* **2007**, *72*, 6714-25.

12. Brombosz, S. M.; Zuccherro, A. J.; Phillips, R. L.; Vazquez, D.; Wilson, A.; Bunz, U. H. *Org. Lett.* **2007**, *9*, 4519-22.
13. Klare J.E., Tulevski S. G. Sugo K., Picciotto A. de, White K.A. Nuckolls C.J. *Am. Chem. Soc.* **2003**, *125*, 6030-6031.
14. Spitler, E. L.; Shirtcliff, L. D.; Haley, M. M. *J. Org. Chem.* **2007**, *72*, 86-96.
15. Tolosa, J.; Bunz, U. H. F. *Chem-Asian. J.* **2009**, *4*, 270-276.
16. Zuccherro, A. J.; Wilson, J. N.; Bunz, U. H. F. *J. Am. Chem. Soc.* **2006**, *128*, 11872-11881.
17. Tolosa, J.; Zuccherro, A. J.; Bunz, U. H. *J. Am. Chem. Soc.* **2008**, *130*, 6498-506.
18. Marsden J.A., Miller J.J., shirtcliff L.D., Haley M.M. *J. Am. Chem. Soc.* **2005**, *127*, 3464-2476.

Chapter 2

1. Petroni, A.; D. Slep, L. D.; Etchenique R. *Inorg. Chem.* **2008**, *47*, 951-956.
2. Belser, P.; Zelewsky, A.V.; Frank, M.; Seel, C.; Vogtle, F.; DeCola, L.; rancesco Barigelletti, F.; Balzani, V.; *J. Am. Chem. SOC.* **1993**, *115*, 4076-4086.
3. Cpmagna, S.; Puntoriero, F.; Nastasi F.; Bergamini G.; Baizani V.; Photochemistry & photophysics of coordination compounds: Ruthenium. *Topics in Current Chemistry* **2007**, *280*, 117-214.
4. Lehn, J. M.; *Chem. Soc. Rev.* **2007**, *36*, 151.
5. Lehn, J.; M.; *Supramolecular Chemistry – Concepts and Chemistry*; VCH: Weinheim, Germany, **1995**.
6. G. R. Newkome, E. He, Moorefield, C. N. *Chem. Rev.* **1999**, *99*, 1689.
7. U. S. Schubert, H. Hofmeier, G. R. Newkome, *Modern Terpyridine Chemistry*, Wiley-VCH, Weinheim, **2006**.
8. Thomas, K. R. J.; Lin, J. T.; Lin, H. M.; Chang, C. P.; Chuen, C. H. *Organometallics* **2001**, *20* (3), 557-563.
9. Ziessel, R.; Hissler, M.; El-ghazoury, A.; Harriman, A. *Coord. Chem. Rev.* 1998, *178-180*, 1251. (b) Sauvage, J.-P.; Collin, J.-P.; Chambron, J.-C.; Guillerez, S. Coudret, C.; Balzani, V.; Barigelletti, F.; De Cola, L.; Flamigni, L. *Chem. Rev.* 1994, *94*, 993.
10. Albano, G.; Balzani, V.; Constable, E. C.; Maestri, M.; Smith, D. R. *Inorg. Chim. Acta* 1998, *277*, 225. (b) Wilson, G. J.; Lavnikonis, A.; Sasse, W. H. F.; Mau, A. W.-H. *J. Phys. Chem. (A)* **1997**, *101*, 4860.

11. Wilson, G. J.; Sasse, W. H. G.; Mau, A. W.-H. *Chem. Phys. Lett.* **1996**, *250*, 583.
12. Harriman, A.; Hissler, M.; Khatr, A.; Ziessel, R. *Chem. Commun.* **1999**, 735. (b) Simon, J. A.; Curry, S. L. Schmehl, R. H.; Schatz, T. R.; Piotrowiak, P.; Jin, X.; Thummel, R. P. *J. Am. Chem. Soc.* **1997**, *119*, 11012. (c) Ford, W. E.; Rodgers, M. A. J. *J. Phys. Chem.* **1992**, *96*, 2917.
13. Ciana, L. D.; Zanarini, S.; Perciaccante, R.; Marzocchi, E.; Valenti G. *J. Phys. Chem. C* **2010**, *114*, 3653–3658.
14. Okujima, T. Mifuji, A.; Nakamura, J.; Yamada, H.; Uno, H.; Ono N. *Org. Lett.* **2009**, *11*, No. 18, 4088-4091.
15. Haberecht, M. C.; Schnorr, J. M.; Andreitchenko, E. V.; Clark, C. G.; Wagner, M.; Mullen K. *Angew. Chem. Int. Ed.* **2008**, *47*, 1662–1667.
16. (a) Rathore, R.; Abdelwhaed, S.H.; Guezi, I.A., *J. Am. Chem. Soc.* **2003**, *125*, 8712-8713. (b) Rathore, R.; Abdelwahed, S.H.; Kiesewetter, M.K.; Reiter, R.C.; Stevenson, C.D., *J. Phys. Chem. B* **2006**, *110*, 1536-1542. (c) Stevenson, C.D.; Kiesewetter, M.K.; Reiter, R.C.; Chebny, V.J.; Rathore, R., *J. Phys. Chem. A* **2006**, *110*, 9602-9609. (d) Stevenson, C.D.; Kiesewetter, M.K.; Reiter, R.C.; Abdelwahed, S.H.; Rathore, R., *J. Am. Chem. Soc.* **2005**, *127*, 5282-5283.
17. Geng, Y.; Trajkovska, A.; Katsis, D.; Ou, J. J.; Culligan, S.W.; Chen, S.H., *J. Am. Chem. Soc.* **2002**, *124*, 8337-8347.